EAI-TR-82-001

# ADVANCED
# SPACE SHUTTLE
# SIMULATION MODEL

Summary Report

Contract NAS8-33818

Prepared for

National Aeronautics and Space Administration
George C. Marshall Space Flight Center
Marshall Space Flight Center, Alabama 35812

Prepared by

Frank B. Tatom
S. Ray Smith

January 11, 1982

ENGINEERING ANALYSIS, INC.

2109 Clinton Ave. W., Suite 432
Huntsville, Alabama 35805
(205)533-9391

TABLE OF CONTENTS

## LIST OF TABLES

## LIST OF ILLUSTRATIONS

## LIST OF ILLUSTRATIONS
(Continued)

## LIST OF ILLUSTRATIONS
(Continued)

## LIST OF ILLUSTRATIONS
(Concluded)

# 1. INTRODUCTION

The effects of atmospheric turbulence in both horizontal and near-horizontal flight, during the return of the Space Shuttle, are important for determining design, control, and "pilot-in-the-loop" effects. A non-recursive model (based on von Karman spectra) for atmospheric turbulence along the flight path of the Shuttle Orbiter has been developed which provides for simulation of instantaneous vertical and horizontal gusts at the vehicle center-of-gravity, and also for simulation of instantaneous gusts gradients. Based on this model the time series for both gusts and gust gradients have been generated and stored on a series of magnetic tapes which are entitled Shuttle Simulation Turbulence Tapes (SSTT). The time series are designed to represent atmospheric turbulence from ground level to an altitude of 120,000 meters.

A description of the turbulence generation procedure is provided in Section 2. The results of validating the simulated turbulence are described in Section 3. Conclusions and recommendations are presented in Section 4 with Section 5 containing references cited. Appendix A contains the tabulated one-dimensional von Karman spectra while Appendix B provides a discussion of the minimum frequency simulated. Appendices C and D present the results of spectral and statistical analyses of the SSTT. A more detailed description of the proper use of the tapes is provided elsewhere [1].

# 2. TURBULENCE GENERATION PROCEDURE

The non-recursive turbulence model used to generate the SSTT is based on von Karman spectra with finite upper limits corresponding to the dimensions of the Space Shuttle, relative to the scale of turbulence in the atmosphere. Because the scale of turbulence increases with altitude while the dimensions of the Space Shuttle are fixed, the finite upper limits of the von Karman spectra increase with altitude. In order to take into account the resulting spectral changes, the atmosphere, extending from ground level to 120,000 meters, was divided into six altitude bands. The subsections which follow provide a description of the development and application of the turbulence generation procedures.

## 2.1 BACKGROUND

The current turbulence model represents the results of the development and evaluation of several different turbulence simulation techniques. Two of the earlier techniques, which were given serious consideration, warrant further discussion.

Initial efforts involved refinement and evaluation of a turbulence model, TBMOD [2], which had been developed elsewhere [3]. This model was based on discretization of the Fourier integral representation of turbulence and was designed for use with von Karman spectra. Several problems were encountered with TBMOD, both theoretical and practical. First, from a theoretical standpoint, the assumptions used in the development of the shear (gust gradient) simulation were difficult to justify. Second, from a practical standpoint, the output of TBMOD, representing turbulent gusts, when subjected to Fast Fourier Transform (FFT) spectral analysis, did not possess the proper von Karman spectral shape. Because of such problems, further development of the model was halted.

The second simulation technique was based on digital filter theory coupled with a combined von Karman - Saffman spectral model [4]. Meromorphic functions were used to approximate the various spectra. Based on z-transform theory, recursive difference equations were derived from such approximations. Such difference equations were then used to generate

the appropriate turbulence gusts and gust gradients. Unfortunately the recursive difference equations, in addition to being somewhat complex, proved numerically unstable and could not be used in their original recursive form [5].

A non-recursive version of the same difference equations was subsequently developed in an effort to overcome the stability problem [5]. These difference equations were also quite complex but resembled in form the output of digital filters, characterized by some impulse response function, with a white noise input. The present model, as described in subsections 2.2 through 2.4, was an outgrowth of this resemblance.

## 2.2 SELECTION OF ATMOSPHERIC BANDS

The standard deviations ($\sigma_1$, $\sigma_2$, $\sigma_3$) and the integral scale lengths ($L_1$, $L_2$, $L_3$) of atmospheric turbulence are functions of altitude, as shown in Table 2-1. Notice should be taken that the values for $\sigma_i$ and $L_i$ presented in this table are consistent with those presented in JSC 7700 [6]. Based on the variation of $\sigma_i$ and $L_i$ presented in Table 2-1, the atmosphere was divided into six altitude bands as presented in Table 2-2. Within each band, as also indicated in Table 2-2, characteristic integral scales of turbulence were selected for use in calculating the finite upper limit of the turbulence spectral model discussed in subsection 2.3.

## 2.3 DEVELOPMENT OF VON KARMAN SPECTRA WITH FINITE UPPER LIMITS

As developed previously [5] the basic three-dimensional von Karman relation to be integrated for the dimensionless gust spectra is,

$$\phi_{ii}(\Omega_1,\Omega_2,\Omega_3) = \frac{55}{36a\pi^2}\frac{(\Omega^2-\Omega_i^2)}{(1+\Omega^2)^{17/6}} \qquad (2\text{-}1)$$

The corresponding von Karman relation for dimensionless gust gradient spectra is

$$\phi_{ii/jj}(\Omega_1,\Omega_2,\Omega_3) = \frac{55}{36\pi^2a^3}\frac{\Omega_j^2(\Omega^2-\Omega_i^2)}{(1+\Omega^2)^{17/6}} \qquad (2\text{-}2)$$

These three-dimensional spectral relations must be integrated over certain ranges of values of $\Omega_2$ and $\Omega_3$ to obtain one-dimensional spectral models $\Phi_{ii}(\Omega_1)$ and $\Phi_{ii/jj}(\Omega_1)$.

TABLE 2-1. VARIATION OF STANDARD DEVIATION AND LENGTH SCALE WITH ALTITUDE*

| ALTITUDE (m) | STANDARD DEVIATION OF TURBULENCE | | | INTEGRAL SCALES OF TURBULENCE | | |
|---|---|---|---|---|---|---|
| | $\sigma_1$(m/sec) | $\sigma_2$(m/sec) | $\sigma_3$(m/sec) | $L_1$(m) | $L_2$(m) | $L_3$(m) |
| 10 | 2.31 | 1.67 | 1.15 | 21 | 11 | 5 |
| 20 | 2.58 | 1.98 | 1.46 | 33 | 19 | 11 |
| 30 | 2.75 | 2.20 | 1.71 | 43 | 28 | 17 |
| 40 | 2.88 | 2.36 | 1.89 | 52 | 35 | 23 |
| 50 | 2.98 | 2.49 | 2.05 | 61 | 42 | 29 |
| 60 | 3.07 | 2.61 | 2.19 | 68 | 49 | 35 |
| 70 | 3.15 | 2.71 | 2.32 | 75 | 56 | 41 |
| 80 | 3.22 | 2.81 | 2.43 | 82 | 63 | 47 |
| 90 | 3.28 | 2.89 | 2.54 | 89 | 69 | 53 |
| 100 | 3.33 | 2.97 | 2.64 | 95 | 75 | 59 |
| 200 | 3.72 | 3.53 | 3.38 | 149 | 134 | 123 |
| 304.8 | 3.95/4.37 | 3.95/4.37 | 3.95/4.39 | 196/300 | 190/300 | 192/300 |
| 400 | 4.39 | 4.39 | 4.39 | 300 | 300 | 300 |
| 500 | 4.39 | 4.39 | 4.39 | 300 | 300 | 300 |
| 600 | 4.39 | 4.39 | 4.39 | 300 | 300 | 300 |
| 700 | 4.39 | 4.39 | 4.39 | 300 | 300 | 300 |
| 762 | 4.39/5.70 | 4.39/5.70 | 4.39/5.70 | 300/533 | 300/533 | 300/533 |
| 800 | 5.70 | 5.70 | 5.70 | 533 | 533 | 533 |
| 900 | 5.70 | 5.70 | 5.70 | 533 | 533 | 533 |
| 1524 | 5.70/5.79 | 5.70/5.79 | 5.70/5.79 | 533 | 533 | 533 |
| 2000 | 5.79 | 5.79 | 5.79 | 533 | 533 | 533 |
| 3048 | 5.79/5.52 | 5.79/5.52 | 5.79/5.52 | 533 | 533 | 533 |
| 4000 | 5.52 | 5.52 | 5.52 | 533 | 533 | 533 |
| 5000 | 5.52 | 5.52 | 5.52 | 533 | 533 | 533 |
| 6096 | 5.52/5.27 | 5.52/5.27 | 5.52/5.27 | 533 | 533 | 533 |
| 7000 | 5.27 | 5.27 | 5.27 | 533 | 533 | 533 |
| 8000 | 5.27 | 5.27 | 5.27 | 533 | 533 | 533 |
| 9144 | 5.27/4.22 | 5.27/4.22 | 5.27/4.22 | 533 | 533 | 533 |
| 10000 | 4.22 | 4.22 | 4.22 | 533 | 533 | 533 |
| 20000 | 6.01 | 6.01 | 4.22 | 6691 | 6691 | 955 |

*Double entries for a tabulated altitude indicate a step change in standard deviation or integral scale at that altitude.

TABLE 2-1. VARIATION OF STANDARD DEVIATION AND LENGTH SCALE WITH ALTITUDE (Continued)

| ALTITUDE (m) | STANDARD DEVIATION OF TURBULENCE | | | INTEGRAL SCALES OF TURBULENCE | | |
|---|---|---|---|---|---|---|
| | $\sigma_1$(m/sec) | $\sigma_2$(m/sec) | $\sigma_3$(m/sec) | $L_1$(m) | $L_2$(m) | $L_3$(m) |
| 27000 | 7.00 | 7.00 | 4.22 | 20000 | 20000 | 1230 |
| 30000 | 8.23 | 8.23 | 4.66 | 23533 | 23533 | 1443 |
| 40000 | 12.82 | 12.82 | 6.09 | 36693 | 36693 | 2231 |
| 50000 | 18.08 | 18.08 | 7.51 | 51786 | 51786 | 3128 |
| 60000 | 23.94 | 23.94 | 8.90 | 68623 | 68623 | 4124 |
| 70000 | 30.36 | 30.36 | 10.28 | 87063 | 87063 | 5208 |
| 80000 | 37.29 | 37.29 | 11.65 | 106998 | 106998 | 6376 |
| 90000 | 44.70 | 44.70 | 13.01 | 128338 | 128338 | 7622 |
| 100000 | 52.58 | 52.58 | 14.35 | 151010 | 151010 | 8941 |
| 110000 | 60.89 | 60.89 | 15.69 | 174950 | 174950 | 10330 |
| 120000 | 69.62 | 69.62 | 17.02 | 200000 | 200000 | 11800 |

### 2.3.1 Upper Limits of Integration

The upper limits of integration for j = 2 and 3 are calculated according to the relation [7]

$$\Omega_{ijmax} = aL_i/\ell_j \qquad (j = 2,3) \qquad (2\text{-}3)$$

where

$a$ = 1.339

$L_i$ = integral scale of turbulence associated with the $\Phi_{ii}(\Omega_1)$ spectrum

$\ell_j$ = characteristic length of Space Shuttle in the $j$th direction

Values of $L_i$ for the six bands are given in Table 2-2 while the characteristic lengths, $\ell_j$, are presented in Table 2-3.

TABLE 2-2. SUMMARY OF TURBULENCE PARAMETERS IN DISCRETE ALTITUDE BANDS

| BAND # | LOWER LIMIT (m) | UPPER LIMIT (m) | TURBULENCE LENGTH SCALE $L_i$(m) | | | TIME INTERVAL $T_i$ (dimensionless) | | | MAXIMUM FREQUENCY $\Omega_{i1max}$(dimensionless) | | |
|---|---|---|---|---|---|---|---|---|---|---|---|
| | | | i = 1 | i = 2 | i = 3 | i = 1 | i = 2 | i = 3 | i = 1 | i = 2 | i = 3 |
| 1 | 0 | 30 | 43.4 | 27.7 | 16.8 | .6520 | 1.022 | 1.684 | 4.818 | 3.075 | 1.866 |
| 2 | 30 | 304.8 | 196 | 190 | 192 | .1444 | .1489 | .1474 | 21.76 | 21.10 | 21.32 |
| 3 | 304.8 | 762 | 300 | 300 | 300 | .09432 | .09432 | .09432 | 33.310 | 33.310 | 33.310 |
| 4 | 762 | 10,000 | 533 | 533 | 533 | .05309 | .05309 | .05309 | 59.180 | 59.180 | 59.180 |
| 5 | 10,000 | 27,000 | 20,000 | 20,000 | 1,230 | .004266 | .004266 | .06785 | 736.5 | 736.5 | 46.30 |
| 6 | 27,000 | 120,000 | 200,000 | 200,000 | 11,800 | .003511 | .003511 | .05950 | 894.9 | 894.9 | 52.80 |

NOTE: i = 1 applies to $u_1$-gust
i = 2 applies to $u_2$-gust and $\partial u_2/\partial x_i$ gust gradients
i = 3 applies to $u_3$-gust and $\partial u_3/\partial x_1$ gust gradients

TABLE 2-3. CHARACTERISTIC DIMENSIONS OF THE SPACE SHUTTLE [8]

| Characteristic Length | Magnitude (ft) | (m) | Explanation |
|---|---|---|---|
| $\ell_1$ | 39.56 | 12.06 | mean aerodynamic chord |
| $\ell_2$ | 39.05 | 11.9 | 1/2 wingspan |
| $\ell_3$ | 10.95 | 3.34 | 1/2 fuselage thickness |

In the case of $\Omega_{i1max}$ special consideration must be given to the *dimensional* frequencies corresponding to the *dimensionless* limits. The dimensional frequency limit satisfies the relation

$$f_{1max} = \Omega_{i1max} V/(2\pi a L_i) \tag{2-4}$$

where

$V$ = vehicle velocity

The maximum dimensional frequency which the Space Shuttle simulators are capable of handling is 4 hertz. Thus any higher frequencies should be excluded from the simulation. For this reason the dimensionless frequency limit $\Omega_{i1max}$ must satisfy the relation

$$\Omega_{i1max} = \min(aL_i/\ell_1, 2\pi a L_i f_{1max}/V) \tag{2-5}$$

where

$f_{1max}$ = 4 hertz

Values of $\Omega_{i1max}$ based on Eq (2-5) are included in Table 2-2.

### 2.3.2 One-Dimensional Spectra

There are six spectra of primary interest for turbulence simulation, as indicated in Table 2-4. Based on second-order numerical integration, the six corresponding three-dimensional gust and gust gradient spectral relations, as given by Eqs (2-1) and (2-2), were integrated over $\Omega_3$ and $\Omega_2$ (with the appropriate upper limits). The resulting one-dimensional spectra for all altitude bands are presented in Appendix A. These spectra were used in establishing the impulse response functions associated with digital filter simulation processes described in subsection 2.4.

TABLE 2-4. TYPES OF SIMULATED TURBULENCE

| Type | Corresponding Spectrum | Comments |
|---|---|---|
| $u_1$ | $\Phi_{11}$ | longitudinal gust |
| $u_2$ | $\Phi_{22}$ | transverse gust |
| $u_3$ | $\Phi_{33}$ | vertical gust |
| $\partial u_2/\partial x_1$ | $\Phi_{22/11}$ | yaw |
| $\partial u_3/\partial x_1$ | $\Phi_{33/11}$ | pitch |
| $\partial u_3/\partial x_2$ | $\Phi_{33/22}$ | roll |

### 2.3.3 Dimensionless Energy Content

The total dimensionless energy content of each one-dimensional spectra in each altitude band was established by integrating the corresponding spectra over the appropriate finite limits, indicated in Table 2-2. The resulting energy content is presented in Table 2-5. As might be expected

TABLE 2-5. DIMENSIONLESS ENERGY CONTENT FOR GUSTS AND GUST GRADIENTS

| ALTITUDE BAND | SPECTRUM | | | | | |
|---|---|---|---|---|---|---|
| | $\Phi_{11}$ | $\Phi_{22}$ | $\Phi_{33}$ | $\Phi_{22/11}$ | $\Phi_{33/11}$ | $\Phi_{33/22}$ |
| 1 | .6225 | .5010 | .2752 | .5877 | .1525 | .1557 |
| 2 | .8595 | .8560 | .8383 | 13.147 | 12.171 | 12.308 |
| 3 | .8956 | .8952 | .8809 | 24.767 | 22.643 | 22.890 |
| 4 | .9298 | .9296 | .9197 | 54.123 | 49.527 | 50.060 |
| 5 | .9977 | .9953 | .9251 | 1740. | 41.71 | 95.62 |
| 6 | 1.000 | .9973 | .9363 | 2309. | 52.08 | 391.6 |

the total dimensionless energy content of each of the turbulent gust series is less than unity. The dimensionless energy* content for each gust gradient, however, is not limited in such a manner and range as high has 391.6. For both gusts and gust gradients the total energy content increases with altitude because of similar increases in the limits of integration.

## 2.4 DIGITAL FILTER SIMULATION

As suggested in subsection 2.1, simulated turbulence, Y(t), can be interpreted as the response or output of a control system [9] with double-sided response functions, h(t), subject to an input consisting of Gaussian white noise I(t). This response can be represented by the convolution integral

$$Y(t) = \int_{-\infty}^{\infty} h(\tau)\, I(t-\tau)\, d\tau \qquad (2\text{-}6)$$

Based on filter theory the double-sided spectrum, $\Phi_{DY}(\Omega)$, of the simulated turbulence satisfies the relation

$$\Phi_{DY}(\Omega_1) = H(\Omega_1)H^*(\Omega_1)\Phi_{DI}(\Omega_1) \qquad (2\text{-}7)$$

where $H(\Omega_1) = F[h(t)]$

$\Phi_{DI}(\Omega_1)$ = double-sided power spectrum for white noise

Generally the standard deviation of any white noise signal has a value of unity. Furthermore in most practical situations the white noise is defined to occur over some interval extending from $-\Omega_{1max}$ to $+\Omega_{1max}$. For this case**,

$$\Phi_{DI}(\Omega_1) = \frac{1}{2\Omega_{1max}}$$

$$= \frac{T}{2\pi} \qquad (2\text{-}8)$$

---

*Actually the term "energy" is not precise when dealing with gust gradients.

**The subscript, i, normally applied to the variables $\Omega_{1max}$ and T, has been suppressed in Eqs (2-8) through (2-13) for simplicity.

where

$T$ = time interval associated with generation process ($=\pi/\Omega_{1max}$)

By substitution,

$$\Phi_{DY}(\Omega_1) = H(\Omega_1)H^*(\Omega_1)\frac{T}{2\pi} \tag{2-9}$$

If $H(\Omega_1)$ is limited to real values,

$$\Phi_{DY}(\Omega_1) = H^2(\Omega_1)\frac{T}{2\pi} \tag{2-10}$$

Rearrangement of Eq (2-10) yields

$$H(\Omega_1) = \sqrt{\frac{2\pi}{T}\Phi_{DY}(\Omega_1)} \tag{2-11}$$

Then based on the definition of the inverse Fourier transform, the double-sided impulse response function h(t) can be expressed as

$$\begin{aligned} h(t) &= F^{-1}[H(\Omega_1)] \\ &= \int_{-\infty}^{\infty}\sqrt{\frac{2\pi}{T}\Phi_{DY}(\Omega_1)}\cos(\Omega_1 t)\,d\Omega_1 \\ &= 2\int_{0}^{\infty}\sqrt{\frac{2\pi}{T}\Phi_{DY}(\Omega_1)}\cos(\Omega_1 t)\,d\Omega_1 \\ &= 2\int_{0}^{\infty}\sqrt{\frac{2\pi}{T}\frac{\Phi_Y(\Omega_1)}{2}}\cos(\Omega_1 t)\,d\Omega_1 \\ &= 2\sqrt{\frac{\pi}{T}}\int_{0}^{\infty}\sqrt{\Phi_Y(\Omega_1)}\cos(\Omega_1 t)\,d\Omega_1 \end{aligned} \tag{2-12}$$

where

$\Phi_Y(\Omega_1)$ = single-sided spectrum of Y(t)

The single-sided spectra tabulated in Appendix A correspond to $\Phi_Y(\Omega_1)$

The discrete version of the convolution integral given in Eq (2-6) yields

$$Y(k) = \sum_{j=-N}^{+N} h(j)\, I(k-j)\, T \qquad (2\text{-}13)$$

where

$Y(k)$ = discrete sampled turbulence output

$h(j)$ = discrete double-sided impulse response function $h(jT)$

$I(k)$ = discrete sampled white noise input

Eq (2-13) represents the basic, non-recursive relation for the generation of simulated turbulence*. The impulse response functions $h(t)$ were evaluated by means of second-order numerical integration of Eq (2-12) using the six spectra from Appendix A. In carrying out this evaluation some maximum value of t must be established, corresponding to the value of N for Eq (2-13), and replacing the infinite limit of Eq (2-6). As discussed in Appendix B this maximum time limit determines the minimum frequency, $\Omega_{i1max}$, for which the corresponding spectrum is accurately simulated.

The values of dimensionless time increment, $T_i$, used for the six altitude bands are included in Table 2-2 and are based on the values of $\Omega_{imax}$ shown in the same table. Thus the Nyquist generation frequencies $\Omega_{iNG}$ for the simulated turbulence correspond to the upper frequency limits for $\Omega_{i1}$ as computed by Eq (2-5) for each altitude band.

---

*In certain references [9,11] to correct for the "effect of digitizing" the series represented by Eq (2-13) has been divided by $\sqrt{T}$. This process can be seen to be dimensionally incorrect and actually results from the use of a white noise spectrum with unit strength instead of a strength of $T/2\pi$.

## 2.5 EFFECTS OF DIGITIZATION

The effects of digitization in turbulence simulation have been considered by a number of investigators [9-12]. As a result of these studies two basic digitization effects have been generally identified.

The first effect results from the assumption of a white noise specrrum with unit *strength* instead of unit *power*, noted in subsection 2.4. To correct for such an "effect" the proposed procedure is to divide the series approximation of the convolution integral by $\sqrt{T}$. This "effect" disappears when the white noise spectrum has unit power.

The second effect involves the *tapering* of the spectrum of simulated white noise, $\Phi_I'$, in the vicinity of the Nyquist generation frequency, $\Omega_{NG}$. Some investigators [10,12] have considered it necessary, because of the tapering effect, to generate the simulated turbulence time series at a rate from four to ten times the rate at which the series will be sampled.

The second effect arises from the discrete processes associated with both the generation and sampling of the simulated turbulence. In the case of discrete white noise with unit variance, the time series involved is basically a train of step functions as shown in Figure 2-1. The autocorrelation function of the train of step functions depicted in Figure 2-1 can

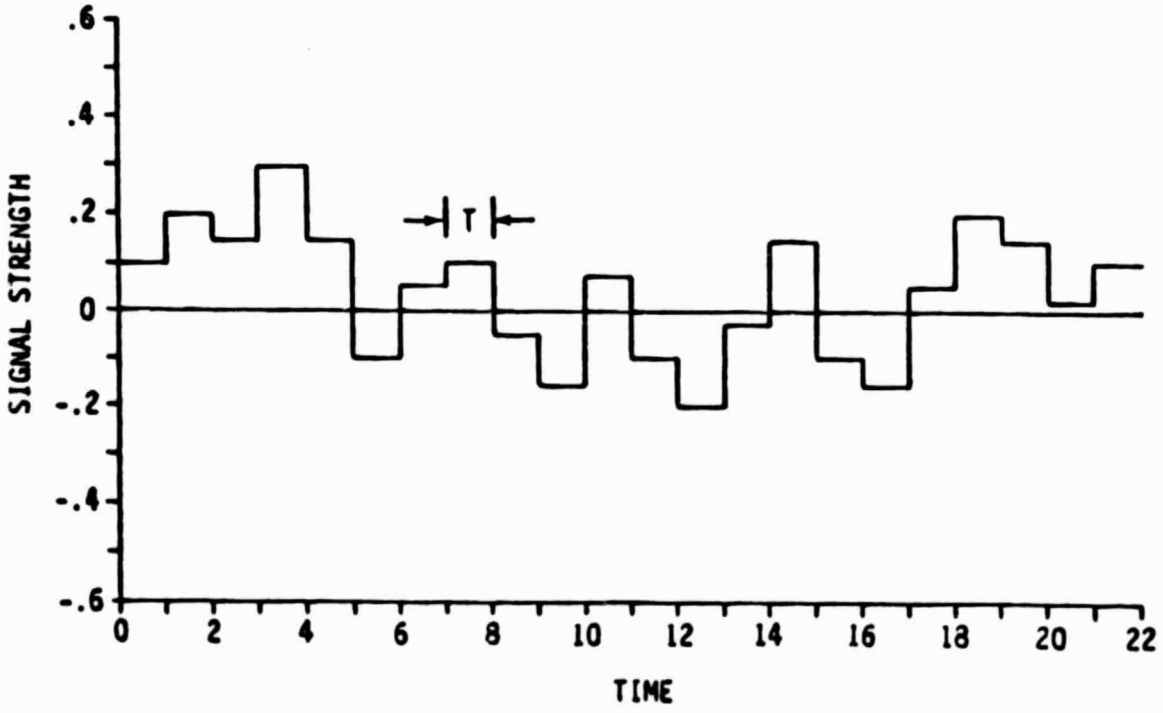


Figure 2-1. Discrete White Noise Series

be shown to be

$$R_{DI}(\tau) = \begin{cases} 1 - \frac{|\tau|}{T_G} & (|\tau| \leq T_G) \\ 0 & (|\tau| > T_G) \end{cases} \tag{2-14}$$

The corresponding double-sided power spectrum by definition is

$$\begin{aligned} \Phi'_{DI}(\Omega) &\equiv \mathcal{F}[R_{DI}(\tau)] \\ &= \frac{T_G}{2\pi} \frac{\sin^2(\Omega T_G/2)}{(\Omega T_G/2)^2} \\ &= \frac{1}{2\Omega_{NG}} \frac{\sin^2(\Omega\pi/2\Omega_{NG})}{(\Omega\pi/2\Omega_{NG})^2} \end{aligned} \tag{2-15}$$

The single-sided version of this power spectrum is shown in Figure 2-2.

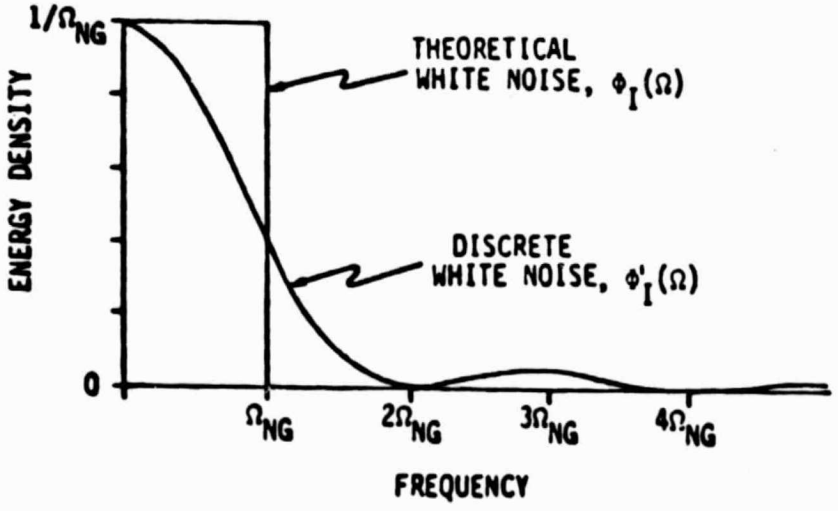


Figure 2-2. White Noise Spectra

Theoretical white noise, by definition, is characterized by a uniform power spectral distribution. In order to avoid infinite power, such a spectral distribution is normally restricted to the frequency band $(-\Omega_{NG} \leq \Omega \leq \Omega_{NG})$ for a double-sided spectrum. For a signal with unit power the spectral density function for such white noise is

$$\Phi_{DI}(\Omega) = \begin{cases} \frac{1}{2\Omega_{NG}} & (-\Omega_{NG} \leq \Omega \leq \Omega_{NG}) \\ 0 & (\Omega_{NG} < |\Omega|) \end{cases} \tag{2-16}$$

Such a theoretical distribution in single-sided form is also shown in Figure 2-2.

It is important to note that the two power spectra shown in Figure 2-2 are both normalized and thus

$$\int_{-\infty}^{\infty} \Phi_{DI}(\Omega)d\Omega = \int_{-\infty}^{\infty} \Phi'_{DI}(\Omega)d\Omega \tag{2-17}$$

$$= 1$$

The theoretical spectrum is basically a rectangular pulse function while the discrete spectrum is characterized by tapering. The difference between these two spectra is generally considered the basis for the second digitization effect.

The preceding descriptions of the two spectra $\Phi_I(\Omega)$ and $\Phi_{DI}(\Omega)$ are based purely on mathematical theory. To observe such spectra in reality the corresponding time series would have to be sampled with an infinitesimal sampling interval. Actually, finite sampling intervals, $T_S$, must be used but this finite (or discrete) sampling process results in *aliasing*. The aliased spectrum, $\Phi^+(\Omega)$, based on the finite sampling process, is related to the original spectrum according to the relation [13]

$$\phi^{+}(\Omega) = \sum_{k=-\infty}^{\infty} \phi(\Omega+2k\Omega_{NS}) \tag{2-18}$$

where

$\Omega_{NS}$ = Nyquist sampling frequency $(=\pi/T_S)$

For the case of the discrete white noise

$$\phi'^{+}_{DI}(\Omega) = \sum_{k=-\infty}^{\infty} \phi'_{DI}(\Omega+2k\Omega_{NS})$$

$$= \frac{1}{2\Omega_{NG}} \sum_{k=-\infty}^{\infty} \frac{\sin^2[(\Omega+2k\Omega_{NS})\pi/2\Omega_{NG}]}{[(\Omega+2k\Omega_{NS})\pi/2\Omega_{NG}]^2} \tag{2-19}$$

Numerical evaluation of this series has been carried out for $\Omega_{NG} = 100$ with various ratios of $\Omega_{NS}/\Omega_{NG}$, including .5, 1, 2, and 4. The resulting aliased spectra are presented in Figure 2-3. It is important to note that the figure indicates that

$$\phi'^{+}_{DI}(\Omega) = \left\{ \begin{array}{ll} \frac{1}{2\Omega_{NG}} & (-\Omega_{NG} \leq \Omega \leq \Omega_{NG}) \\ 0 & (\Omega_{NG} < |\Omega|) \end{array} \right\} (\Omega_{NG} = \Omega_{NS}) \tag{2-20}$$

In this case, by comparision with $\Phi_{DI}(\Omega)$,

$$\phi'^{+}_{DI}(\Omega) = \Phi_{DI}(\Omega) \qquad (\Omega_{NG} = \Omega_{NS}) \tag{2-21}$$

Thus for white noise *the aliasing due to discrete sampling exactly offsets the tapering due to discrete generation when the sampling frequency equals the generation frequency*. Based on this fundamental point, it is clear that in the simulation of white noise no tapering of the spectrum occurs as long as the sampling rate equals the generation rate. Under most conditions this equality is automatically satisfied.

The process of convolving the white noise with the appropriate impulse response function is also carried out in a discrete manner. The process involves selecting (or sampling) values of the white noise signal and the impulse response function at equal intervals in time and then approximating the convolution integral by a summation of products. It is important to note that the discrete sampling of both the white noise and the impulse response function normally occurs at the same rate as the generation rate for the white noise. Thus the resulting spectra for the sampled discrete white noise, as previously shown, will be uniform. According to the convolution theorem, the spectrum of the output signal equals the spectrum of the input white noise multiplied by the product of the Fourier transform of the impulse response function and its complex conjugate. Thus, as previously noted in subsection 2.4, for a continuous signal,

$$\Phi_{DY}(\Omega) = \Phi_{DI}(\Omega)H(\Omega)H^*(\Omega) \tag{2-22}$$

The Fourier transform $H(\Omega)$ for the *continuous* impulse function, $h(t)$, is

$$H(\Omega) = F[h(t)]$$

$$= \sqrt{\frac{2\pi}{T}\,\Phi_{DY}(\Omega)} \tag{2-23}$$

The corresponding output spectrum for a discrete signal would be

$$\Phi'_{DY}(\Omega) = \Phi'_{DI}(\Omega)H'(\Omega)H'^*(\Omega) \tag{2-24}$$

The Fourier transform $H'(\Omega)$ of the *discrete* impulse response function, $h'(t)$, is

$$H'(\Omega) = F[h'(t)] \tag{2-25}$$

Based on the preceding development, for cases in which the sampling frequency equals the generation frequency, any difference between the discrete turbulence spectrum and the continuous spectrum apparently originates because of some difference between $H(\Omega)$ and $H'(\Omega)$.

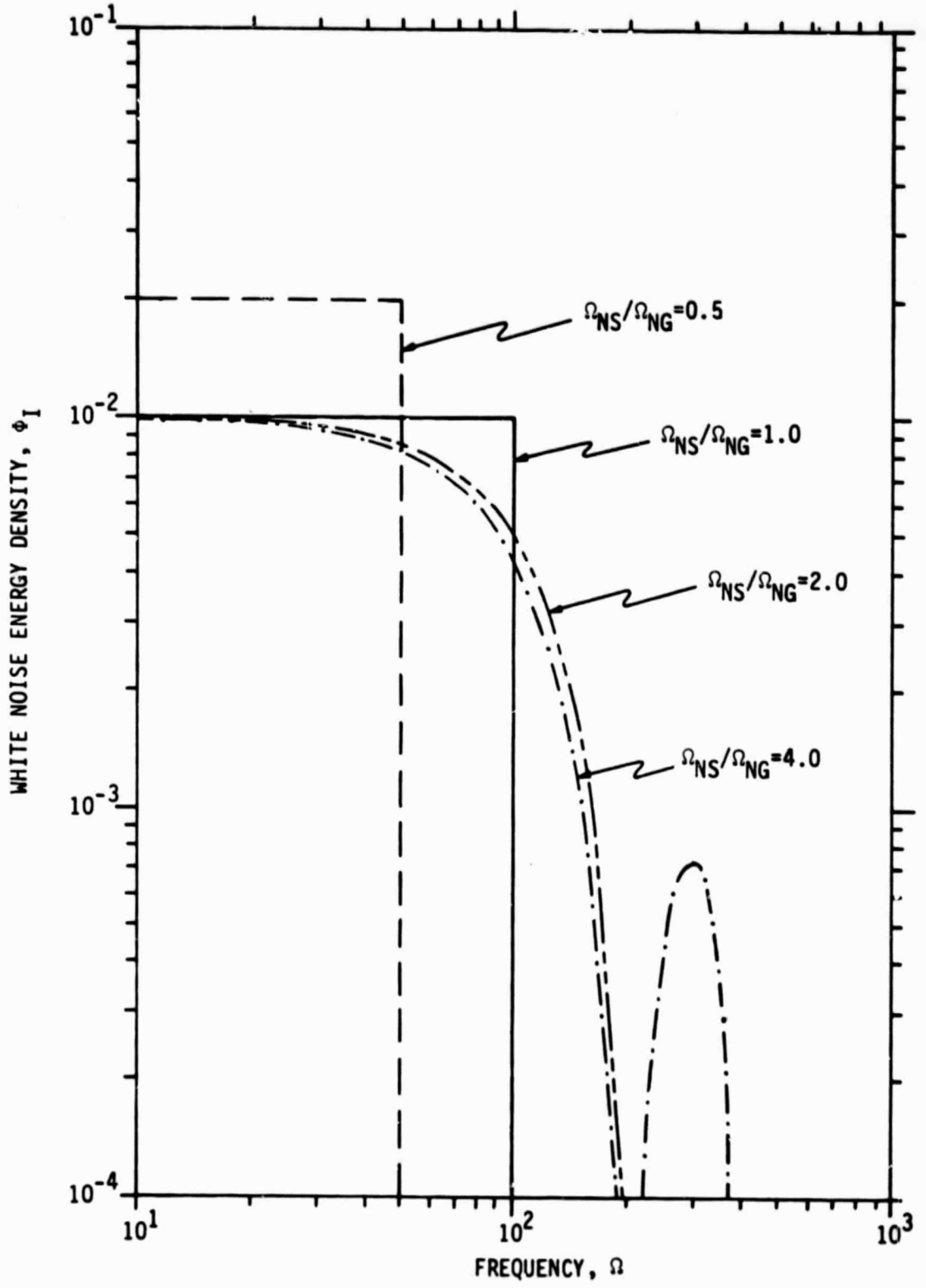


Figure 2-3. Effects of Aliasing on White Noise Spectrum

# 3. SIMULATED TURBULENCE TAPES

The turbulence generation procedure described in Section 2 has been used to generate six dimensionless simulated turbulence time series which are stored on magnetic tapes as summarized in Table 3-1. The appropriate procedures for using the tapes are described elsewhere [1]. Subsection 3.1 provides a description of the results of validating the tapes while subsection 3.2 presents an explanation of the process for converting from dimensionless to dimensional values.

TABLE 3-1. INDEX OF SHUTTLE SIMULATED TURBULENCE TAPES (SSTT)

| Tape | Time Series | Comments |
|---|---|---|
| SSTT-1 | $u_1$ - gust | longitudinal gust |
| SSTT-2 | $u_2$ - gust | transverse gust |
| SSTT-3 | $u_3$ - gust | vertical gust |
| SSTT-4 | $\partial u_2/\partial x_1$ - gust gradient | yaw |
| SSTT-5 | $\partial u_3/\partial x_1$ - gust gradient | pitch |
| SSTT-6 | $\partial u_3/\partial x_2$ - gust gradient | roll |

## 3.1 VALDIATION OF SIMULATED TURBULENCE

A spectral analysis of each of the dimensionless time series has been carried out by means of a Fast Fourier Transform FFT4 [14]. The results, which are presented in Appendix C, demonstrate that the simulated turbulence possesses the proper von Karman spectral characteristics.

All of the dimensionless time series have also been analyzed statistically to determine the gust and gust gradient probability density functions. As shown in Appendix D the results of these analyses indicate that both the simulated gusts and gust gradients are normally distributed, with near-zero means and standard deviations consistent with the energy content presented in Table 2-5.

## 3.2 CONVERSION TO DIMENSIONAL VALUES

The dimensionless time series on each tape must be converted to dimensional form before actual use in a simulation exercise. The conversion process generally involves multiplication and/or division by the appropriate turbulence parameters. For dimensionless gusts, $u_i$, the corresponding standard deviation, $\sigma_i$, should be used. Thus

$$u_i^* = \sigma_i u_i \tag{3-1}$$

where

$u_i^*$ = dimensional gust

For dimensionless gust gradient, $\frac{\partial u_i}{\partial x_j}$, the parameters $\sigma_i$ and $L_j$ are used. Thus

$$\frac{\partial u_i^*}{\partial x_j^*} = \frac{\sigma_i}{L_j} \frac{\partial u_i}{\partial x_j} \tag{3-2}$$

where

$\partial u_i^*/\partial x_j^*$ = dimensional gust gradient

In the case of dimensionless time it is necessary to develop the procedures for converting both from dimensionless to dimensional form and also to dimensionless from dimensional. In proceeding from dimensionless to dimensional time the dimensionless time step, $T_i$, represents the basic unit to be converted. The conversion involves the vehicle velocity, V, and the turbulence scale, $L_i$. Thus

$$\Delta t_i^* = aL_iT_i/V \tag{3-3}$$

where

$\Delta t_i^*$ = dimensional time step

It is important to note that because both $L_i$ and V vary with altitude, the resulting dimensional time step $\Delta t_i^*$ is not a constant. To obtain dimensional time, $t_i^*$, a summation process is involved as follows:

$$t_{iN}^* = \sum_{n=1}^{N} \Delta t_{in}^* \qquad (3\text{-}4)$$

$$= aT_i \sum_{n=1}^{N} L_{in}/V_n$$

where

$$L_{in} = L_i(Z_n)$$

$$V_n = V(Z_n)$$

$$Z_n = \text{altitude at } n\text{th step}$$

In converting to dimensionless from dimensional time the basic unit, the dimensional time step, $\delta t^*$, will normally be a constant. The corresponding dimensionless time interval, $T_{im}$, will be

$$T_{im} = \frac{V_m \delta t^*}{aL_{im}} \qquad (3\text{-}5)$$

The total dimensionless time, $t_{iM}$, will be

$$t_{iM} = \sum_{m=1}^{M} T_{im}$$

$$= \sum_{m=1}^{M} \frac{V_m \delta t^*}{aL_{im}}$$

$$= \frac{\delta t^*}{a} \sum_{m=1}^{M} V_m/L_{im} \qquad (3\text{-}6)$$

The dimensionless time, $t_{iM}$, corresponds to some M' dimensionless time intervals, $T_i$, plus some fractional interval, T', as follows:

$$t_{iM} = M'T_i + T' \tag{3-7}$$

where

$$0 \leq T' \leq T_i$$

Thus the number of dimensionless time intervals, M', can be computed as

$$M' = \text{Int}(t_{iM}/T_i)$$

$$= \text{Int}\left(\frac{\delta t^*}{aT_i} \sum_{m=1}^{M} V_m/L_{im}\right) \tag{3-8}$$

where

Int( ) = integer value of ( )

The fractional interval, T', can be computed by the relation

$$T' = t_{iM} - M'T_i \tag{3-9}$$

The interpolation process will involve interpolating between $t_{iM'}$ and $t_{iM'+1}$ at the point $t_{iM}$ as shown in Figure 3-1.

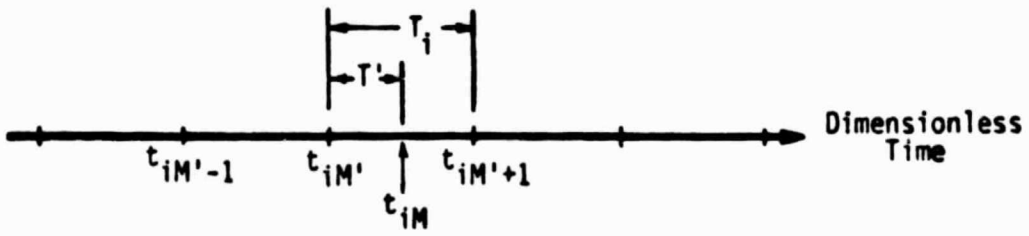


Figure 3-1. Relationship Between $t_{iM}$, $t_{iM'}$, and $t_{iM'+1}$

In the conversion to or from dimensional values three parameters are required: standard deviation, integral scale of turbulence, and vehicle

speed. The variation of the turbulence standard deviation, $\sigma_i$, with altitude was presented in Table 2-1. The same table contains the turbulence scale, $L_i$, as a function of altitude. The vehicle speed, V, is a function of altitude but also may vary from one trajectory to another. Table 3-2 provides *representative* values of V as a function of altitude.

TABLE 3-2. VARIATION OF SHUTTLE SPEED WITH ALTITUDE [12]

| ALTITUDE (m) | V (m/sec) |
|---|---|
| 100 | 152 |
| 300 | 156 |
| 500 | 158 |
| 2000 | 170 |
| 4000 | 188 |
| 6000 | 200 |
| 8000 | 240 |
| 10000 | 300 |
| 20000 | 500 |
| 40000 | 1928 |
| 60000 | 4695 |
| 80000 | 7468 |
| 100000 | 7521 |
| 120000 | 7510 |

# 4. CONCLUSIONS AND RECOMMENDATIONS

By means of a non-recursive discrete generation process, based on a von Karman spectral model with finite upper limits, dimensionless simulated turbulence time series have been developed and stored on six magnetic tapes. Longitudinal, transverse, and vertical gusts are simulated as well as the gust gradients associated with yaw, pitch, and roll. For each gust or gust gradient six separate time series (corresponding to the six altitude bands extending from ground level to 120,000 meters) have been stored on each tape.

The results of spectral analyses of each tape reveals that the simulated turbulence possesses the appropriate von Karman spectral characteristics. Statistical analyses of the tapes indicate that both the simulated gust and gust gradients are normally distributed with near-zero means. Furthermore the standard deviation of each series is constant with the theoretical energy content.

The Shuttle Simulated Turbulence Tapes (SSTT) are now ready for actual use for simulating turbulence at altitudes up to 120,000 meters.

## 5. REFERENCES CITED


1. Tatom, Frank B., and Smith, S. Ray, "Space Shuttle Simulation Model", *EAI-TR-80-003A*, Final Report, Engineering Analysis, Inc., Huntsville, AL, November 17, 1980.

2. Tatom, Frank B., and King, Richard L., "Turbulence Simulation Mechanization for Space Shuttle Orbiter Dynamics and Control Studies", *SAI-78-766-HU*, Summary Report, Science Applications, Inc., Huntsville, AL, December 1977.

3. Scharf, L. L., Wells, M. K., and Winn, C. B., "The Simulation of Atmospheric Turbulence for Space Shuttle Response Studies", Colorado State University, Fort Collins, Colorado.

4. Tatom, Frank B., and Smith, S. Ray, "Shuttle Orbiter Turbulence Simulation Model Development", *EAI-TR-79-001*, Summary Report, Engineering Analysis, Inc., Huntsville, AL, March 27, 1979.

5. Tatom, Frank B., and Smith, S. Ray, "Atmospheric Turbulence Simulation for Shuttle Orbiter", *EAI-TR-79-004*, Engineering Analysis, Inc., Huntsville, AL, August 31, 1979.

6. Space Shuttle Program: Natural Environment Design Requirements. Appendix 10.10, Space Shuttle Flight and Ground Specification, Level II Program Definition and Requirements, *JSC 07700*, Vol. X, Revision B. NASA-Lyndon B. Johnson Space Center, Houston, TX, August 18, 1975.

7. Etkin, B., *Dynamics of Atmospheric Flight*, John Wiley & Sons, Inc., New York, 1972.

8. Rockwell International Corporation, "Aerodynamic Design Substantiation Report", *SD74-SH-0206*, 1974.

9. Fichtl, George H., Perlmutter, Morris, and Frost, Walter, "Monte Carlo Turbulence Simulation", *Handbook of Turbulence*, Vol. 1, Chapter 14, Plenum Publishing Corporation, 1977.

10. Neuman, Frank, and Foster, John D., "Investigation of a Digital Automatic Aircraft Landing System in Turbulence", *NASA TN D-66066*, National Aeronautics and Space Administration, Washington, D.C.. October 1970.

11. Perlmutter, Morris, "Stochastic Simulation of Ocean Waves for SRB Simulation", *NASA TR-230-1446*, George C. Marshall Space Flight Center, Marshall Space Flight Center, Alabama, May 1975.

12. Fichtl, George H., "A Technique for Simulating Turbulence for Aerospace Vehicle Flight Simulation Studies", *NASA TM 78141*, George C. Marshall Space Flight Center, Marshall Space Flight Center, Alabama, November 1977.

13. Bloomfield, Peter, *Fourier Analysis of Time Series: An Introduction*, John Wiley & Sons, Inc., 1976.

14. Maynard, Harry W., "An Evaluation of Ten Fast Fourier Transform (FFT) Programs", *Research and Development Technical Report ECOM-5476*, U.S. Army Electronics Command, Fort Monmouth, NJ, March 1973.

# APPENDIX A

## DIMENSIONLESS VON KARMAN SPECTRA WITH FINITE UPPER LIMITS

For each altitude band, the three-dimensional spectral model for gusts, as given by Eq (2-1), and the three-dimensional model for gust gradients, as given by Eq (2-2), have been integrated with respect to $\Omega_2$ and $\Omega_3$ over the finite limits calculated according to Eq (2-3). The six resulting one-dimensional spectra are presented in Tables A-1 through A-6, corresponding to Altitude Bands #1 through 6 respectively. These spectra were used in the numerical evaluation of the impulse response functions described in subsection 2.4.

TABLE A-1. DIMENSIONLESS SPECTRUM FOR ALTITUDE BAND # 1

| i=1 | | i=2 | | | i=3 | | | |
|---|---|---|---|---|---|---|---|---|
| DIMENSIONLESS WAVE NUMBER | DIMENSIONLESS SPECTRUM | DIMENSIONLESS WAVE NUMBER | DIMENSIONLESS SPECTRUM | | DIMENSIONLESS WAVE NUMBER | DIMENSIONLESS SPECTRUM | | |
| $\Omega_1$ | $\Phi_{11}$ | $\Omega_1$ | $\Phi_{22}$ | $\Phi_{22/11}$ | $\Omega_1$ | $\Phi_{33}$ | $\Phi_{33/11}$ | $\Phi_{33/22}$ |
| 0.00000 | .44171 | 0.00000 | .21638 | 0.0000 | 0.00000 | .14709 | 0.0000 | .10454 |
| .01000 | .44167 | .01000 | .21640 | .12070E-04 | .01000 | .14711 | .82051E-05 | .10454 |
| .02000 | .44156 | .02000 | .21646 | .48293E-04 | .02000 | .14717 | .32834E-04 | .10454 |
| .03000 | .44136 | .03000 | .21656 | .10871E-03 | .03000 | .14728 | .73930E-04 | .10453 |
| .04000 | .44108 | .04000 | .21670 | .19339E-03 | .04000 | .14742 | .13156E-03 | .10452 |
| .05000 | .44072 | .05000 | .21688 | .30242E-03 | .05000 | .14761 | .20582E-03 | .10451 |
| .06000 | .44029 | .06000 | .21710 | .43591E-03 | .06000 | .14783 | .29684E-03 | .10450 |
| .07000 | .43978 | .07000 | .21735 | .59402E-03 | .07000 | .14810 | .40475E-03 | .10449 |
| .08000 | .43919 | .09000 | .21765 | .77691E-03 | .09000 | .14840 | .52974E-03 | .10447 |
| .09000 | .43852 | .09000 | .21797 | .98475E-03 | .09000 | .14875 | .67200E-03 | .10445 |
| .10000 | .43779 | .10000 | .21834 | .12178E-02 | .10000 | .14912 | .83173E-03 | .10443 |
| .19000 | .42785 | .19000 | .22295 | .44890E-02 | .19000 | .15395 | .30997E-02 | .10413 |
| .28000 | .41270 | .28000 | .22910 | .10018E-01 | .28000 | .16046 | .70165E-02 | .10355 |
| .37000 | .39348 | .37000 | .23541 | .17975E-01 | .37000 | .16726 | .12771E-01 | .10262 |
| .46000 | .37147 | .46000 | .24056 | .28391E-01 | .46000 | .17305 | .20423E-01 | .10127 |
| .55000 | .34786 | .55000 | .24364 | .41107E-01 | .55000 | .17692 | .29850E-01 | .99460E-01 |
| .64000 | .32369 | .64000 | .24419 | .55787E-01 | .64000 | .17841 | .40757E-01 | .97177E-01 |
| .73000 | .29979 | .73000 | .24217 | .71978E-01 | .73000 | .17745 | .52742E-01 | .94454E-01 |
| .82000 | .27671 | .82000 | .23780 | .89181E-01 | .82000 | .17429 | .65360E-01 | .91349E-01 |
| .91000 | .25485 | .91000 | .23148 | .10692 | .91000 | .16928 | .78187E-01 | .87935E-01 |
| 1.00000 | .23441 | 1.00000 | .22368 | .12476 | 1.00000 | .16290 | .90859E-01 | .84293E-01 |
| 1.38186 | .16426 | 1.20755 | .20235 | .16457 | 1.08653 | .15596 | .10263 | .80650E-01 |
| 1.76373 | .11685 | 1.41510 | .17955 | .20054 | 1.17305 | .14827 | .11379 | .76934E-01 |
| 2.14559 | .84980E-01 | 1.62264 | .15772 | .23161 | 1.25958 | .14039 | .12423 | .73201E-01 |
| 2.52745 | .63167E-01 | 1.83019 | .13792 | .25766 | 1.34611 | .13246 | .13387 | .69498E-01 |
| 2.90931 | .47895E-01 | 2.03774 | .12048 | .27903 | 1.43264 | .12463 | .14267 | .65865E-01 |
| 3.29117 | .36960E-01 | 2.24529 | .10535 | .29623 | 1.51916 | .11702 | .15063 | .62331E-01 |
| 3.67304 | .28969E-01 | 2.45284 | .92322E-01 | .30980 | 1.60569 | .10971 | .15776 | .58919E-01 |
| 4.05490 | .23021E-01 | 2.66039 | .81130E-01 | .32026 | 1.69222 | .10274 | .16410 | .55643E-01 |
| 4.43676 | .18521E-01 | 2.86793 | .71517E-01 | .32809 | 1.77875 | .96161E-01 | .16969 | .52514E-01 |
| 4.81862 | .15066E-01 | 3.07548 | .63248E-01 | .33366 | 1.86527 | .89967E-01 | .17458 | .49538E-01 |

TABLE A-2. DIMENSIONLESS SPECTRUM FOR ALTITUDE BAND # 2

| i=1 | | i=2 | | | i=3 | | | |
|---|---|---|---|---|---|---|---|---|
| DIMENSIONLESS WAVE NUMBER | DIMENSIONLESS SPECTRUM | DIMENSIONLESS WAVE NUMBER | DIMENSIONLESS SPECTRUM | | DIMENSIONLESS WAVE NUMBER | DIMENSIONLESS SPECTRUM | | |
| $\Omega_1$ | $\phi_{11}$ | $\Omega_1$ | $\phi_{22}$ | $\phi_{22/11}$ | $\Omega_1$ | $\phi_{33}$ | $\phi_{33/11}$ | $\phi_{33/22}$ |
| 0.00000 | .47130 | 0.00000 | .23623 | 0.0000 | 0.00000 | .23492 | 0.0000 | 1.4485 |
| .01000 | .47126 | .01000 | .23625 | .13177E-04 | .01000 | .23494 | .13104E-04 | 1.4484 |
| .02000 | .47114 | .02000 | .23632 | .52702E-04 | .02000 | .23500 | .52429E-04 | 1.4484 |
| .03000 | .47094 | .03000 | .23642 | .11868E-03 | .03000 | .23510 | .11802E-03 | 1.4484 |
| .04000 | .47066 | .04000 | .23656 | .21110E-03 | .04000 | .23524 | .20993E-03 | 1.4483 |
| .05000 | .47030 | .05000 | .23674 | .33010E-03 | .05000 | .23543 | .32827E-03 | 1.4483 |
| .06000 | .46986 | .06000 | .23696 | .47579E-03 | .06000 | .23565 | .47315E-03 | 1.4482 |
| .07000 | .46934 | .07000 | .23722 | .64831E-03 | .07000 | .23590 | .64472E-03 | 1.4481 |
| .08000 | .46875 | .09000 | .23751 | .84783E-03 | .08000 | .23620 | .84314E-03 | 1.4480 |
| .09000 | .46808 | .09000 | .23785 | .10745E-02 | .09000 | .23653 | .10686E-02 | 1.4479 |
| .10000 | .46733 | .10000 | .23821 | .13286E-02 | .10000 | .23690 | .13213E-02 | 1.4478 |
| .19000 | .45731 | .19000 | .24289 | .48905E-02 | .19000 | .24158 | .48641E-02 | 1.4461 |
| .28000 | .44205 | .28000 | .24914 | .10894E-01 | .28000 | .24783 | .10837E-01 | 1.4433 |
| .37000 | .42269 | .37000 | .25555 | .19512E-01 | .37000 | .25423 | .19412E-01 | 1.4393 |
| .46000 | .40053 | .46000 | .26079 | .30778E-01 | .46000 | .25948 | .30624E-01 | 1.4341 |
| .55000 | .37679 | .55000 | .26395 | .44533E-01 | .55000 | .26264 | .44312E-01 | 1.4276 |
| .64000 | .35250 | .64000 | .26455 | .60437E-01 | .64000 | .26324 | .60138E-01 | 1.4198 |
| .73000 | .32848 | .73000 | .26254 | .78033E-01 | .73000 | .26123 | .77645E-01 | 1.4110 |
| .82000 | .30531 | .82000 | .25817 | .96823E-01 | .82000 | .25687 | .96333E-01 | 1.4010 |
| .91000 | .28336 | .91000 | .25185 | .11632 | .91000 | .25055 | .11572 | 1.3902 |
| 1.00000 | .26282 | 1.00000 | .24404 | .13611 | 1.00000 | .24274 | .13539 | 1.3785 |
| 1.90000 | .13051 | 1.90000 | .15244 | .30693 | 1.90000 | .15117 | .30438 | .42978 |
| 2.80000 | .74892E-01 | 2.80000 | .95050E-01 | .41563 | 2.80000 | .93828E-01 | .41028 | .38314 |
| 3.70000 | .48151E-01 | 3.70000 | .63922E-01 | .48809 | 3.70000 | .62751E-01 | .47914 | .34244 |
| 4.60000 | .33430E-01 | 4.60000 | .45937E-01 | .54097 | 4.60000 | .44718E-01 | .52776 | .30684 |
| 5.50000 | .24468E-01 | 5.50000 | .34499E-01 | .58207 | 5.50000 | .33429E-01 | .56401 | .27562 |
| 6.40000 | .18602E-01 | 6.40000 | .26931E-01 | .61526 | 6.40000 | .25906E-01 | .59182 | .24817 |
| 7.30000 | .14550E-01 | 7.30000 | .21622E-01 | .64267 | 7.30000 | .20637E-01 | .61339 | .22400 |
| 8.20000 | .11636E-01 | 8.20000 | .17747E-01 | .66558 | 8.20000 | .16801E-01 | .63009 | .20265 |
| 9.10000 | .94722E-02 | 9.10000 | .14828E-01 | .68486 | 9.10000 | .13919E-01 | .64286 | .18376 |
| 10.00000 | .78233E-02 | 10.00000 | .12570E-01 | .70107 | 10.00000 | .11697E-01 | .65240 | .16700 |

TABLE A-2. DIMENSIONLESS SPECTRUM FOR ALTITUDE BAND # 2 (continued)

| i=1 | | i=2 | | | i=3 | | | |
|---|---|---|---|---|---|---|---|---|
| DIMENSION-LESS WAVE NUMBER | DIMENSIONLESS SPECTRUM | DIMENSION-LESS WAVE NUMBER | DIMENSIONLESS SPECTRUM | | DIMENSION-LESS WAVE NUMBER | DIMENSIONLESS SPECTRUM | | |
| $\Omega_1$ | $\phi_{11}$ | $\Omega_1$ | $\phi_{22}$ | $\phi_{22/11}$ | $\Omega_1$ | $\phi_{33}$ | $\phi_{33/11}$ | $\phi_{33/22}$ |
| 11.17616 | .62035E-02 | 11.10954 | .10423E-01 | .71748 | 11.13174 | .95590E-02 | .66066 | 1.2419 |
| 12.35231 | .50019E-02 | 12.21907 | .87718E-02 | .73047 | 12.26348 | .79344E-02 | .66555 | 1.1067 |
| 13.52846 | .40891E-02 | 13.32861 | .74735E-02 | .74052 | 13.39522 | .66722E-02 | .66774 | .98783 |
| 14.70461 | .33820E-02 | 14.43814 | .64331E-02 | .74796 | 14.52696 | .56732E-02 | .66776 | .88476 |
| 15.88077 | .28252E-02 | 15.54768 | .55859E-02 | .75312 | 15.65870 | .49701E-02 | .66602 | .79506 |
| 17.05692 | .23807E-02 | 16.65722 | .48867E-02 | .75624 | 16.79045 | .42156E-02 | .66287 | .71653 |
| 18.23307 | .20217E-02 | 17.76675 | .43030E-02 | .75757 | 17.92219 | .36760E-02 | .65857 | .64736 |
| 19.40922 | .17287E-02 | 18.87629 | .39107E-02 | .75731 | 19.05393 | .32265E-02 | .65334 | .58615 |
| 20.58537 | .14875E-02 | 19.98582 | .33919E-02 | .75566 | 20.18567 | .28486E-02 | .64737 | .53180 |
| 21.76152 | .12872E-02 | 21.09536 | .30329E-02 | .75279 | 21.31741 | .25283E-02 | .64031 | .48338 |

TABLE A-3. DIMENSIONLESS SPECTRUM FOR ALTITUDE BAND # 3

| i=1 | | i=2 | | | i=3 | | | |
|---|---|---|---|---|---|---|---|---|
| DIMENSIONLESS WAVE NUMBER | DIMENSIONLESS SPECTRUM | DIMENSIONLESS WAVE NUMBER | DIMENSIONLESS SPECTRUM | | DIMENSIONLESS WAVE NUMBER | DIMENSIONLESS SPECTRUM | | |
| $\Omega_1$ | $\phi_{11}$ | $\Omega_1$ | $\phi_{22}$ | $\phi_{22/11}$ | $\Omega_1$ | $\phi_{33}$ | $\phi_{33/11}$ | $\phi_{33/22}$ |
| 0.00000 | .47307 | 0.00000 | .23698 | 0.0000 | 0.00000 | .23610 | 0.0000 | 1.8735 |
| .01000 | .47303 | .01000 | .23700 | .13213E-04 | .01000 | .23612 | .13169E-04 | 1.8735 |
| .02000 | .47291 | .02000 | .23706 | .52987E-04 | .02000 | .23618 | .52691E-04 | 1.8735 |
| .03000 | .47271 | .03000 | .23716 | .11905E-03 | .03000 | .23628 | .11861E-03 | 1.8735 |
| .04000 | .47243 | .04000 | .23730 | .21177E-03 | .04000 | .23642 | .21098E-03 | 1.8734 |
| .05000 | .47207 | .05000 | .23748 | .33114E-03 | .05000 | .23660 | .32991E-03 | 1.8734 |
| .06000 | .47164 | .06000 | .23770 | .47728E-03 | .06000 | .23682 | .47551E-03 | 1.8733 |
| .07000 | .47112 | .07000 | .23796 | .65034E-03 | .07000 | .23708 | .64793E-03 | 1.8732 |
| .08000 | .47052 | .08000 | .23826 | .85047E-03 | .08000 | .23737 | .84733E-03 | 1.8731 |
| .09000 | .46985 | .09000 | .23859 | .10779E-02 | .09000 | .23771 | .10739E-02 | 1.8730 |
| .10000 | .46910 | .10000 | .23896 | .13328E-02 | .10000 | .23807 | .13279E-02 | 1.8729 |
| .19000 | .45909 | .19000 | .24363 | .49055E-02 | .19000 | .24275 | .48878E-02 | 1.8712 |
| .28000 | .44382 | .28000 | .24988 | .10927E-01 | .28000 | .24900 | .10888E-01 | 1.8683 |
| .37000 | .42447 | .37000 | .25629 | .19569E-01 | .37000 | .25541 | .19502E-01 | 1.8643 |
| .46000 | .40230 | .46000 | .26153 | .30966E-01 | .46000 | .26065 | .30762E-01 | 1.8589 |
| .55000 | .37855 | .55000 | .26469 | .44658E-01 | .55000 | .26381 | .44510E-01 | 1.8524 |
| .64000 | .35426 | .64000 | .26529 | .60606E-01 | .64000 | .26441 | .60406E-01 | 1.8446 |
| .73000 | .33025 | .73000 | .26328 | .78253E-01 | .73000 | .26241 | .77995E-01 | 1.8356 |
| .82000 | .30707 | .82000 | .25891 | .97099E-01 | .82000 | .25804 | .96774E-01 | 1.8255 |
| .91000 | .28512 | .91000 | .25259 | .11666 | .91000 | .25172 | .11626 | 1.8146 |
| 1.00000 | .26458 | 1.00000 | .24477 | .13652 | 1.00000 | .24391 | .13604 | 1.8029 |
| 1.90000 | .13222 | 1.90000 | .15316 | .30838 | 1.90000 | .15235 | .30675 | 1.6640 |
| 2.80000 | .76534E-01 | 2.80000 | .95746E-01 | .11867 | 2.80000 | .94999E-01 | .41541 | 1.5254 |
| 3.70000 | .49712E-01 | 3.70000 | .64591E-01 | .49319 | 3.70000 | .63915E-01 | .48803 | 1.4019 |
| 4.60000 | .34905E-01 | 4.60000 | .46476E-01 | .54851 | 4.60000 | .45866E-01 | .54131 | 1.2930 |
| 5.50000 | .25860E-01 | 5.50000 | .35110E-01 | .59237 | 5.50000 | .34555E-01 | .58301 | 1.1965 |
| 6.40000 | .19915E-01 | 6.40000 | .27517E-01 | .62864 | 6.40000 | .27002E-01 | .61688 | 1.1101 |
| 7.30000 | .15792E-01 | 7.30000 | .22187E-01 | .65945 | 7.30000 | .21699E-01 | .64496 | 1.0323 |
| 8.20000 | .12812E-01 | 8.20000 | .18295E-01 | .68612 | 8.20000 | .17825E-01 | .66848 | .96174 |
| 9.10000 | .10588E-01 | 9.10000 | .15363E-01 | .70955 | 9.10000 | .14902E-01 | .68827 | .89746 |
| 10.00000 | .88940E-02 | 10.00000 | .13095E-01 | .73035 | 10.00000 | .12639E-01 | .70496 | .83868 |

TABLE A-3. DIMENSIONLESS SPECTRUM FOR ALTITUDE BAND # 3 (continued)

| i=1 | | i=2 | | | i=3 | | | |
|---|---|---|---|---|---|---|---|---|
| DIMENSIONLESS WAVE NUMBER | DIMENSIONLESS SPECTRUM | DIMENSIONLESS WAVE NUMBER | DIMENSIONLESS SPECTRUM | | DIMENSIONLESS WAVE NUMBER | DIMENSIONLESS SPECTRUM | | |
| $\Omega_1$ | $\phi_{11}$ | $\Omega_1$ | $\phi_{22}$ | $\phi_{22/11}$ | $\Omega_1$ | $\phi_{33}$ | $\phi_{33/11}$ | $\phi_{33/22}$ |
| 12.33085 | .59522E-02 | 12.33085 | .91368E-02 | .77485 | 12.33085 | .86903E-02 | .73698 | .70768 |
| 14.66170 | .42188E-02 | 14.66170 | .67485E-02 | .80912 | 14.66170 | .63163E-02 | .75731 | .60124 |
| 16.99254 | .31087E-02 | 16.99254 | .51879E-02 | .83551 | 16.99254 | .47784E-02 | .76956 | .51377 |
| 19.32339 | .23566E-02 | 19.32339 | .41069E-02 | .85530 | 19.32339 | .37255E-02 | .77588 | .44127 |
| 21.65423 | .18260E-02 | 21.65423 | .33244E-02 | .86943 | 21.65423 | .29733E-02 | .77762 | .38079 |
| 23.98508 | .14401E-02 | 23.98508 | .27383E-02 | .87863 | 23.98508 | .24177E-02 | .77575 | .33006 |
| 26.31592 | .11528E-02 | 26.31592 | .22875E-02 | .88358 | 26.31592 | .19961E-02 | .77102 | .28731 |
| 28.64677 | .93463E-03 | 28.64677 | .19333E-02 | .88489 | 28.64677 | .16693E-02 | .76404 | .25114 |
| 30.97761 | .76627E-03 | 30.97761 | .16499E-02 | .88309 | 30.97761 | .14113E-02 | .75533 | .22040 |
| 33.30846 | .63450E-03 | 33.30846 | .14200E-02 | .87869 | 33.30846 | .12045E-02 | .74533 | .19419 |

TABLE A-4. DIMENSIONLESS SPECTRUM FOR ALTITUDE BAND # 4

| i=1 | | i=2 | | | i=3 | | | |
|---|---|---|---|---|---|---|---|---|
| DIMENSIONLESS WAVE NUMBER $\Omega_1$ | DIMENSIONLESS SPECTRUM $\phi_{11}$ | DIMENSIONLESS WAVE NUMBER $\Omega_1$ | DIMENSIONLESS SPECTRUM $\phi_{22}$ | $\phi_{22/11}$ | DIMENSIONLESS WAVE NUMBER $\Omega_1$ | DIMENSIONLESS SPECTRUM $\phi_{33}$ | $\phi_{33/11}$ | $\phi_{33/22}$ |
| 0.00000 | .47403 | 0.00000 | .23725 | 0.0000 | 0.00000 | .23678 | 0.0000 | 2.5189 |
| .01000 | .47399 | .01000 | .23727 | .13234E-04 | .01000 | .23680 | .13207E-04 | 2.5189 |
| .02000 | .47387 | .02000 | .23733 | .52949E-04 | .02000 | .23686 | .52843E-04 | 2.5189 |
| .03000 | .47367 | .03000 | .23744 | .11919E-03 | .03000 | .23696 | .11895E-03 | 2.5188 |
| .04000 | .47339 | .04000 | .23758 | .21201E-03 | .04000 | .23710 | .21159E-03 | 2.5188 |
| .05000 | .47303 | .05000 | .23776 | .33152E-03 | .05000 | .23728 | .33086E-03 | 2.5187 |
| .06000 | .47259 | .06000 | .23798 | .47784E-03 | .06000 | .23750 | .47689E-03 | 2.5187 |
| .07000 | .47208 | .07000 | .23824 | .65109E-03 | .07000 | .23776 | .64979E-03 | 2.5186 |
| .08000 | .47148 | .08000 | .23853 | .85146E-03 | .08000 | .23805 | .84976E-03 | 2.5185 |
| .09000 | .47081 | .09000 | .23886 | .10791E-02 | .09000 | .23839 | .10770E-02 | 2.5184 |
| .10000 | .47006 | .10000 | .23923 | .13343E-02 | .10000 | .23875 | .13317E-02 | 2.5182 |
| .19000 | .46005 | .19000 | .24391 | .49111E-02 | .19000 | .24343 | .49014E-02 | 2.5165 |
| .28000 | .44478 | .28000 | .25016 | .10939E-01 | .28000 | .24968 | .10918E-01 | 2.5136 |
| .37000 | .42542 | .37000 | .25656 | .19590E-01 | .37000 | .25609 | .19554E-01 | 2.5096 |
| .46000 | .40326 | .46000 | .26181 | .30899E-01 | .46000 | .26133 | .30843E-01 | 2.5042 |
| .55000 | .37951 | .55000 | .26496 | .44704E-01 | .55000 | .26449 | .44625E-01 | 2.4976 |
| .64000 | .35522 | .64000 | .26556 | .60669E-01 | .64000 | .26509 | .60561E-01 | 2.4897 |
| .73000 | .33120 | .73000 | .26356 | .78336E-01 | .73000 | .26309 | .78196E-01 | 2.4807 |
| .82000 | .30803 | .82000 | .25919 | .97204E-01 | .82000 | .25872 | .97028E-01 | 2.4706 |
| .91000 | .28607 | .91000 | .25287 | .11679 | .91000 | .25240 | .11658 | 2.4595 |
| 1.00000 | .26553 | 1.00000 | .24505 | .13668 | 1.00000 | .24459 | .13642 | 2.4476 |
| 1.90000 | .13316 | 1.90000 | .15344 | .30895 | 1.90000 | .15301 | .30809 | 2.3076 |
| 2.80000 | .77440E-01 | 2.80000 | .96030E-01 | .41992 | 2.80000 | .95655E-01 | .41828 | 2.1670 |
| 3.70000 | .50590E-01 | 3.70000 | .64876E-01 | .49537 | 3.70000 | .64556E-01 | .49292 | 2.0408 |
| 4.60000 | .35757E-01 | 4.60000 | .46762E-01 | .55188 | 4.60000 | .46492E-01 | .54870 | 1.9286 |
| 5.50000 | .26687E-01 | 5.50000 | .35394E-01 | .59716 | 5.50000 | .35166E-01 | .59331 | 1.8291 |
| 6.40000 | .20721E-01 | 6.40000 | .27797E-01 | .63503 | 6.40000 | .27599E-01 | .63052 | 1.7372 |
| 7.30000 | .16579E-01 | 7.30000 | .22463E-01 | .66765 | 7.30000 | .22284E-01 | .66234 | 1.6543 |
| 8.20000 | .13584E-01 | 8.20000 | .18567E-01 | .69632 | 8.20000 | .18398E-01 | .68999 | 1.5782 |
| 9.10000 | .11346E-01 | 9.10000 | .15631E-01 | .72195 | 9.10000 | .15465E-01 | .71430 | 1.5077 |
| 10.00000 | .96272E-02 | 10.00000 | .13361E-01 | .74519 | 10.00000 | .13194E-01 | .73587 | 1.4423 |

TABLE A-4. DIMENSIONLESS SPECTRUM FOR ALTITUDE BAND #4 (continued)

| i=1 | | i=2 | | | i=3 | | | |
|---|---|---|---|---|---|---|---|---|
| DIMENSIONLESS WAVE NUMBER $\Omega_1$ | DIMENSIONLESS SPECTRUM $\Phi_{11}$ | DIMENSIONLESS WAVE NUMBER $\Omega_1$ | DIMENSIONLESS SPECTRUM $\Phi_{22}$ | $\Phi_{22/11}$ | DIMENSIONLESS WAVE NUMBER $\Omega_1$ | DIMENSIONLESS SPECTRUM $\Phi_{33}$ | $\Phi_{33/11}$ | $\Phi_{33/22}$ |
| 14.91760 | .47319E-02 | 14.91780 | .68101E-02 | .84529 | 14.91780 | .66213E-02 | .82185 | 1.1506 |
| 19.83561 | .27884E-02 | 19.83561 | .41833E-02 | .91802 | 19.83561 | .39942E-02 | .87653 | .93474 |
| 24.75341 | .18076E-02 | 24.75341 | .28455E-02 | .97244 | 24.75341 | .26687E-02 | .91204 | .76806 |
| 29.67122 | .12440E-02 | 29.67122 | .20620E-02 | 1.0125 | 29.67122 | .19004E-02 | .93314 | .63641 |
| 34.58902 | .89257E-03 | 34.58902 | .15598E-02 | 1.0408 | 34.58902 | .14135E-02 | .94319 | .53107 |
| 39.50682 | .66065E-03 | 39.50682 | .12170E-02 | 1.0594 | 39.50682 | .10854E-02 | .94489 | .44603 |
| 44.42462 | .50109E-03 | 44.42462 | .97201E-03 | 1.0699 | 44.42462 | .85433E-03 | .94040 | .37691 |
| 49.34242 | .38773E-03 | 49.34242 | .79069E-03 | 1.0737 | 49.34242 | .69586E-03 | .93136 | .32040 |
| 54.26022 | .30509E-03 | 54.26022 | .65279E-03 | 1.0719 | 54.26022 | .55968E-03 | .91905 | .27394 |
| 59.17802 | .24355E-03 | 59.17802 | .54558E-03 | 1.0657 | 59.17802 | .46304E-03 | .90444 | .23553 |

TABLE A-5. DIMENSIONLESS SPECTRUM FOR ALTITUDE BAND # 5

| i=1 | | i=2 | | | i=3 | | | |
|---|---|---|---|---|---|---|---|---|
| DIMENSIONLESS WAVE NUMBER | DIMENSIONLESS SPECTRUM | DIMENSIONLESS WAVE NUMBER | DIMENSIONLESS SPECTRUM | | DIMENSIONLESS WAVE NUMBER | DIMENSIONLESS SPECTRUM | | |
| $\Omega_1$ | $\phi_{11}$ | $\Omega_1$ | $\phi_{22}$ | $\phi_{22/11}$ | $\Omega_1$ | $\phi_{33}$ | $\phi_{33/11}$ | $\phi_{33/22}$ |
| 0.00000 | .47517 | 0.00000 | .23758 | 0.0000 | 0.00000 | .23748 | 0.0000 | 3.7129 |
| .01000 | .47513 | .01000 | .23760 | .13252E-04 | .01000 | .23750 | .13246E-04 | 3.7129 |
| .02000 | .47501 | .02000 | .23766 | .53023E-04 | .02000 | .23756 | .52999E-04 | 3.7129 |
| .03000 | .47481 | .03000 | .23777 | .11935E-03 | .03000 | .23766 | .11930E-03 | 3.7128 |
| .04000 | .47453 | .04000 | .23791 | .21231E-03 | .04000 | .23780 | .21221E-03 | 3.7128 |
| .05000 | .47417 | .05000 | .23809 | .33198E-03 | .05000 | .23798 | .33183E-03 | 3.7127 |
| .06000 | .47373 | .06000 | .23831 | .47850E-03 | .06000 | .23820 | .47828E-03 | 3 27 |
| .07000 | .47321 | .07000 | .23857 | .65200E-03 | .07000 | .23946 | .65170E-03 | 3 26 |
| .08000 | .47262 | .08000 | .23886 | .85264E-03 | .08000 | .23876 | .85226E-03 | 3.7125 |
| .09000 | .47195 | .09000 | .23919 | .10806E-02 | .09000 | .23909 | .10801E-02 | 3.7124 |
| .10000 | .47120 | .10000 | .23956 | .13362E-02 | .10000 | .23946 | .13356E-02 | 3.7122 |
| .19000 | .46118 | .19000 | .24424 | .49177E-02 | .19000 | .24413 | .49156E-02 | 3.7105 |
| .28000 | .44591 | .28000 | .25049 | .10953E-01 | .28000 | .25038 | .10949E-01 | 3.7076 |
| .37000 | .42656 | .37000 | .25689 | .19615E-01 | .37000 | .25679 | .19607E-01 | 3.7035 |
| .46000 | .40439 | .46000 | .26214 | .30938E-01 | .46000 | .26203 | .30925E-01 | 3.6981 |
| .55000 | .38064 | .55000 | .26530 | .44760E-01 | .55000 | .26519 | .44742E-01 | 3.6915 |
| .64000 | .35635 | .64000 | .26590 | .60745E-01 | .64000 | .26579 | .60720E-01 | 3.6835 |
| .73000 | .33232 | .73000 | .26389 | .78434E-01 | .73000 | .26378 | .78403E-01 | 3.6744 |
| .82000 | .30915 | .82000 | .25952 | .97328E-01 | .82000 | .25941 | .97288E-01 | 3.6643 |
| .91000 | .28719 | .91000 | .25320 | .11695 | .91000 | .25309 | .11690 | 3.6531 |
| 1.00000 | .26664 | 1.00000 | .24539 | .13686 | 1.00000 | .24528 | .13680 | 3.6411 |
| 1.90000 | .13421 | 1.90000 | .15378 | .30964 | 1.90000 | .15368 | .30942 | 3.4999 |
| 2.80000 | .78413E-01 | 2.80000 | .96383E-01 | .42146 | 2.80000 | .96276E-01 | .42099 | 3.3575 |
| 3.70000 | .51470E-01 | 3.70000 | .65236E-01 | .49812 | 3.70000 | .65129E-01 | .49730 | 3.2290 |
| 4.60000 | .36545E-01 | 4.60000 | .47121E-01 | .55612 | 4.60000 | .47014E-01 | .55486 | 3.1143 |
| 5.50000 | .27395E-01 | 5.50000 | .35746E-01 | .60310 | 5.50000 | .35639E-01 | .60129 | 3.0113 |
| 6.40000 | .21364E-01 | 6.40000 | .28134E-01 | .64274 | 6.40000 | .28028E-01 | .64030 | 2.9178 |
| 7.30000 | .17173E-01 | 7.30000 | .22781E-01 | .67709 | 7.30000 | .22674E-01 | .67392 | 2.8323 |
| 8.20000 | .14143E-01 | 8.20000 | .18863E-01 | .70741 | 8.20000 | .18756E-01 | .70340 | 2.7534 |
| 9.10000 | .11882E-01 | 9.10000 | .15904E-01 | .73457 | 9.10000 | .15797E-01 | .72964 | 2.6801 |
| 10.00000 | .10150E-01 | 10.00000 | .13612E-01 | .75923 | 10.00000 | .13506E-01 | .75328 | 2.6116 |

TABLE A-5. DIMENSIONLESS SPECTRUM FOR ALTITUDE BAND #5 (continued)

| i=1 | | i=2 | | | i=3 | | | |
|---|---|---|---|---|---|---|---|---|
| DIMENSIONLESS WAVE NUMBER | DIMENSIONLESS SPECTRUM | DIMENSIONLESS WAVE NUMBER | DIMENSIONLESS SPECTRUM | | DIMENSIONLESS WAVE NUMBER | DIMENSIONLESS SPECTRUM | | |
| $\Omega_1$ | $\phi_{11}$ | $\Omega_1$ | $\phi_{22}$ | $\phi_{22/11}$ | $\Omega_1$ | $\phi_{33}$ | $\phi_{33/11}$ | $\phi_{33/22}$ |
| 19.00000 | .35256E-02 | 19.00000 | .46734E-02 | .94138 | 19.00000 | .45700E-02 | .92017 | 2.0899 |
| 28.00001 | .18620E-02 | 28.00001 | .24617E-02 | 1.0765 | 28.00001 | .23585E-02 | 1.0313 | 1.7286 |
| 37.00001 | .11733E-02 | 37.00001 | .15535E-02 | 1.1862 | 37.00001 | .14531E-02 | 1.1095 | 1.4530 |
| 46.00001 | .81625E-03 | 46.00001 | .10839E-02 | 1.2793 | 46.00001 | .98684E-03 | 1.1647 | 1.2335 |
| 55.00001 | .60468E-03 | 55.00001 | .80633E-03 | 1.3604 | 55.00001 | .71299E-03 | 1.2030 | 1.0545 |
| 64.00002 | .46794E-03 | 64.00002 | .62698E-03 | 1.4324 | 64.00002 | .53764E-03 | 1.2283 | .90651 |
| 73.00002 | .37409E-03 | 73.00002 | .50358E-03 | 1.4968 | 73.00002 | .41833E-03 | 1.2434 | .78297 |
| 82.00002 | .30690E-03 | 82.00002 | .41460E-03 | 1.5549 | 82.00002 | .33340E-03 | 1.2504 | .67918 |
| 91.00002 | .25687E-03 | 91.00002 | .34810E-03 | 1.6078 | 91.00002 | .27084E-03 | 1.2509 | .59154 |
| 100.00002 | .21879E-03 | 100.00002 | .29698E-03 | 1.6564 | 100.00002 | .22347E-03 | 1.2464 | .51721 |
| 190.00003 | .74480E-04 | 190.00003 | .10056E-03 | 2.0248 | 103.65648 | .20748E-03 | 1.2434 | .49029 |
| 280.00006 | .38592E-04 | 280.00006 | .52567E-04 | 2.2986 | 107.31294 | .19302E-03 | 1.2398 | .46505 |
| 370.00006 | .23822E-04 | 370.00006 | .32946E-04 | 2.5156 | 110.96941 | .17991E-03 | 1.2357 | .44138 |
| 460.00006 | .16216E-04 | 460.00006 | .22822E-04 | 2.6935 | 114.62587 | .16798E-03 | 1.2310 | .41918 |
| 550.00012 | .11742E-04 | 550.00012 | .16851E-04 | 2.8430 | 118.28233 | .15711E-03 | 1.2260 | .39833 |
| 640.00012 | .88702E-05 | 640.00012 | .13003E-04 | 2.9705 | 121.93880 | .14718E-03 | 1.2206 | .37874 |
| 730.00012 | .69113E-05 | 730.00012 | .10363E-04 | 3.0800 | 125.59526 | .13808E-03 | 1.2148 | .36032 |
| 820.00012 | .55136E-05 | 820.00012 | .84644E-05 | 3.1744 | 129.25174 | .12973E-03 | 1.2088 | .34301 |
| 910.00012 | .44814E-05 | 910.00012 | .70491E-05 | 3.2558 | 132.90820 | .12205E-03 | 1.2025 | .32671 |
| 1000.00010 | .36980E-05 | 1000.00010 | .59628E-05 | 3.3257 | 136.56467 | .11497E-03 | 1.1959 | .31137 |
| 1000.00020 | .36980E-05 | 1000.00020 | .59628E-05 | 3.3257 | | | | |
| 1122.05660 | .29062E-05 | 1122.05660 | .48484E-05 | 3.4046 | | | | |
| 1244.11300 | .23262E-05 | 1244.11300 | .40164E-05 | 3.4673 | | | | |
| 1366.16940 | .18901E-05 | 1366.16940 | .33773E-05 | 3.5158 | | | | |
| 1488.22580 | .15551E-05 | 1488.22580 | .28750E-05 | 3.5515 | | | | |
| 1610.28220 | .12931E-05 | 1610.28220 | .24726E-05 | 3.5760 | | | | |
| 1732.33860 | .10852E-05 | 1732.33860 | .21450E-05 | 3.5903 | | | | |
| 1854.39500 | .91821E-06 | 1854.39500 | .18748E-05 | 3.5957 | | | | |
| 1976.45140 | .78255E-06 | 1976.45140 | .16492E-05 | 3.5932 | | | | |
| 2098.50780 | .67131E-06 | 2098.50780 | .14591E-05 | 3.5838 | | | | |
| 2220.56400 | .57933E-06 | 2220.56400 | .12974E-05 | 3.5682 | | | | |

TABLE A-6. DIMENSIONLESS SPECTRUM FOR ALTITUDE BAND # 6

| i=1 | | i=2 | | | i=3 | | | |
|---|---|---|---|---|---|---|---|---|
| DIMENSIONLESS WAVE NUMBER | DIMENSIONLESS SPECTRUM | DIMENSIONLESS WAVE NUMBER | DIMENSIONLESS SPECTRUM | | DIMENSIONLESS WAVE NUMBER | DIMENSIONLESS SPECTRUM | | |
| $\Omega_1$ | $\phi_{11}$ | $\Omega_1$ | $\phi_{22}$ | $\phi_{22/11}$ | $\Omega_1$ | $\phi_{33}$ | $\phi_{33/11}$ | $\phi_{33/22}$ |
| 0.00000 | .47517 | 0.00000 | .23758 | 0.0000 | 0.00000 | .23758 | 0.0000 | 9.2415 |
| .01000 | .47513 | .01000 | .23760 | .13252E-04 | .01000 | .23760 | .13252E-04 | 9.2415 |
| .02000 | .47501 | .02000 | .23767 | .53023E-04 | .02000 | .23766 | .53022E-04 | 9.2415 |
| .03000 | .47481 | .03000 | .23777 | .11935E-03 | .03000 | .23776 | .11935E-03 | 9.2414 |
| .04000 | .47453 | .04000 | .23791 | .21231E-03 | .04000 | .23791 | .21231E-03 | 9.2414 |
| .05000 | .47417 | .05000 | .23809 | .33198E-03 | .05000 | .23809 | .33198E-03 | 9.2413 |
| .06000 | .47373 | .06000 | .23831 | .47850E-03 | .06000 | .23831 | .47849E-03 | 9.2413 |
| .07000 | .47322 | .07000 | .23857 | .65200E-03 | .07000 | .23856 | .65199E-03 | 9.2412 |
| .08000 | .47262 | .08000 | .23886 | .85264E-03 | .08000 | .23886 | .85264E-03 | 9.2411 |
| .09000 | .47195 | .09000 | .23920 | .10806E-02 | .09000 | .23919 | .10806E-02 | 9.2410 |
| .10000 | .47120 | .10000 | .23956 | .13362E-02 | .10000 | .23956 | .13361E-02 | 9.2408 |
| .19000 | .46118 | .19000 | .24424 | .49177E-02 | .19000 | .24424 | .49177E-02 | 9.2391 |
| .28000 | .44592 | .28000 | .25049 | .10953E-01 | .28000 | .25049 | .10953E-01 | 9.2362 |
| .37000 | .42656 | .37000 | .25689 | .19615E-01 | .37000 | .25689 | .19615E-01 | 9.2321 |
| .46000 | .40439 | .46000 | .26214 | .30938E-01 | .46000 | .26214 | .30937E-01 | 9.2267 |
| .55000 | .38064 | .55000 | .26530 | .44760E-01 | .55000 | .26529 | .44760E-01 | 9.2200 |
| .64000 | .35635 | .64000 | .26590 | .60745E-01 | .64000 | .26589 | .60744E-01 | 9.2121 |
| .73000 | .33233 | .73000 | .26389 | .78435E-01 | .73000 | .26389 | .78434E-01 | 9.2030 |
| .82000 | .30915 | .82000 | .25952 | .97329E-01 | .82000 | .25952 | .97328E-01 | 9.1928 |
| .91000 | .28719 | .91000 | .25320 | .11695 | .91000 | .25320 | .11694 | 9.1816 |
| 1.00000 | .26665 | 1.00000 | .24539 | .13686 | 1.00000 | .24538 | .13686 | 9.1697 |
| 1.90000 | .13421 | 1.90000 | .15378 | .30964 | 1.90000 | .15378 | .30964 | 9.0282 |
| 2.80000 | .78414E-01 | 2.80000 | .96384E-01 | .42146 | 2.80000 | .96382E-01 | .42145 | 8.8855 |
| 3.70000 | .51471E-01 | 3.70000 | .65237E-01 | .49812 | 3.70000 | .65234E-01 | .49810 | 8.7566 |
| 4.60000 | .36547E-01 | 4.60000 | .47122E-01 | .55613 | 4.60000 | .47119E-01 | .55610 | 8.6413 |
| 5.50000 | .27396E-01 | 5.50000 | .35746E-01 | .60311 | 5.50000 | .35744E-01 | .60307 | 8.5376 |
| 6.40000 | .21365E-01 | 6.40000 | .28135E-01 | .64276 | 6.40000 | .28133E-01 | .64270 | 8.4433 |
| 7.30000 | .17175E-01 | 7.30000 | .22781E-01 | .67711 | 7.30000 | .22779E-01 | .67704 | 8.3568 |
| 8.20000 | .14145E-01 | 8.20000 | .18863E-01 | .70743 | 8.20000 | .18861E-01 | .70734 | 8.2769 |
| 9.10000 | .11884E-01 | 9.10000 | .15905E-01 | .73459 | 9.10000 | .15902E-01 | .73448 | 8.2024 |
| 10.00000 | .10152E-01 | 10.00000 | .13613E-01 | .75926 | 10.00000 | .13611E-01 | .75913 | 8.1326 |

TABLE A-6. DIMENSIONLESS SPECTRUM FOR ALTITUDE BAND #6 (continued)

| i=1 | | i=2 | | | i=3 | | | |
|---|---|---|---|---|---|---|---|---|
| DIMENSIONLESS WAVE NUMBER | DIMENSIONLESS SPECTRUM | DIMENSIONLESS WAVE NUMBER | DIMENSIONLESS SPECTRUM | | DIMENSIONLESS WAVE NUMBER | DIMENSIONLESS SPECTRUM | | |
| $\Omega_1$ | $\Phi_{11}$ | $\Omega_1$ | $\Phi_{22}$ | $\Phi_{22/11}$ | $\Omega_1$ | $\Phi_{33}$ | $\Phi_{33/11}$ | $\Phi_{33/22}$ |
| 19.00000 | .35273E-02 | 19.00000 | .46760E-02 | .94149 | 19.00000 | .98722E-04 | .94100 | 7.5915 |
| 28.00001 | .18637E-02 | 28.00001 | .24623E-02 | 1.0767 | 28.00001 | .50774E-04 | 1.0756 | 7.1997 |
| 37.00001 | .11750E-02 | 37.00001 | .15541E-02 | 1.1866 | 37.00001 | .31210E-04 | 1.1848 | 6.8838 |
| 46.00001 | .81798E-03 | 46.00001 | .10845E-02 | 1.2799 | 46.00001 | .21153E-04 | 1.2770 | 6.6155 |
| 55.00001 | .60640E-03 | 55.00001 | .80690E-03 | 1.3614 | 55.00001 | .15252E-04 | 1.3573 | 6.3806 |
| 64.00002 | .46966E-03 | 64.00002 | .62756E-03 | 1.4337 | 64.00002 | .11478E-04 | 1.4281 | 6.1709 |
| 73.00002 | .37581E-03 | 73.00002 | .50415E-03 | 1.4985 | 73.00002 | .89135E-05 | 1.4912 | 5.9809 |
| 82.00002 | .30851E-03 | 82.00002 | .41517E-03 | 1.5570 | 82.00002 | .70905E-05 | 1.5479 | 5.8068 |
| 91.00002 | .25858E-03 | 91.00002 | .34867E-03 | 1.6104 | 91.00002 | .57493E-05 | 1.5991 | 5.6460 |
| 100.00002 | .22050E-03 | 100.00002 | .29755E-03 | 1.6596 | 100.00002 | .47355E-05 | 1.6460 | 5.4962 |
| 190.00003 | .76128E-04 | 190.00003 | .10113E-03 | 2.0362 | 190.00003 | .46735E-02 | 1.9877 | 4.3655 |
| 280.00006 | .40158E-04 | 280.00006 | .53133E-04 | 2.3234 | 280.00006 | .24598E-02 | 2.2202 | 3.5890 |
| 370.00006 | .25293E-04 | 370.00006 | .33505E-04 | 2.5583 | 370.00006 | .15516E-02 | 2.3831 | 2.9997 |
| 460.00006 | .17593E-04 | 460.00006 | .23369E-04 | 2.7580 | 460.00006 | .10821E-02 | 2.4964 | 2.5328 |
| 550.00012 | .13031E-04 | 550.00012 | .17380E-04 | 2.9324 | 550.00012 | .80445E-03 | 2.5733 | 2.1540 |
| 640.00012 | .10083E-04 | 640.00012 | .13513E-04 | 3.0870 | 640.00012 | .62511E-03 | 2.6223 | 1.8424 |
| 730.00012 | .80609E-05 | 730.00012 | .10852E-04 | 3.2255 | 730.00012 | .50171E-03 | 2.6493 | 1.5838 |
| 820.00012 | .66106E-05 | 820.00012 | .89342E-05 | 3.3506 | 820.00012 | .41273E-03 | 2.6591 | 1.3677 |
| 910.00012 | .55347E-05 | 910.00012 | .75009E-05 | 3.4645 | 910.00012 | .34623E-03 | 2.6555 | 1.1963 |
| 1000.00010 | .47141E-05 | 1000.00010 | .63991E-05 | 3.5691 | 1000.00010 | .29511E-03 | 2.6412 | 1.0332 |
| 1000.00020 | .47141E-05 | 1000.00020 | .63991E-05 | 3.5691 | 1000.00020 | .29511E-03 | 2.6412 | 1.0332 |
| 1900.00050 | .16047E-05 | 1900.00050 | .21666E-05 | 4.3624 | 1031.01340 | .44433E-05 | 2.6344 | .98605 |
| 2800.00100 | .83145E-06 | 2800.00100 | .11325E-05 | 4.9523 | 1062.02660 | .41753E-05 | 2.6266 | .94155 |
| 3700.00150 | .51323E-06 | 3700.00150 | .70980E-06 | 5.4198 | 1093.03980 | .39288E-05 | 2.6180 | .89947 |
| 4600.00200 | .34936E-06 | 4600.00200 | .49170E-06 | 5.8030 | 1124.05300 | .37019E-05 | 2.6088 | .85969 |
| 5500.00200 | .25297E-06 | 5500.00200 | .36304E-06 | 6.1252 | 1155.06620 | .34924E-05 | 2.5988 | .82204 |
| 6400.00200 | .19110E-06 | 6400.00200 | .28014E-06 | 6.3998 | 1186.07930 | .32987E-05 | 2.5883 | .78641 |
| 7300.00200 | .14890E-06 | 7300.00200 | .22326E-06 | 6.6353 | 1217.09250 | .31194E-05 | 2.5772 | .75267 |
| 8200.00200 | .11879E-06 | 8200.00200 | .18236E-06 | 6.8391 | 1248.10570 | .29530E-05 | 2.5657 | .72070 |
| 9100.00200 | .96550E-07 | 9100.00200 | .15187E-06 | 7.0144 | 1279.11890 | .27984E-05 | 2.5537 | .69041 |
| 10000.00200 | .79671E-07 | 10000.00200 | .12846E-06 | 7.1651 | 1310.13210 | .26546E-05 | 2.5414 | .66168 |

TABLE A-6. DIMENSIONLESS SPECTRUM FOR ALTITUDE BAND # 6 (concluded)

| i=1 | | i=2 | | | i=3 | | | |
|---|---|---|---|---|---|---|---|---|
| DIMENSIONLESS WAVE NUMBER $\Omega_1$ | DIMENSIONLESS SPECTRUM $\Phi_{11}$ | DIMENSIONLESS WAVE NUMBER $\Omega_1$ | DIMENSIONLESS SPECTRUM $\Phi_{22}$ | $\Phi_{22/11}$ | DIMENSIONLESS WAVE NUMBER $\Omega_1$ | DIMENSIONLESS SPECTRUM $\Phi_{33}$ | $\Phi_{33/11}$ | $\Phi_{33/22}$ |
| 11220.566 | .62612E-07 | 11220.566 | .10446E-06 | 7.3351 | | | | |
| 12441.131 | .50118E-07 | 12441.131 | .86531E-07 | 7.4701 | | | | |
| 13661.695 | .40722E-07 | 13661.695 | .72762E-07 | 7.5745 | | | | |
| 14882.260 | .33503E-07 | 14882.260 | .61940E-07 | 7.6515 | | | | |
| 16102.824 | .27859E-07 | 16102.824 | .53270E-07 | 7.7042 | | | | |
| 17323.387 | .23381E-07 | 17323.387 | .46213E-07 | 7.7351 | | | | |
| 18543.949 | .19782E-07 | 18543.949 | .40390E-07 | 7.7468 | | | | |
| 19764.512 | .16860E-07 | 19764.512 | .35531E-07 | 7.7414 | | | | |
| 20985.074 | .14463E-07 | 20985.074 | .31435E-07 | 7.7210 | | | | |
| 22205.637 | .12481E-07 | 22205.637 | .27952E-07 | 7.6875 | | | | |

## APPENDIX B

### ESTABLISHMENT OF LOWER FREQUENCY LIMITS

The maximum time limit, $t_{max}$, for which the impulse response function is computed, determines the minimum frequency, $\Omega_{i1min}$, for which the corresponding spectrum is accurately simulated according to the relation

$$\Omega_{i1min} = \pi/t_{max} \tag{B-1}$$

The simulated turbulence may contain lower frequencies, depending on the total length of the time series, but the shape of the actual spectrum for any frequencies less than $\Omega_{i1min}$ will not in general match the theoretical spectral shape. To verify this point for the $\Phi_{33/11}$ spectrum two impulse response functions were generated, the first extending out to a $t_{max}$ of 42.10573 and the second extending out to a $t_{max}$ of 85.895689. Two separate turbulence time series were then generated, one for each impulse function. The results of spectral analysis of these two time series is presented in Figures B-1 and B-2. As indicated in each figure, the observed spectrum tends to drift away from the theoretical spectrum for frequencies below $\pi/t_{max}$. The impulse response function with the larger $t_{max}$ produces a time series whose spectral shape matches the theoretical spectrum to the lower frequency.

Based on various characteristics of the Space Shuttle simulators, a minimum frequency, $f_{1min}$, of .04 hertz was established for generating simulated turbulence. The dimensional frequency, $f_{1min}$, is related to the dimensionless frequency, $\Omega_{i1min}$, according to the relation

$$\Omega_{i1min} = 2\pi a L_i f_{1min}/V \tag{B-2}$$

By substitution and rearrangement,

$$t_{max} = V/(2aL_i f_{1min}) \tag{B-3}$$

To satisfy the requirement for a minimum simulation frequency of .04 hertz, values of each impulse response function were computed for 100 dimensionless time intervals. As shown in Table B-1, by using a constant number of time

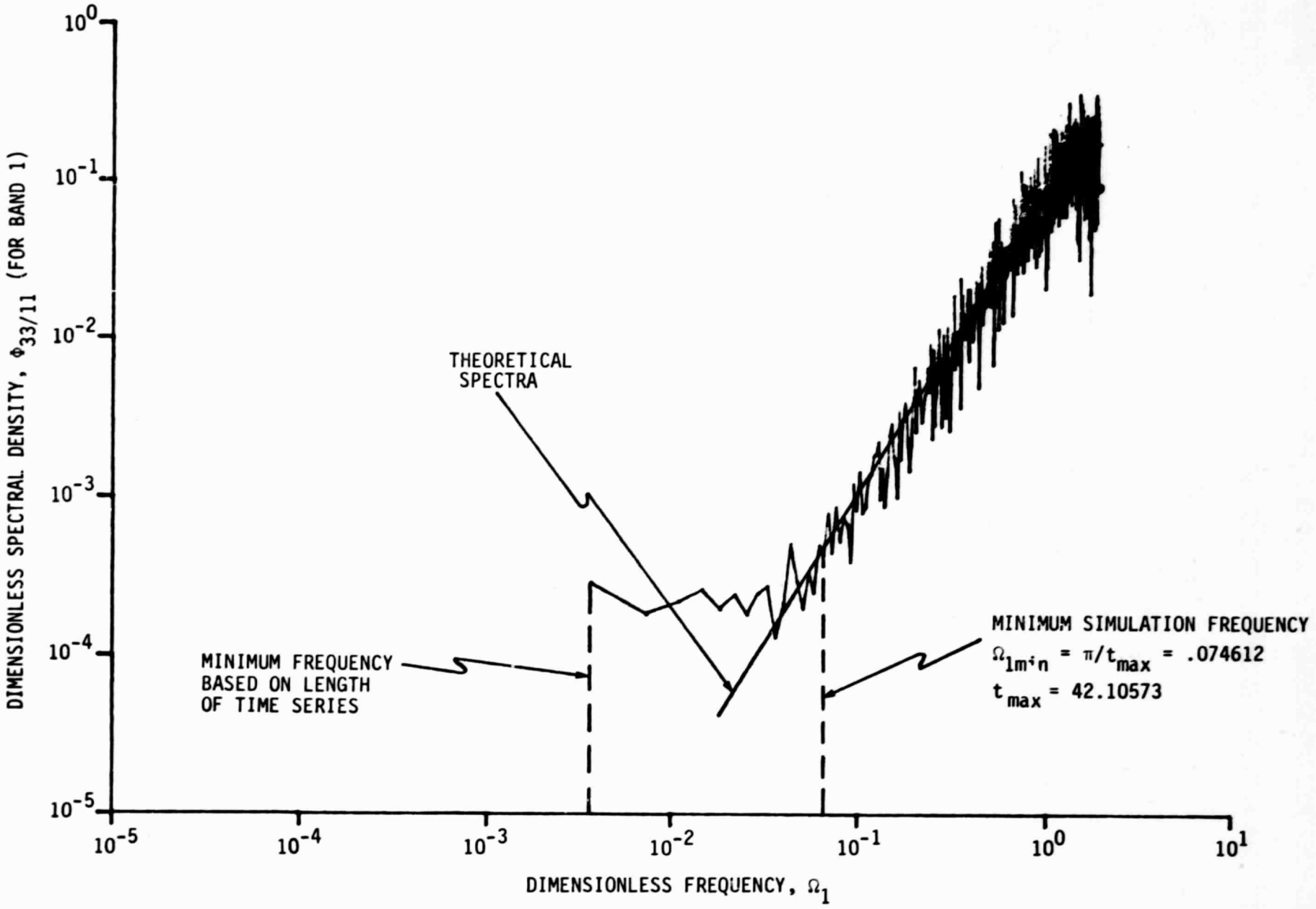


Figure B-1. Spectrum of $\Phi_{33/11}$ for Impulse Response Function with $t_{max} = 42.10573$

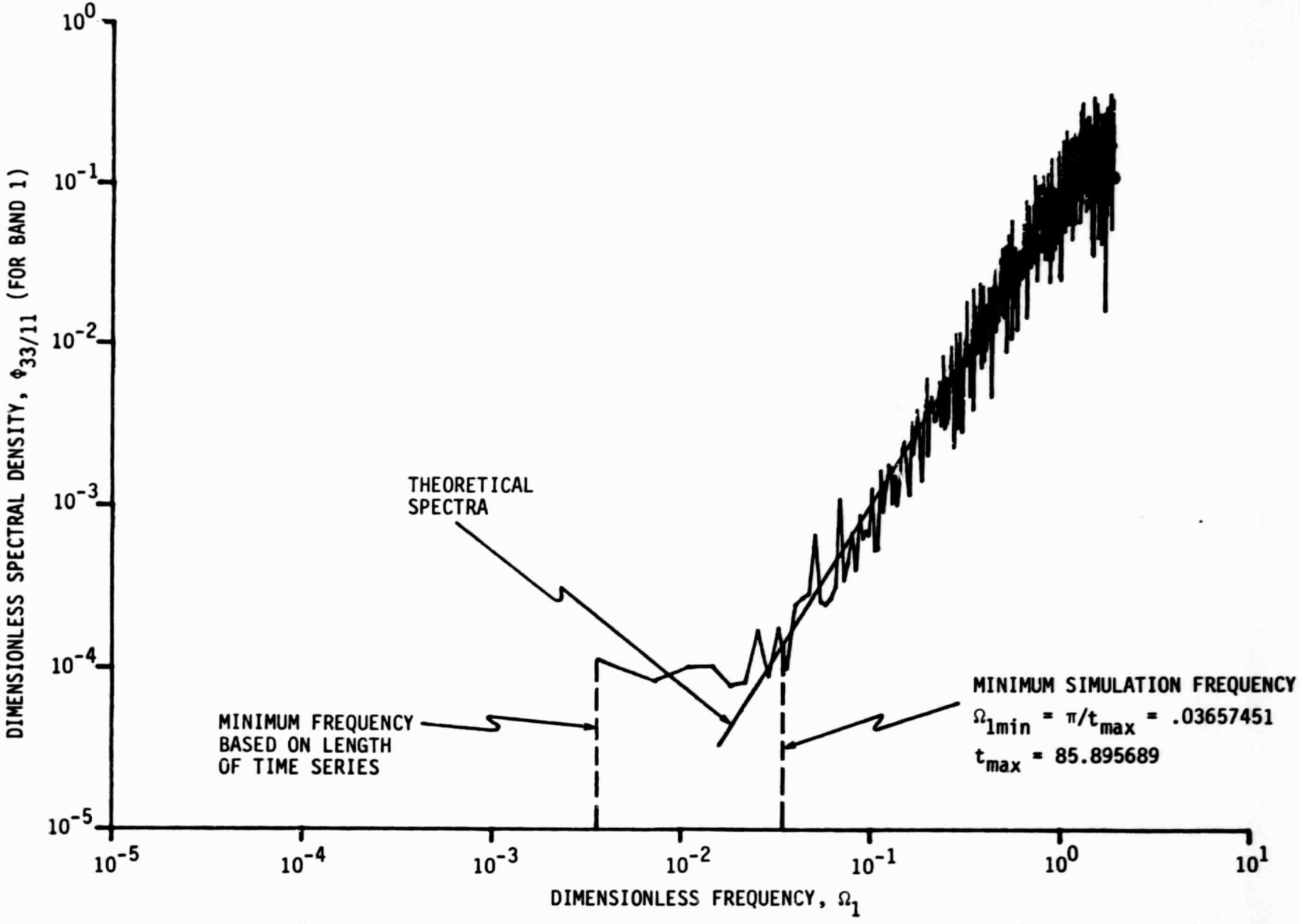


Figure B-2. Spectrum of $\Phi_{33/11}$ for Impulse Response Function with $t_{max} = 85.895689$

intervals, the actual minimum simulation frequency varies from .0174 hertz in Band 1 to .04 hertz in Band 6. Thus, at the lower altitudes the turbulence simulation will actually be valid for frequencies somewhat lower than the required minimum as given by Eq (B-2).

TABLE B-1. DIMENSIONAL AND DIMENSIONLESS MINIMUM FREQUENCY LIMITS

| | | | MINIMUM SIMULATION FREQUENCY LIMITS | |
|---|---|---|---|---|
| | | | DIMENSIONAL | DIMENSIONLESS |
| i | SPECTRA | BAND | $f_{1min}$ (hertz) | $\Omega_{i1min}$ |
| 1 | $\Phi_{11}$ | 1 | .0174 | .04818 |
| | | 2 | .0212 | .2176 |
| | | 3 | .0211 | .3331 |
| | | 4 | .0396 | .5918 |
| | | 5 | .04 | 7.365 |
| | | 6 | .04 | 8.949 |
| 2 | $\Phi_{22}$, $\Phi_{22/11}$ | 1 | .0174 | .03075 |
| | | 2 | .0206 | .2110 |
| | | 3 | .0211 | .3331 |
| | | 4 | .0396 | .5918 |
| | | 5 | .04 | 7.365 |
| | | 6 | .04 | 8.949 |
| 3 | $\Phi_{33}$, $\Phi_{33/11}$, $\Phi_{33/22}$ | 1 | .0174 | .01865 |
| | | 2 | .0208 | .2132 |
| | | 3 | .0211 | .3331 |
| | | 4 | .0396 | .5918 |
| | | 5 | .04 | .4630 |
| | | 6 | .04 | .5280 |

# APPENDIX C

## SPECTRAL ANALYSIS OF SIMULATED TURBULENCE

By means of a Fast Fourier Transform [14] spectral analyses of all simulated turbulence have been performed*. The results are presented in dimensionless form in Figures C-1 through C-36. Table C-1 provides a summary of these figures. Also included in each figure is the theoretical von Karman spectra. The agreement between the theoretical spectra and the computed spectra is quite satisfactory.

TABLE C-1. MATRIX OF SPECTRAL ANALYSIS FIGURES

| SERIES TYPE | ALTITUDE BAND | | | | | |
|---|---|---|---|---|---|---|
| | 1 | 2 | 3 | 4 | 5 | 6 |
| $u_1$ | C-1 | C-2 | C-3 | C-4 | C-5 | C-6 |
| $u_2$ | C-7 | C-8 | C-9 | C-10 | C-11 | C-12 |
| $u_3$ | C-13 | C-14 | C-15 | C-16 | C-17 | C-18 |
| $\partial u_2/\partial x_1$ | C-19 | C-20 | C-21 | C-22 | C-23 | C-24 |
| $\partial u_3/\partial x_1$ | C-25 | C-26 | C-27 | C-28 | C-29 | C-30 |
| $\partial u_3/\partial x_2$ | C-31 | C-32 | C-33 | C-34 | C-35 | C-36 |

*The spectral analysis involved the first 4096 terms of each time series except for bands 5 and 6 for the $u_1$ and $u_2$ gusts. For these cases 8192 terms were used.

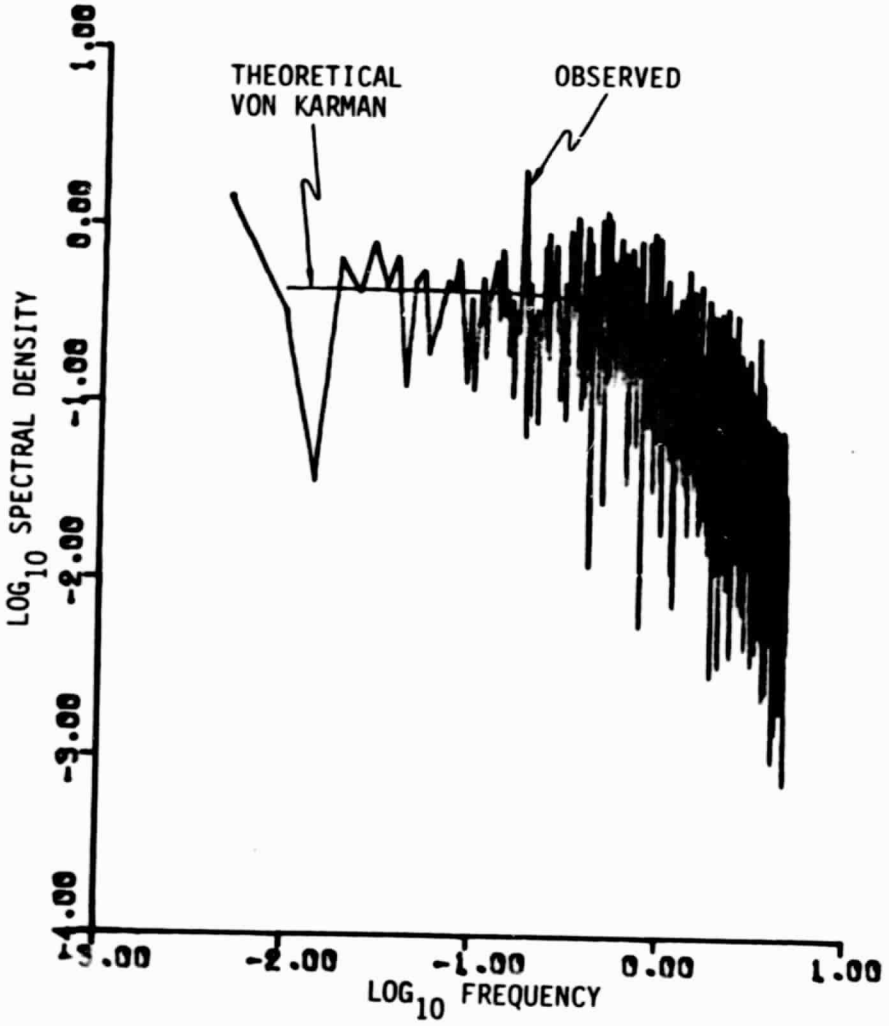


Figure C-1. $u_1$ - Gust Spectrum, Altitude Band #1

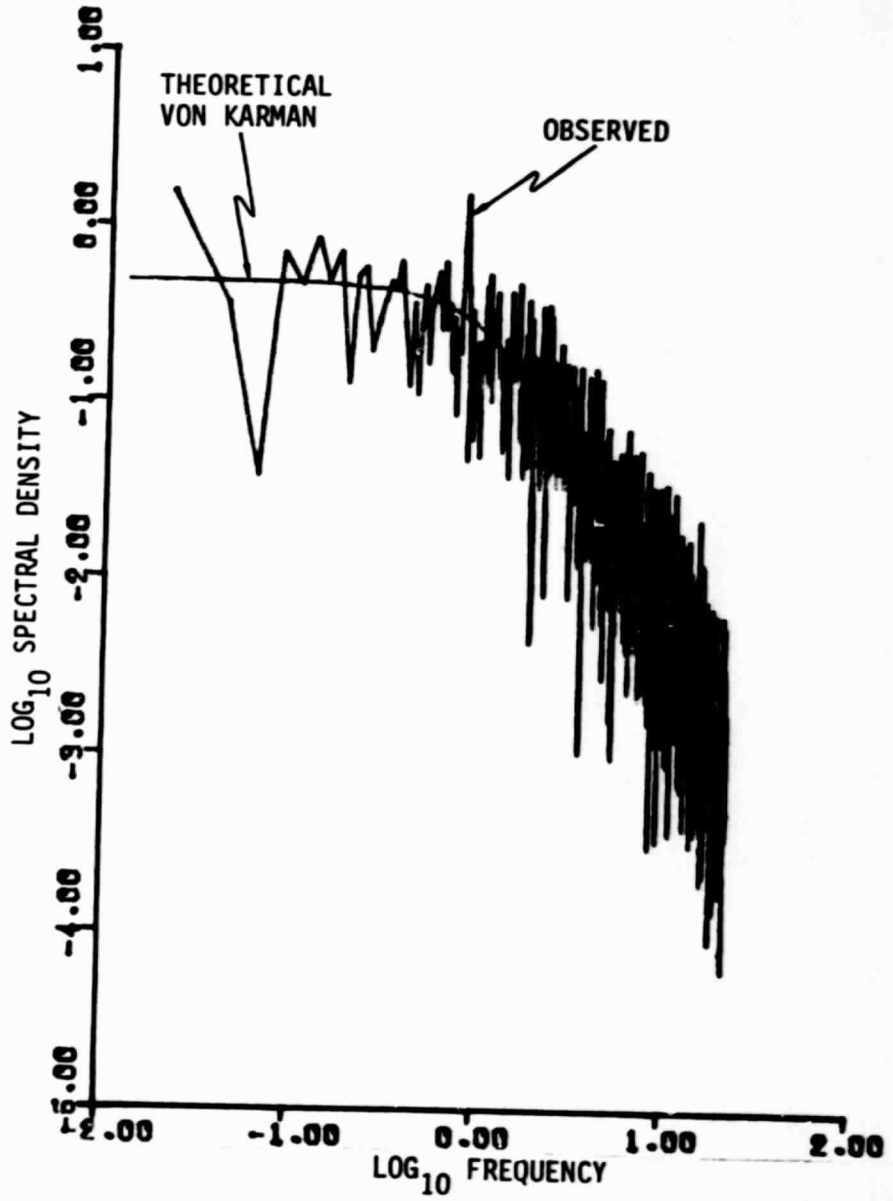


Figure C-2. $u_1$ - Gust Spectrum, Altitude Band #2

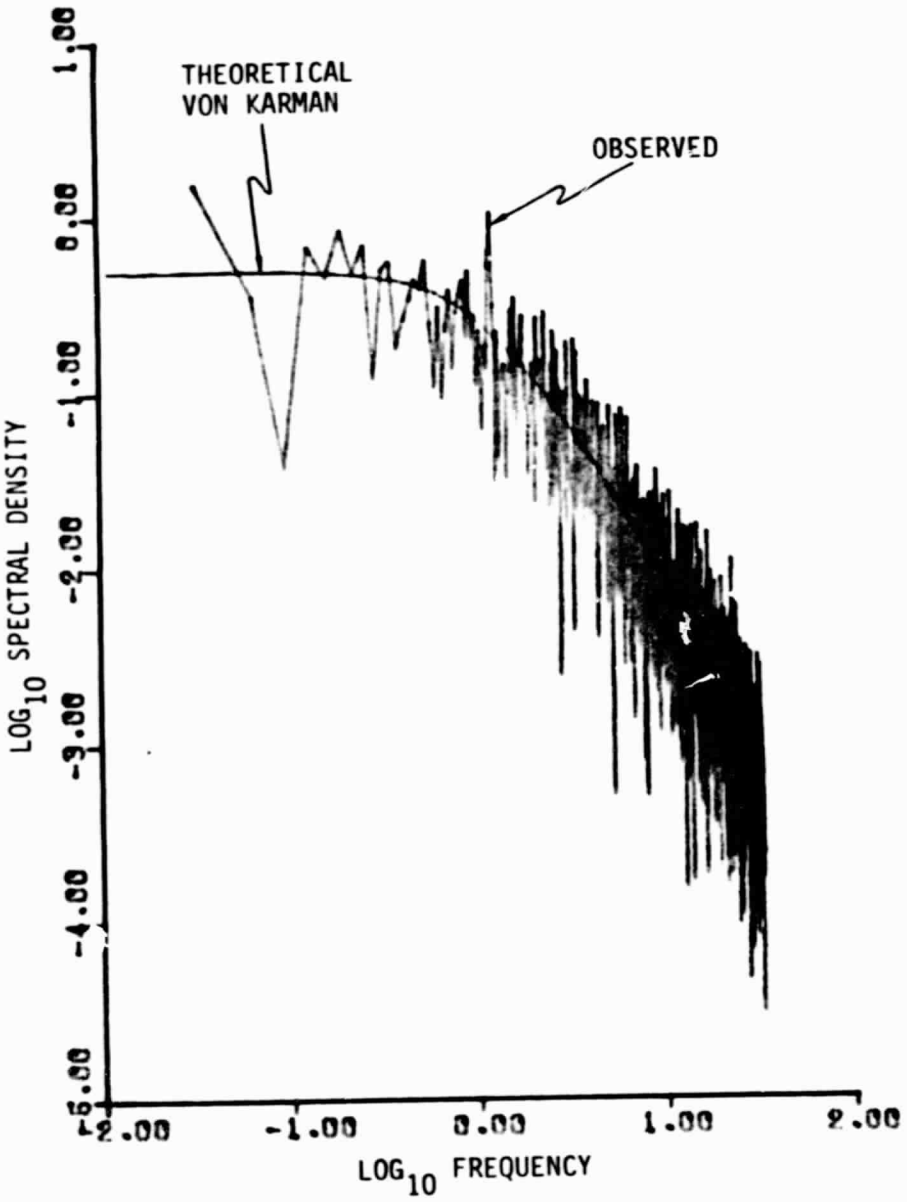


Figure C-3. $u_1$ - Gust Spectrum, Altitude Band #3

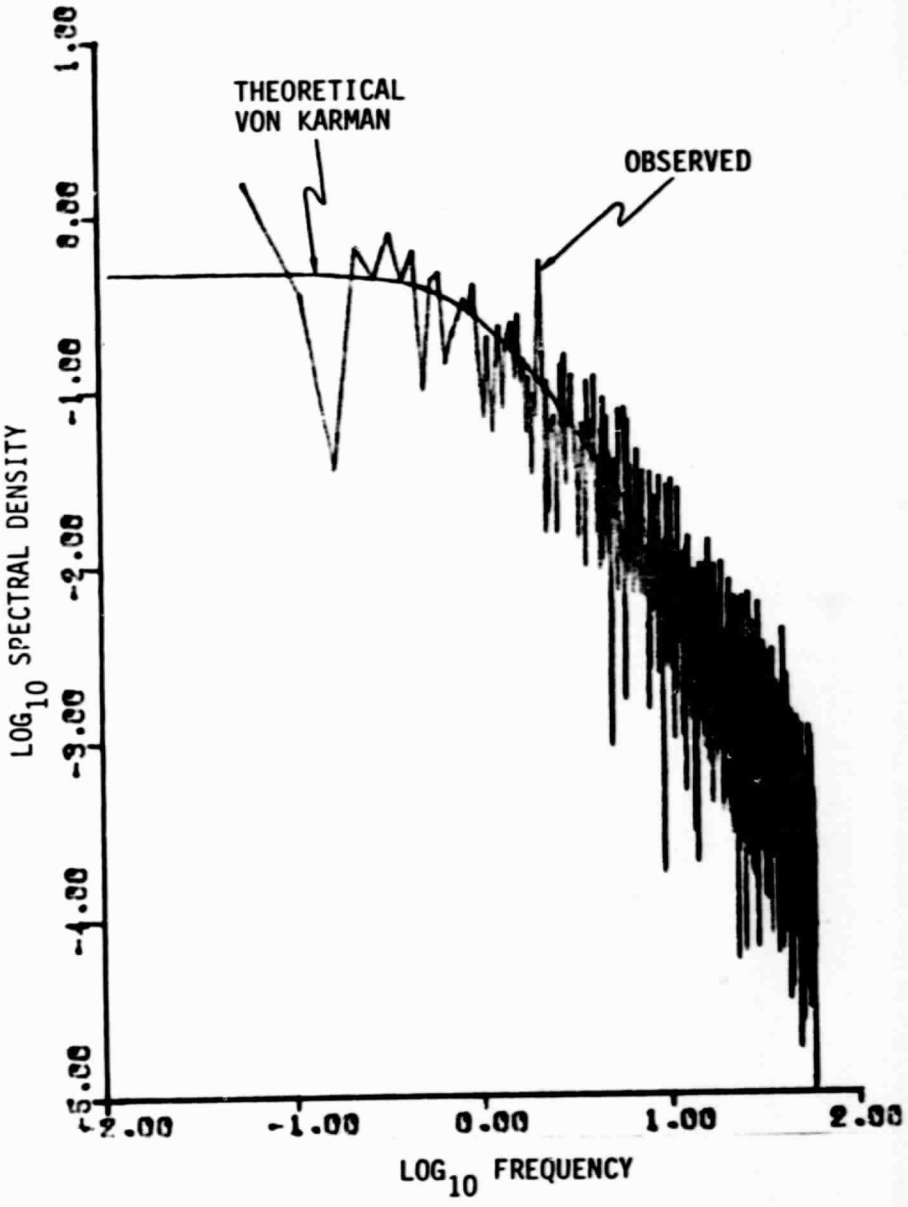


Figure C-4. $u_1$ - Gust Spectrum, Altitude Band #4

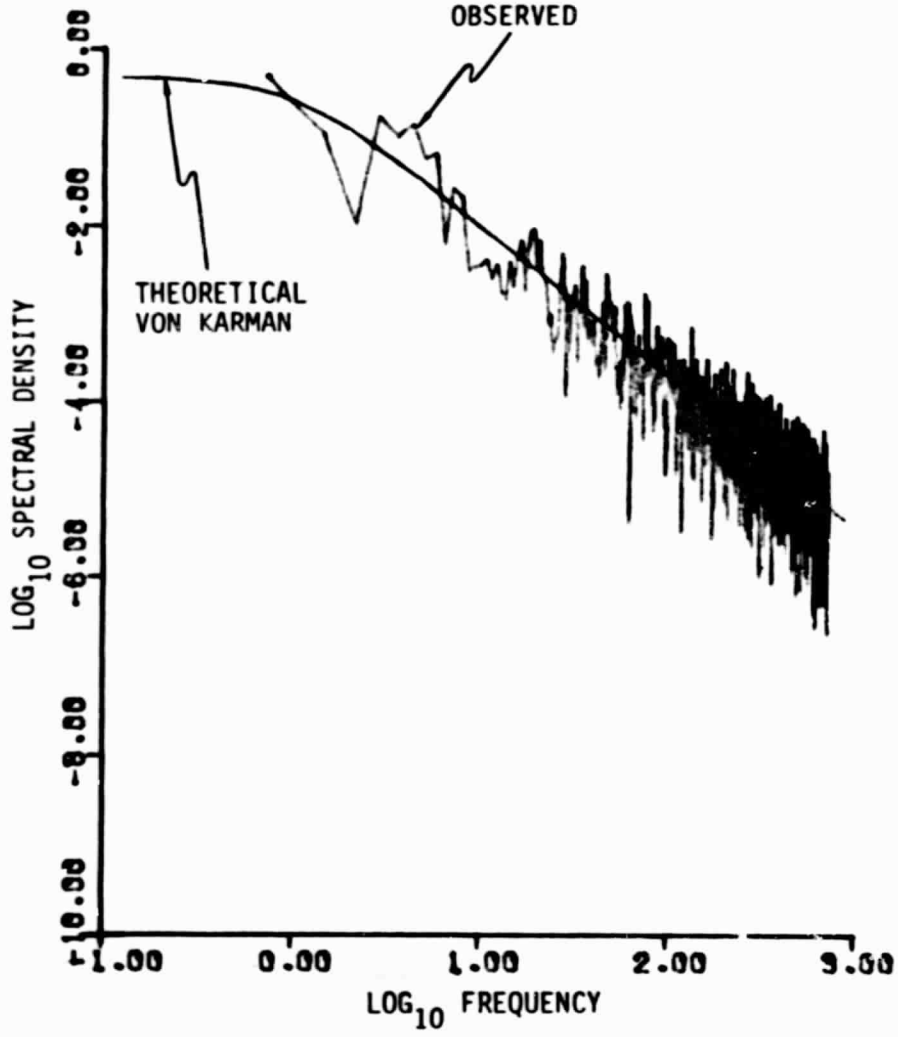


Figure C-5. $u_1$ - Gust Spectrum, Altitude Band #5

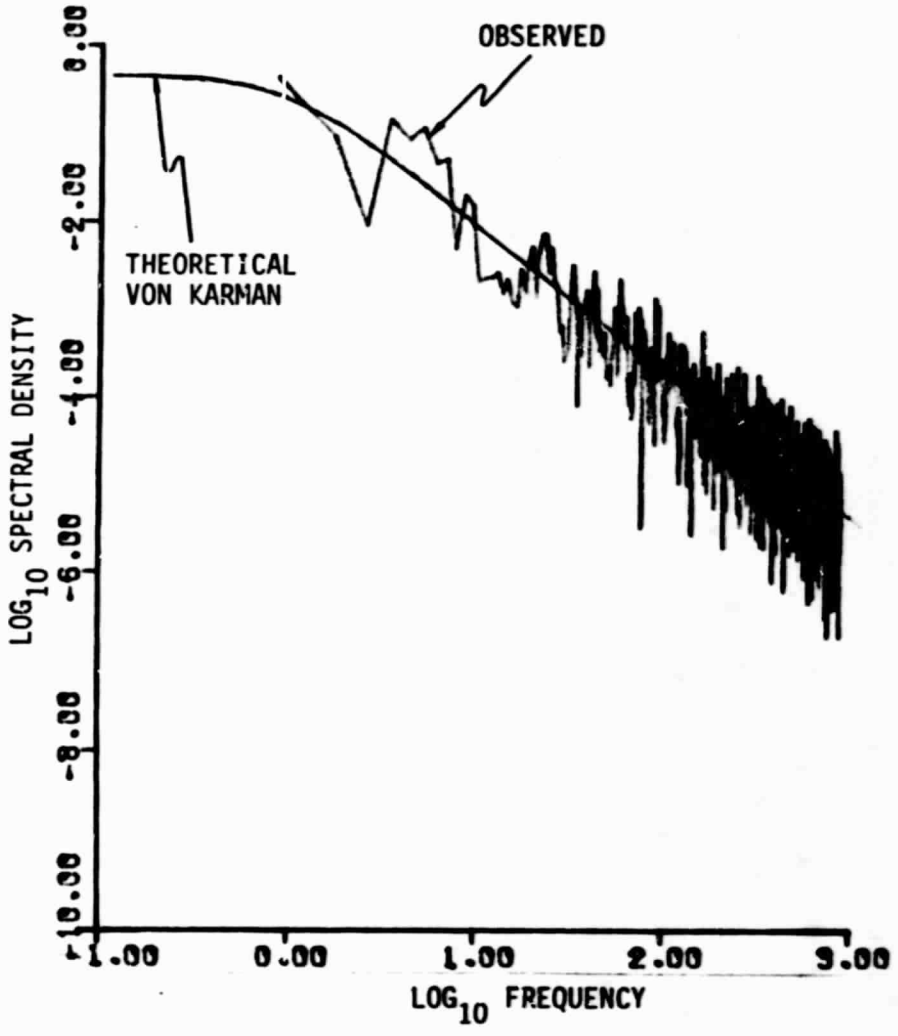


Figure C-6. $u_1$ - Gust Spectrum, Altitude Band #6

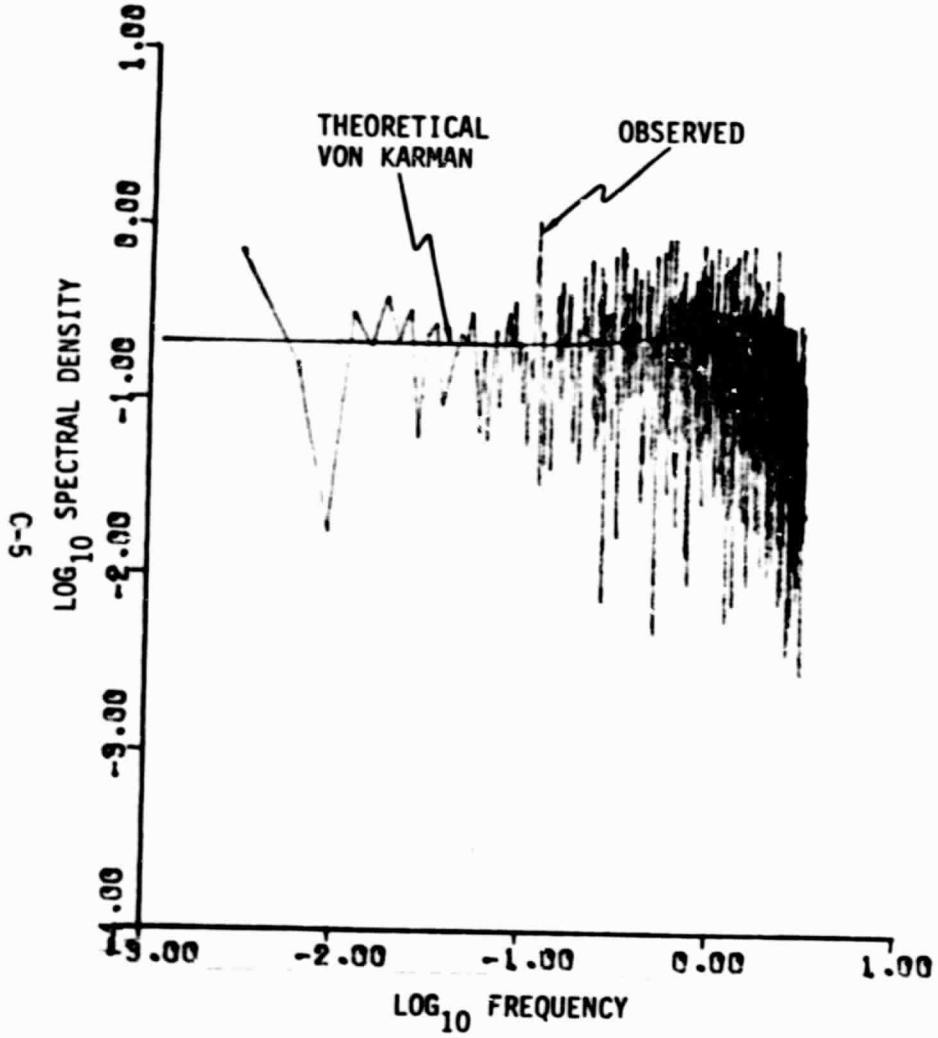


Figure C-7. $u_2$ - Gust Spectrum, Altitude Band #1

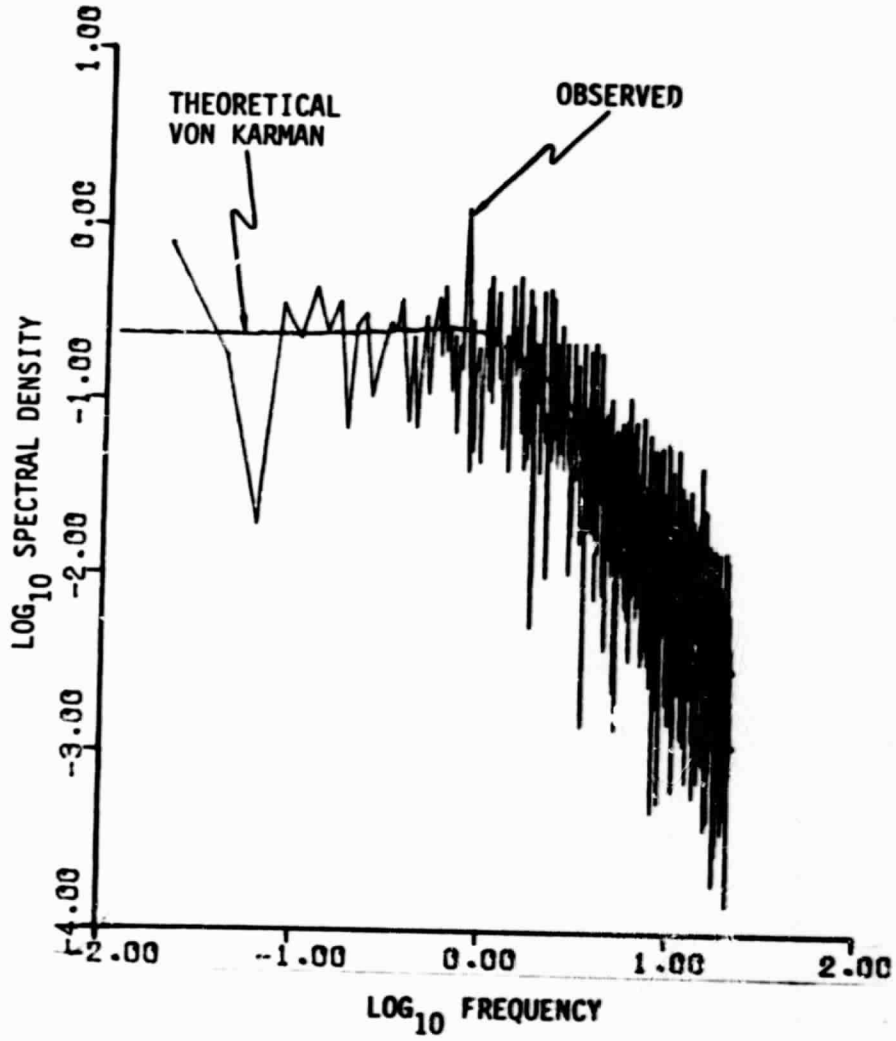


Figure C-8. $u_2$ - Gust Spectrum, Altitude Band #2

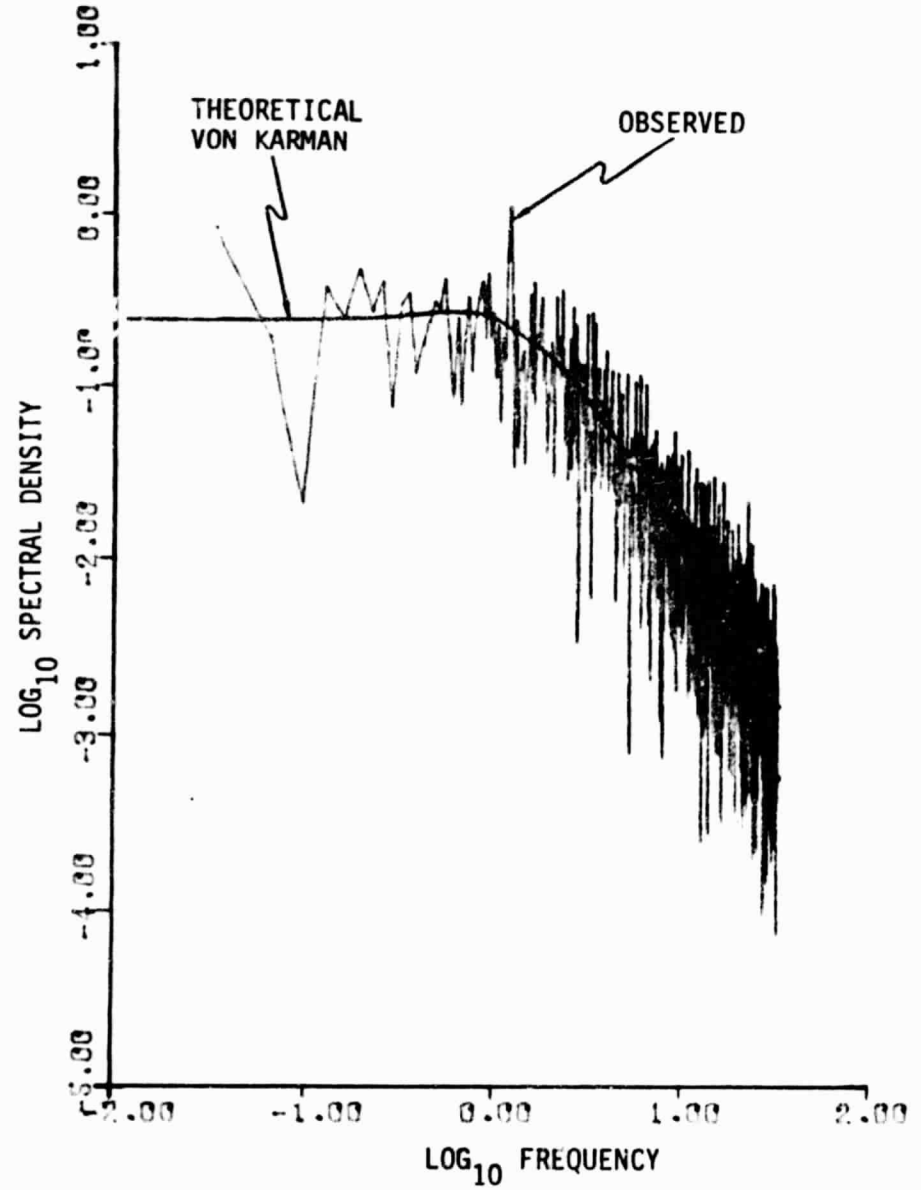


Figure C-9. $u_2$ - Gust Spectrum, Altitude Band #3

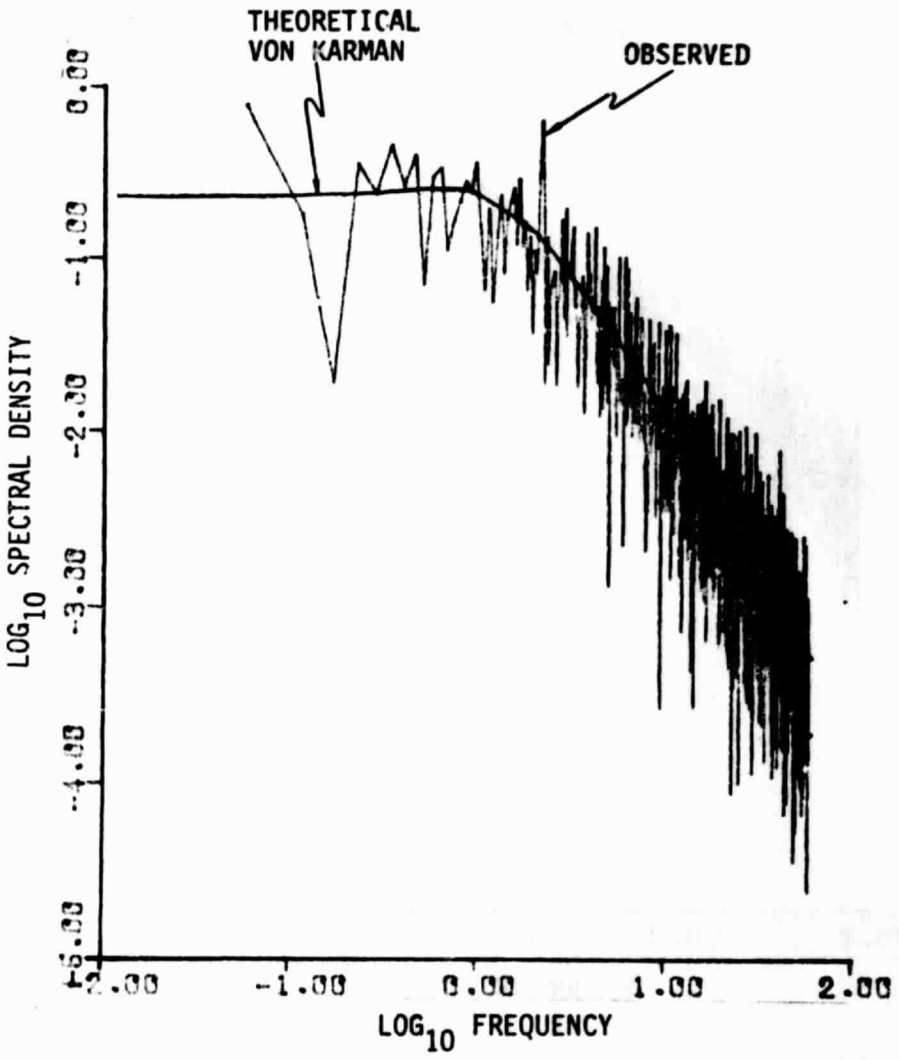


Figure C-10. $u_2$ - Gust Spectrum, Altitude Band #4

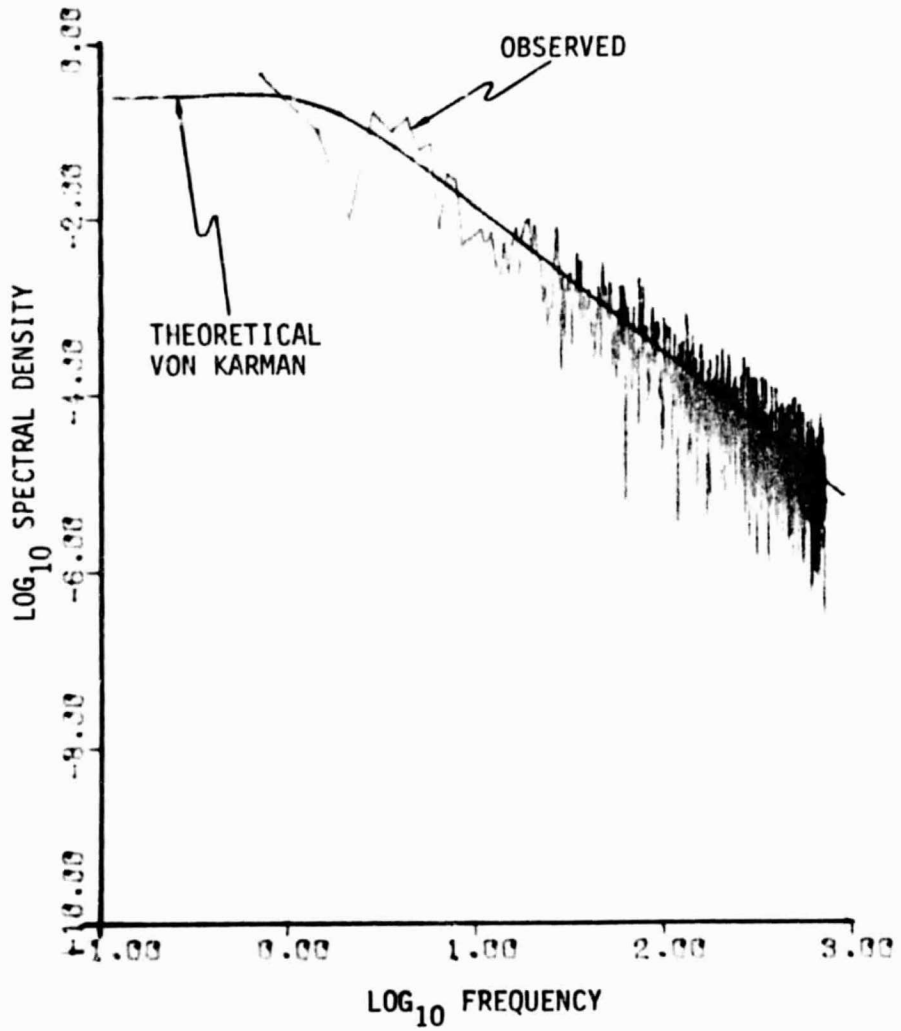


Figure C-11. $u_2$ - Gust Spectrum, Altitude Band #5

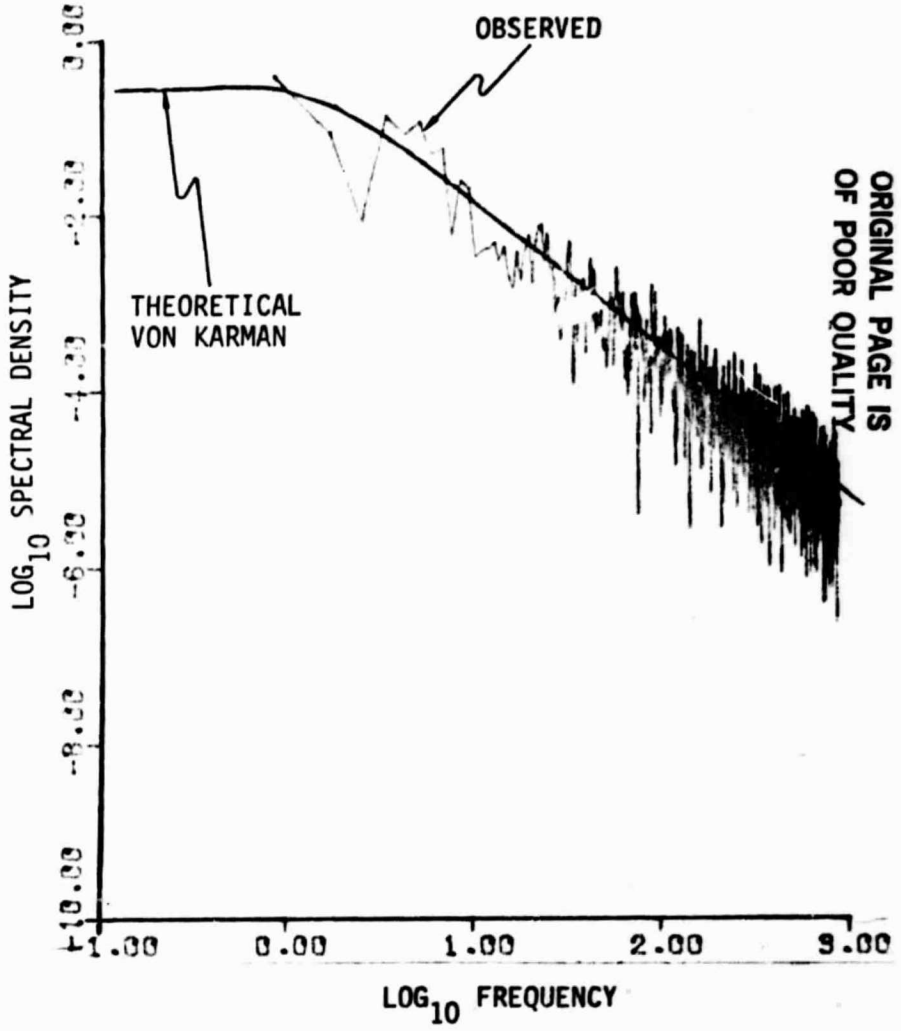


Figure C-12. $u_2$ - Gust Spectrum, Altitude Band #6

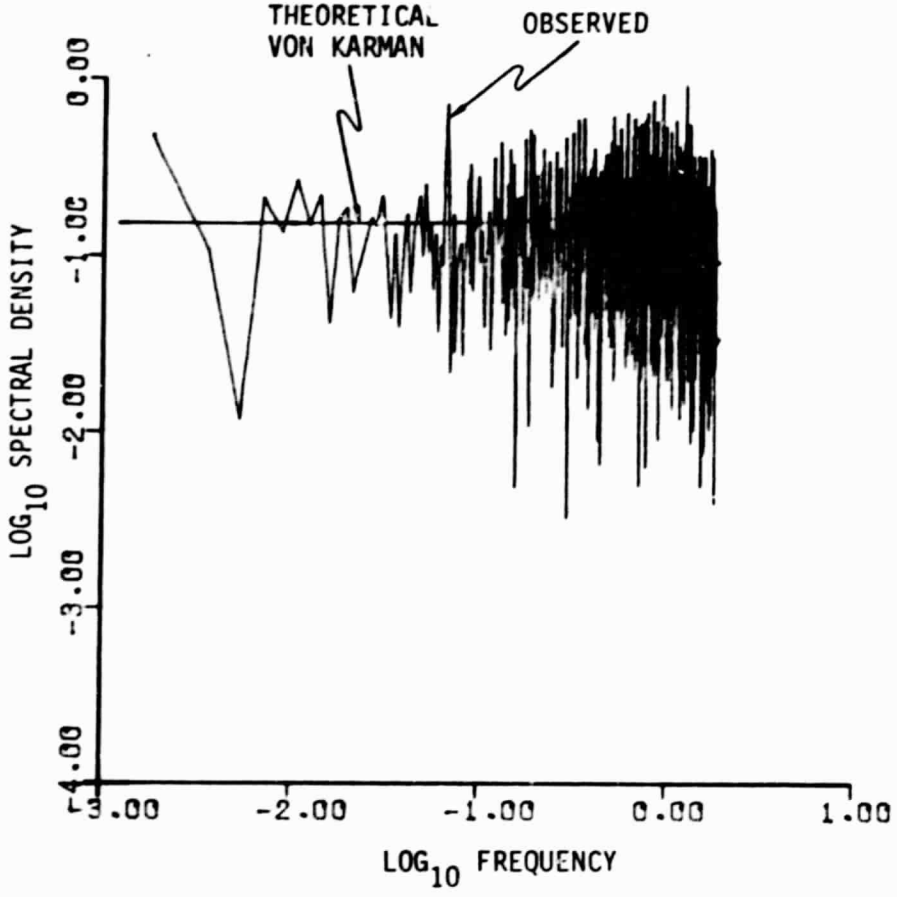


Figure C-13 $u_3$ - Gust Spectrum, Altitude Band #1

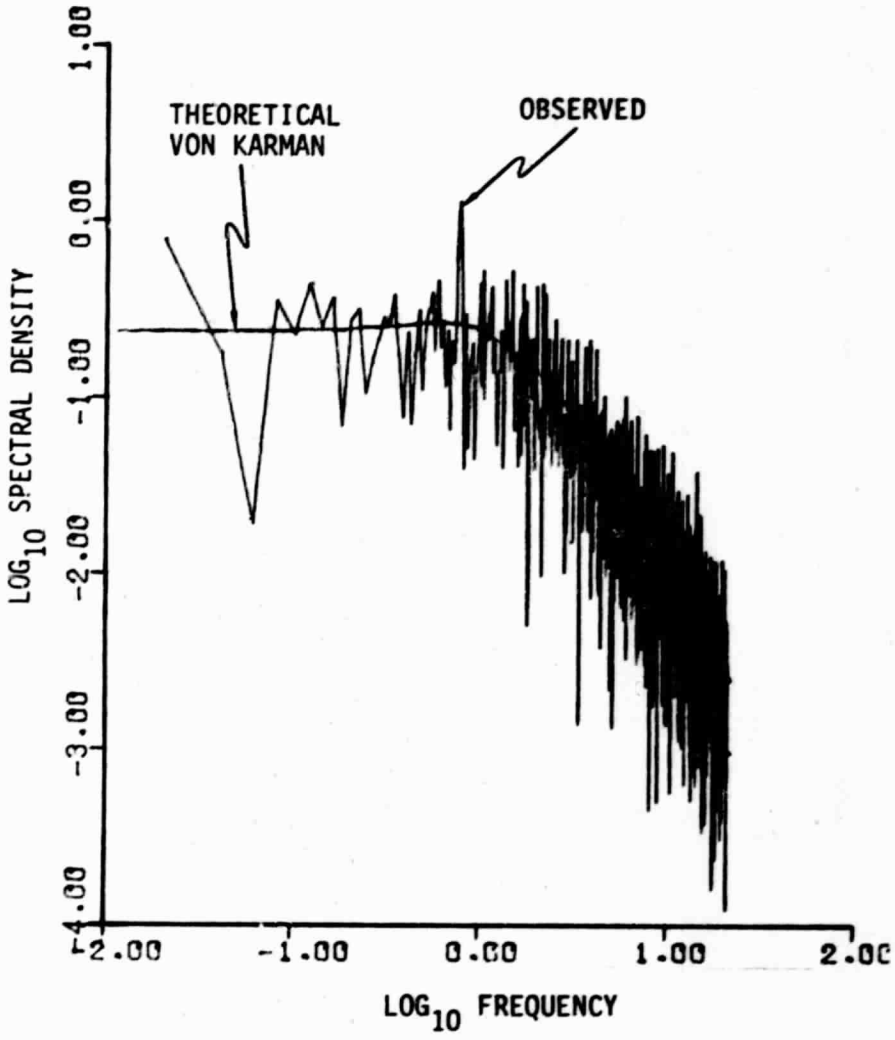


Figure C-14. $u_3$ - Gust Spectrum, Altitude Band #2

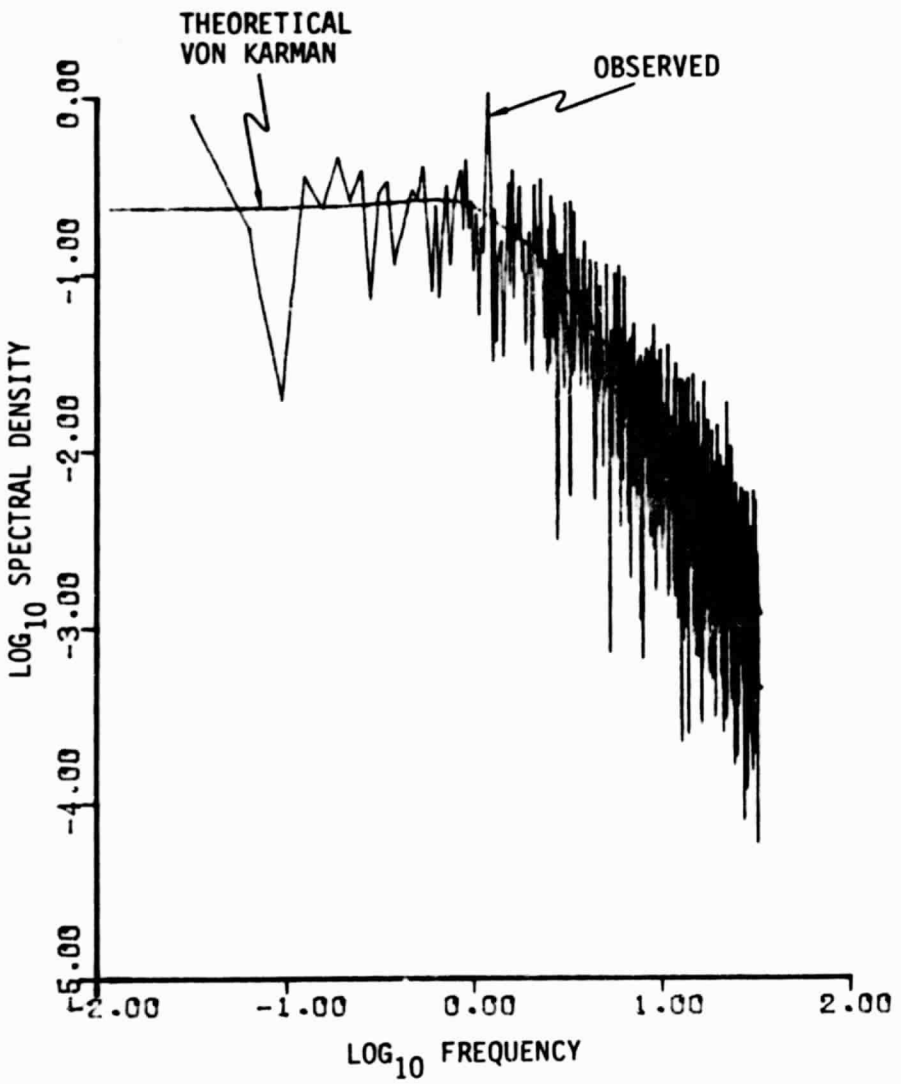


Figure C-15. $u_3$ - Gust Spectrum, Altitude Band #3

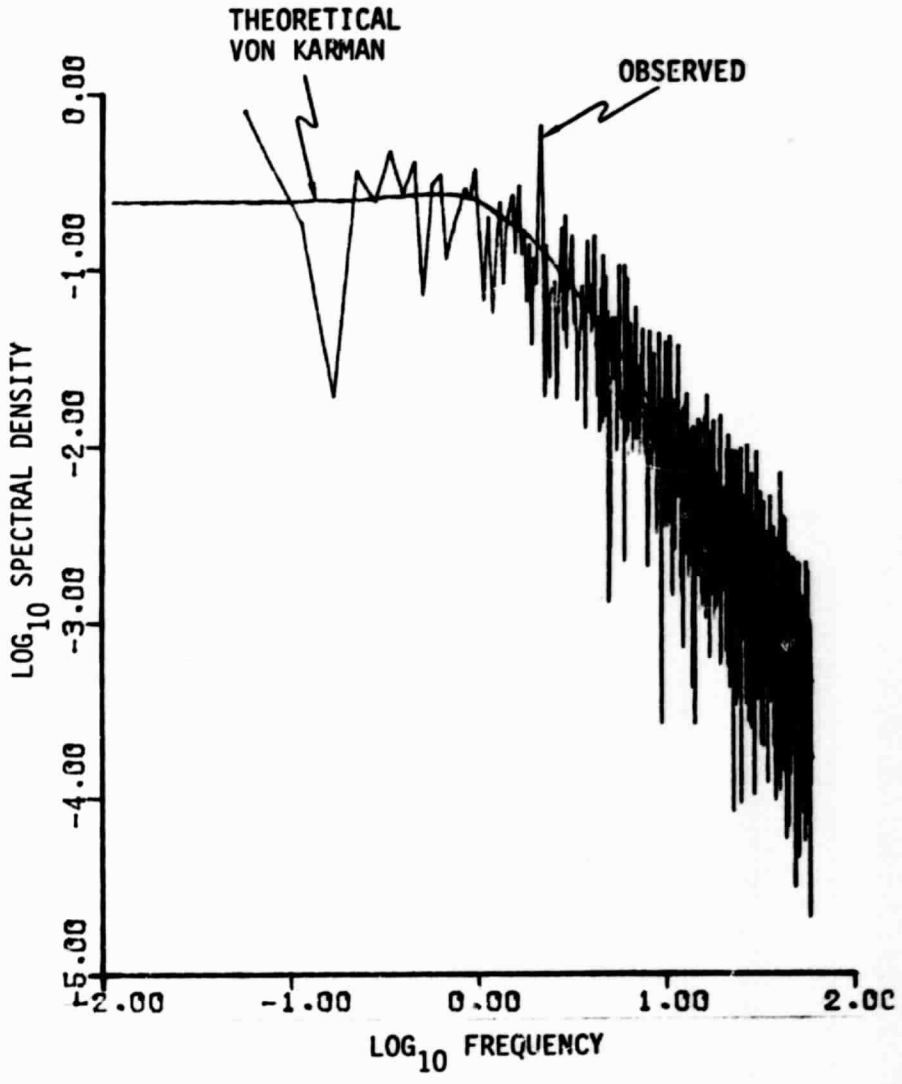


Figure C-16. $u_3$ - Gust Spectrum, Altitude Band #4

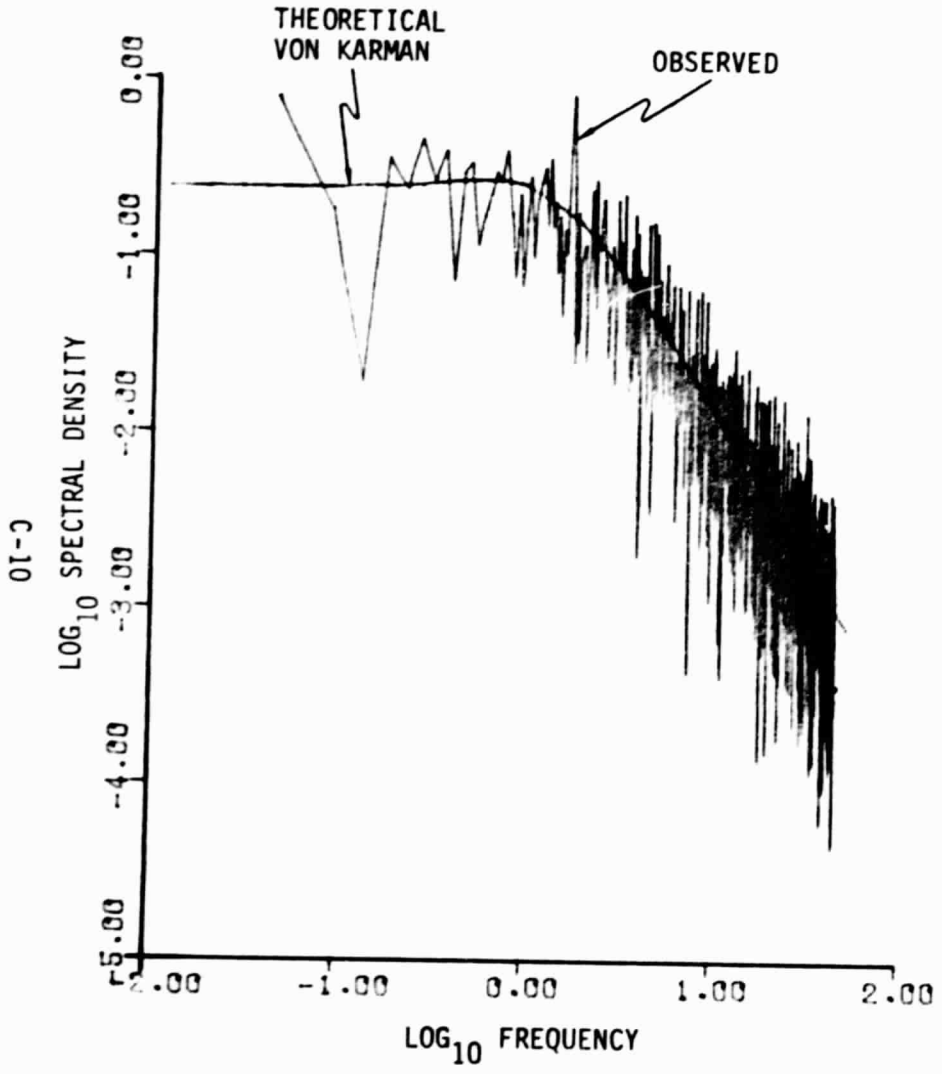


Figure C-17. $u_3$ - Gust Spectrum, Altitude Band #5

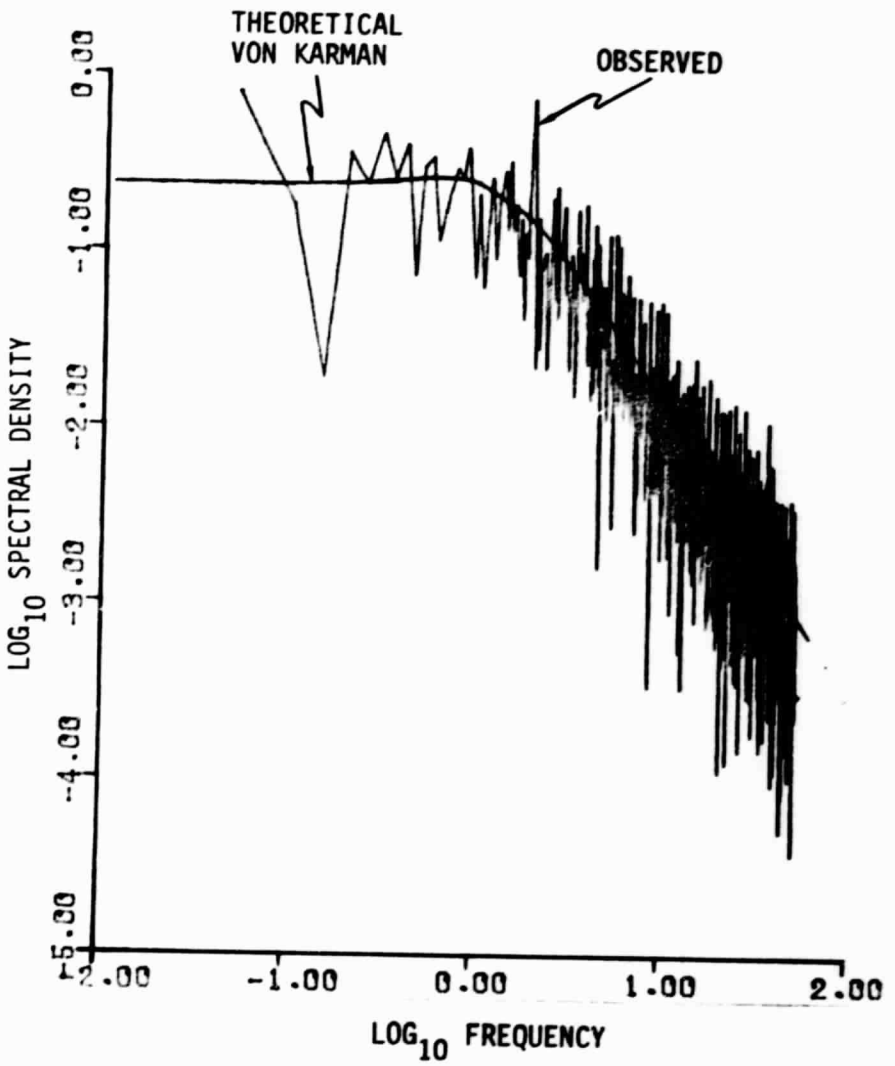


Figure C-18. $u_3$ - Gust Spectrum, Altitude Band #6

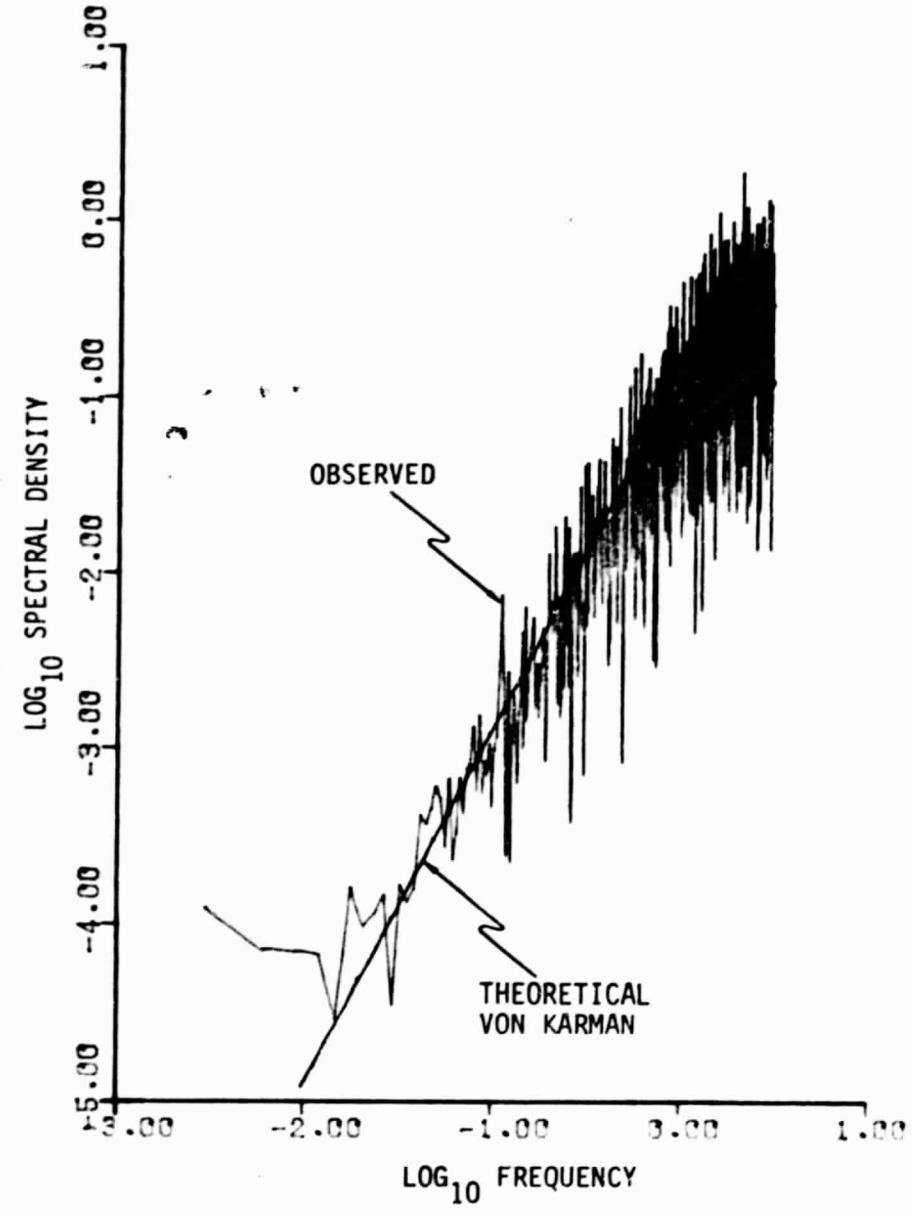


Figure C-19. $\partial u_2/\partial x_1$ - Gust Gradient Spectrum, Altitude Band #1

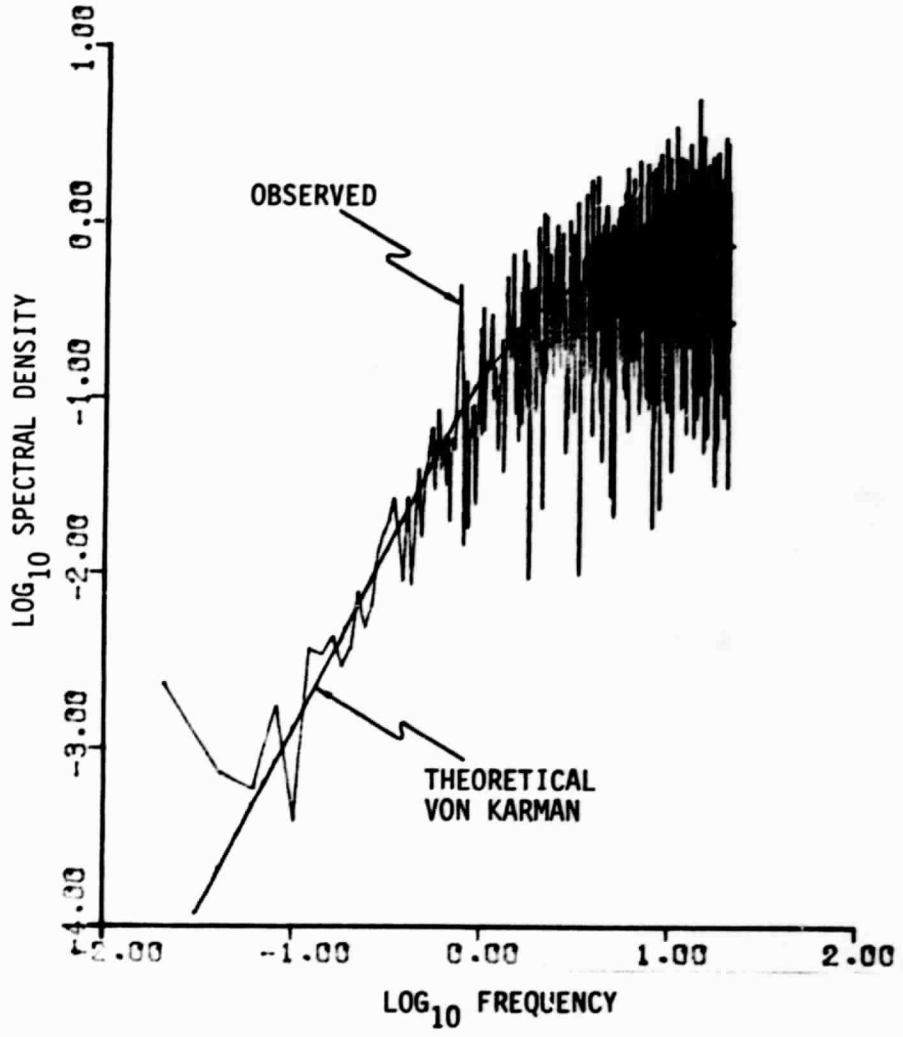


Figure C-20. $\partial u_2/\partial x_1$ - Gust Gradient Spectrum, Altitude Band #2

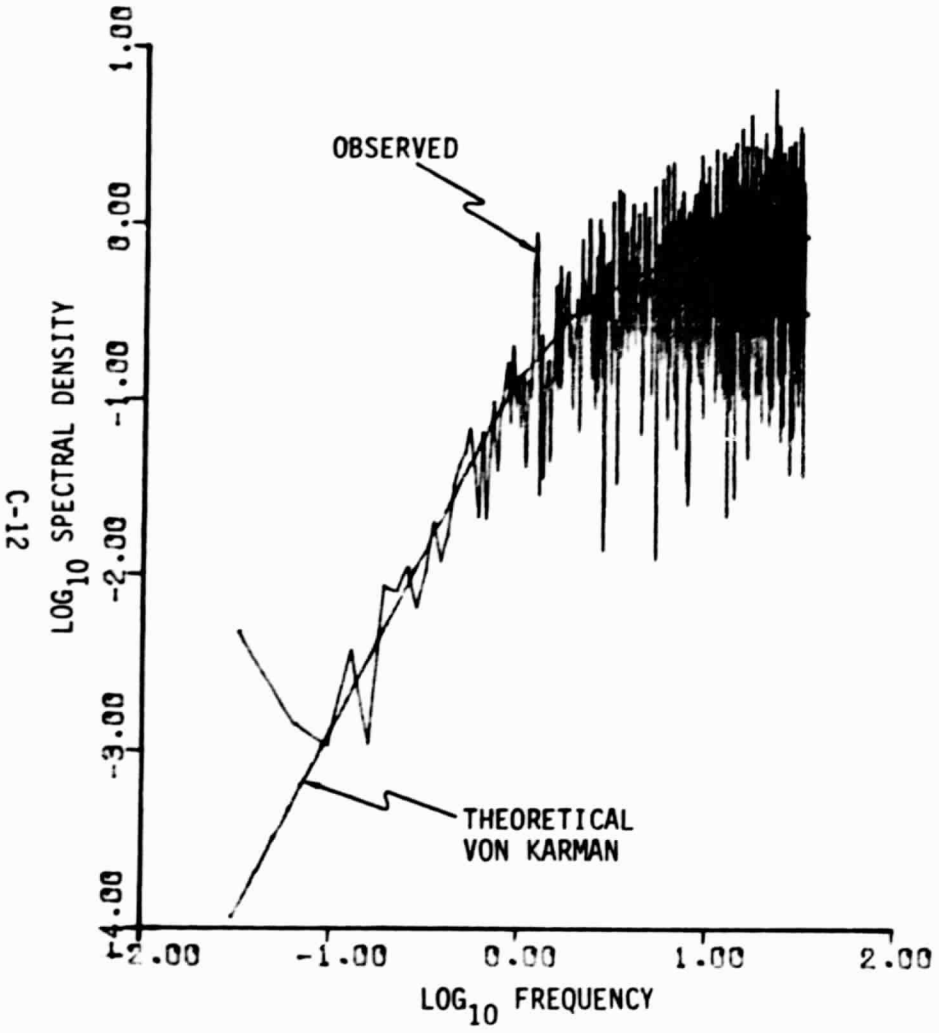


Figure C-21. $\partial u_2/\partial x_1$ - Gust Gradient Spectrum, Altitude Band #3

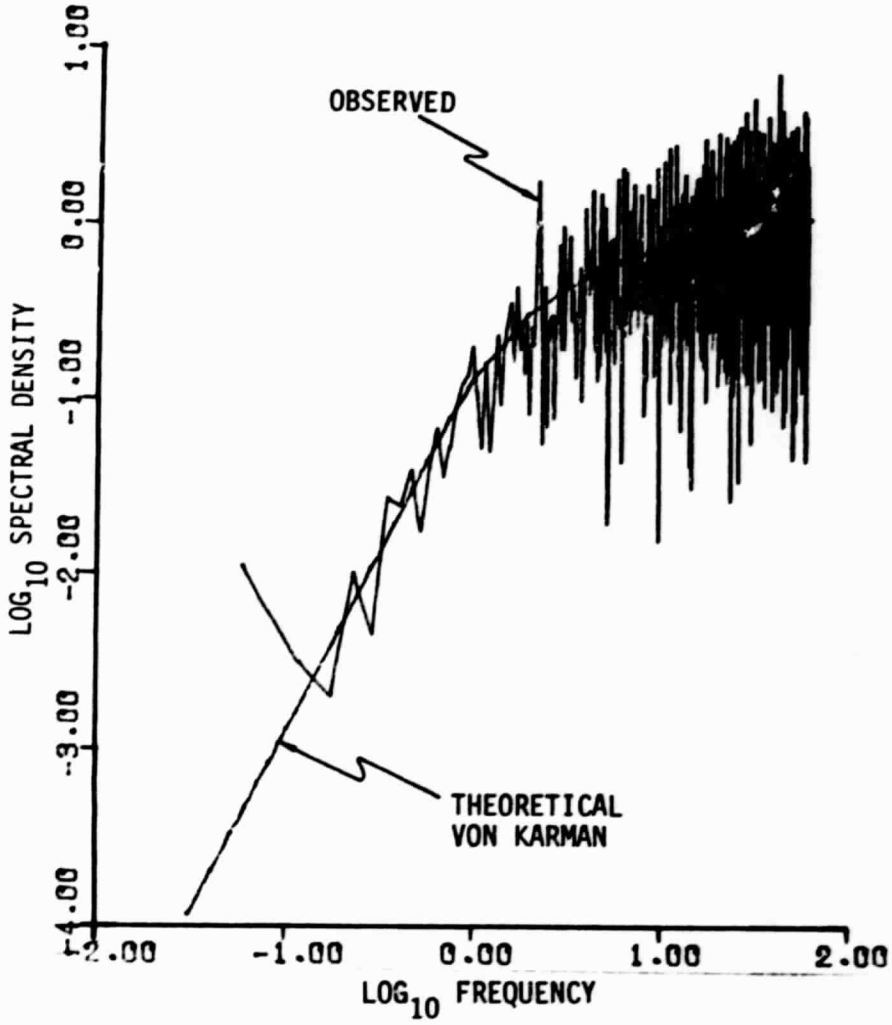


Figure C-22. $\partial u_2/\partial x_1$ - Gust Gradient Spectrum, Altitude Band #4

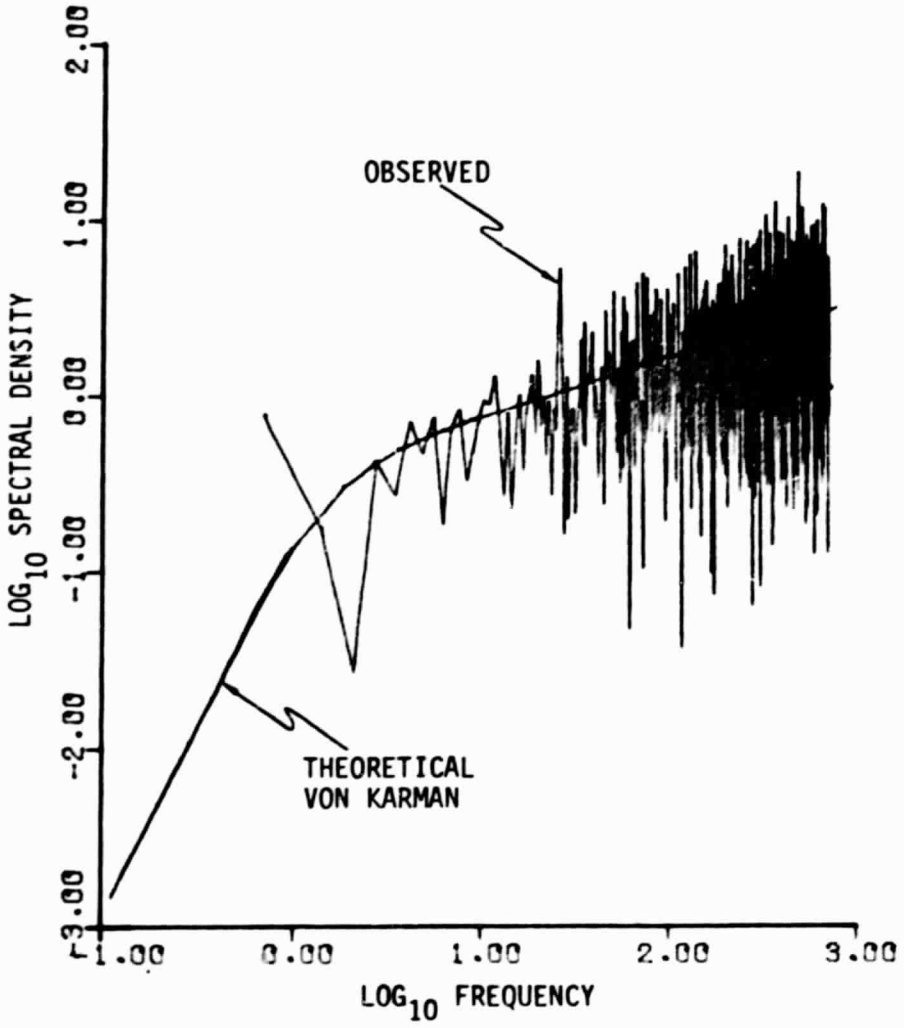


Figure C-23. $\partial u_2/\partial x_1$ - Gust Gradient Spectrum, Altitude Band #5

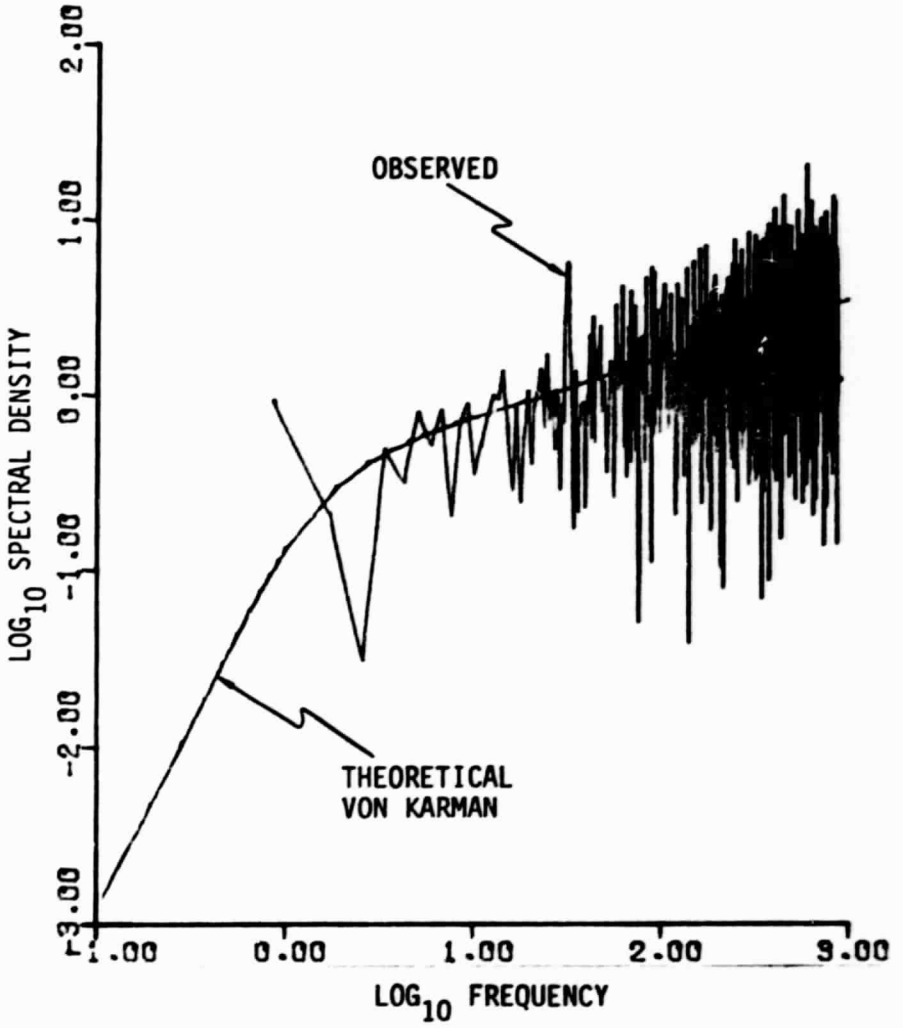


Figure C-24. $\partial u_2/\partial x_1$ - Gust Gradient Spectrum, Altitude Band #6

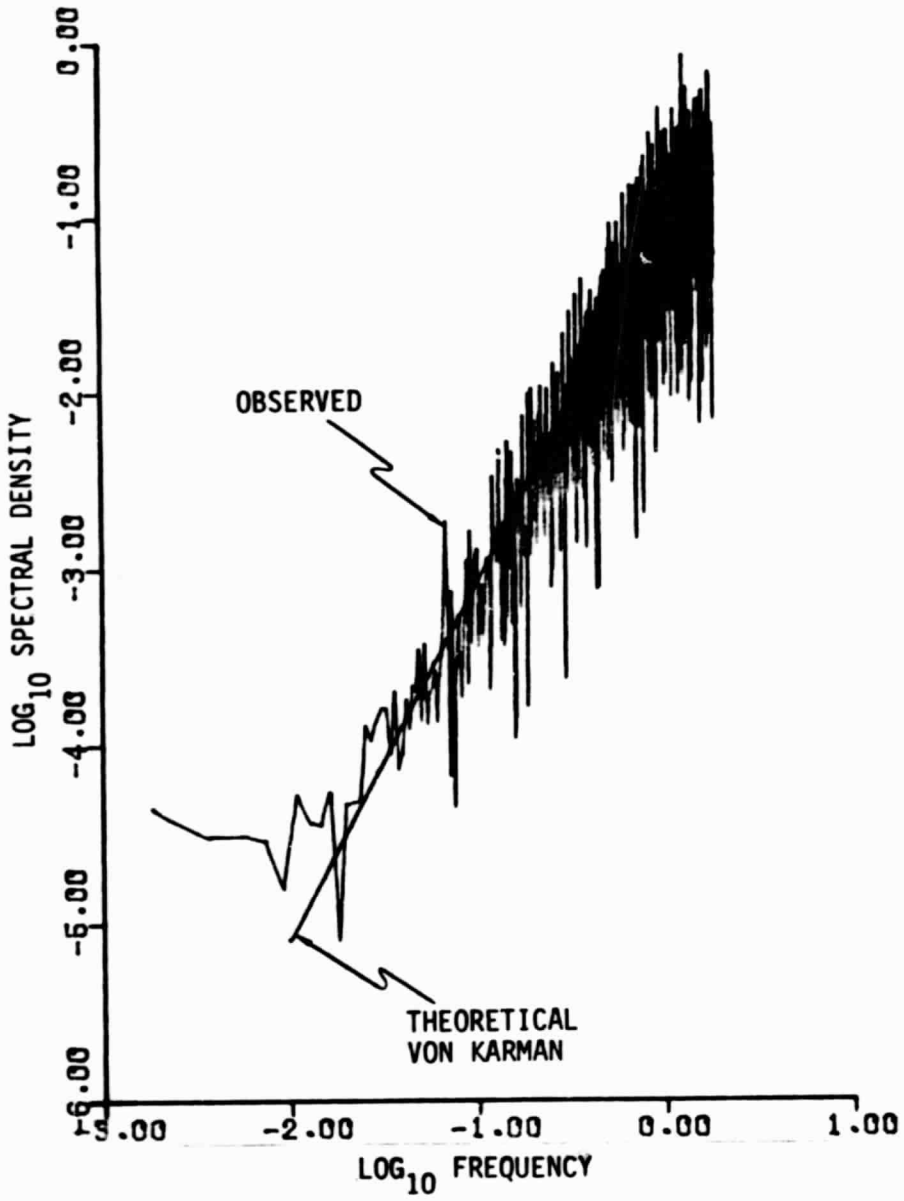


Figure C-25. $\partial u_3/\partial x_1$ - Gust Gradient Spectrum, Altitude Band #1

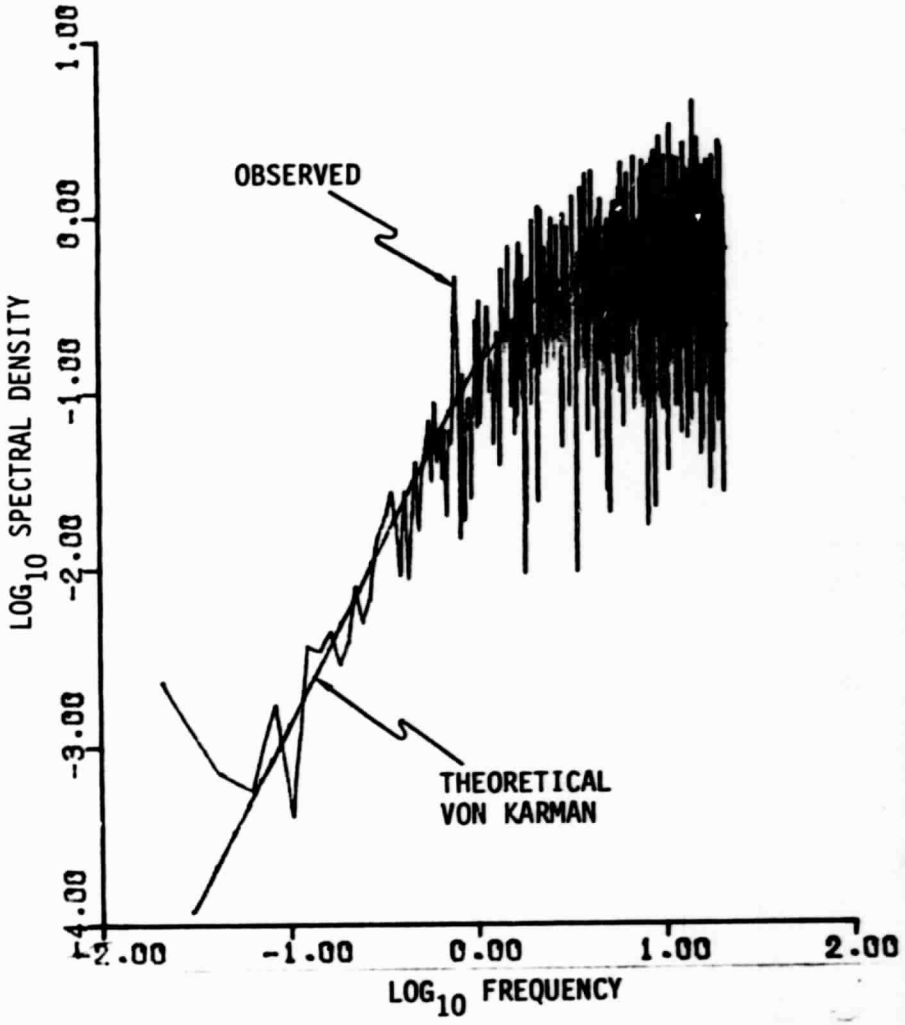


Figure C-26. $\partial u_3/\partial x_1$ - Gust Gradient Spectrum, Altitude Band #2

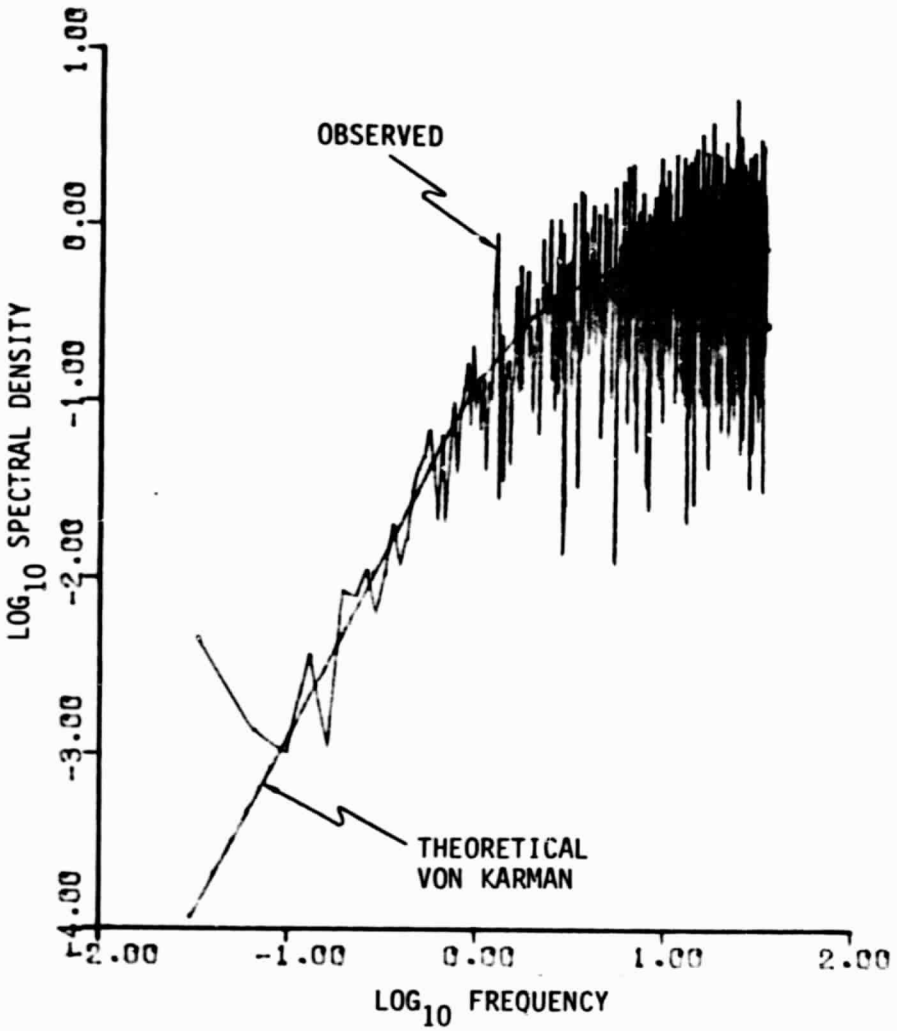


Figure C-27. $\partial u_3/\partial x_1$ - Gust Gradient Spectrum, Altitude Band #3

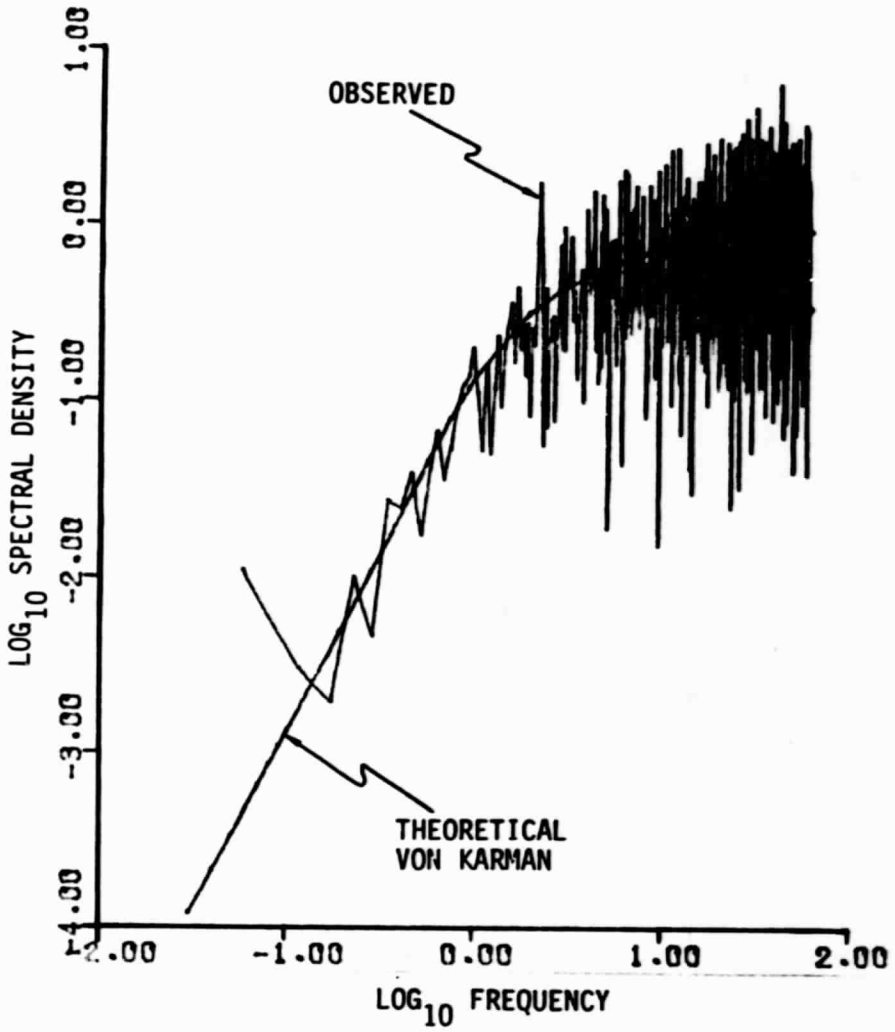


Figure C-28. $\partial u_3/\partial x_1$ - Gust Gradient Spectrum, Altitude Band #4

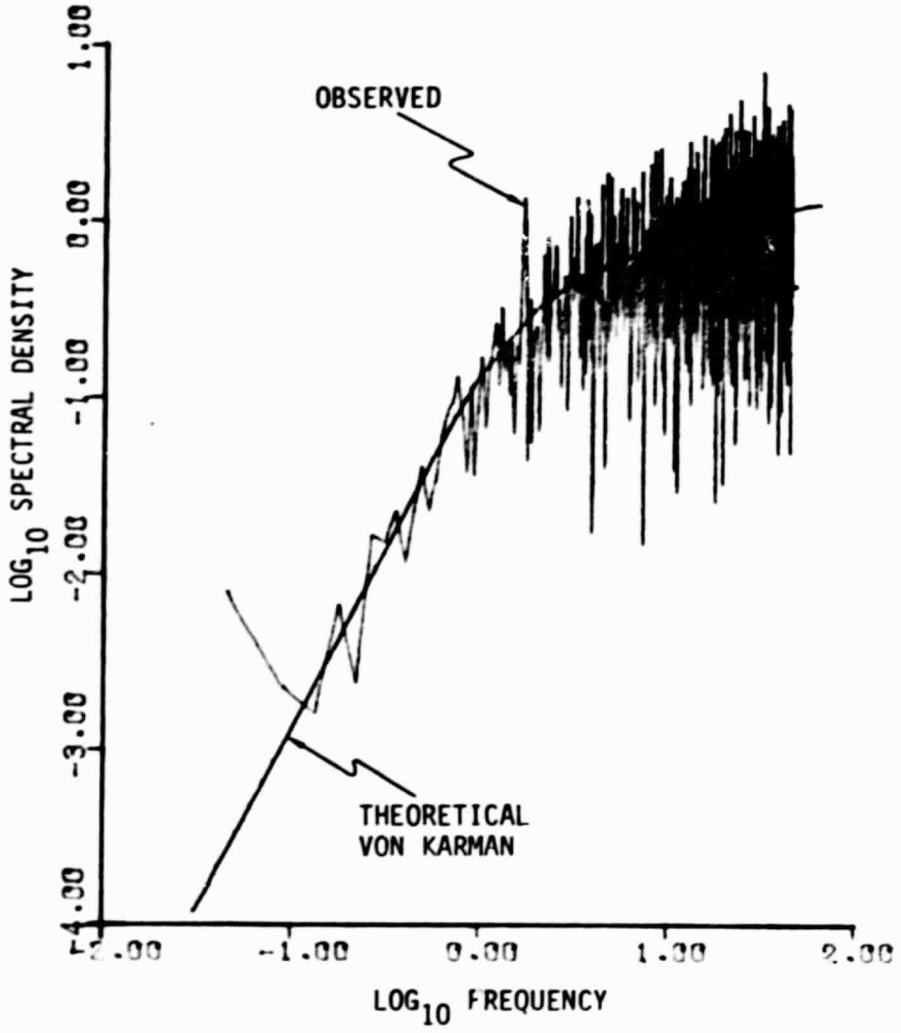


Figure C-29. $\partial u_3/\partial x_1$ - Gust Gradient Spectrum, Altitude Band #5

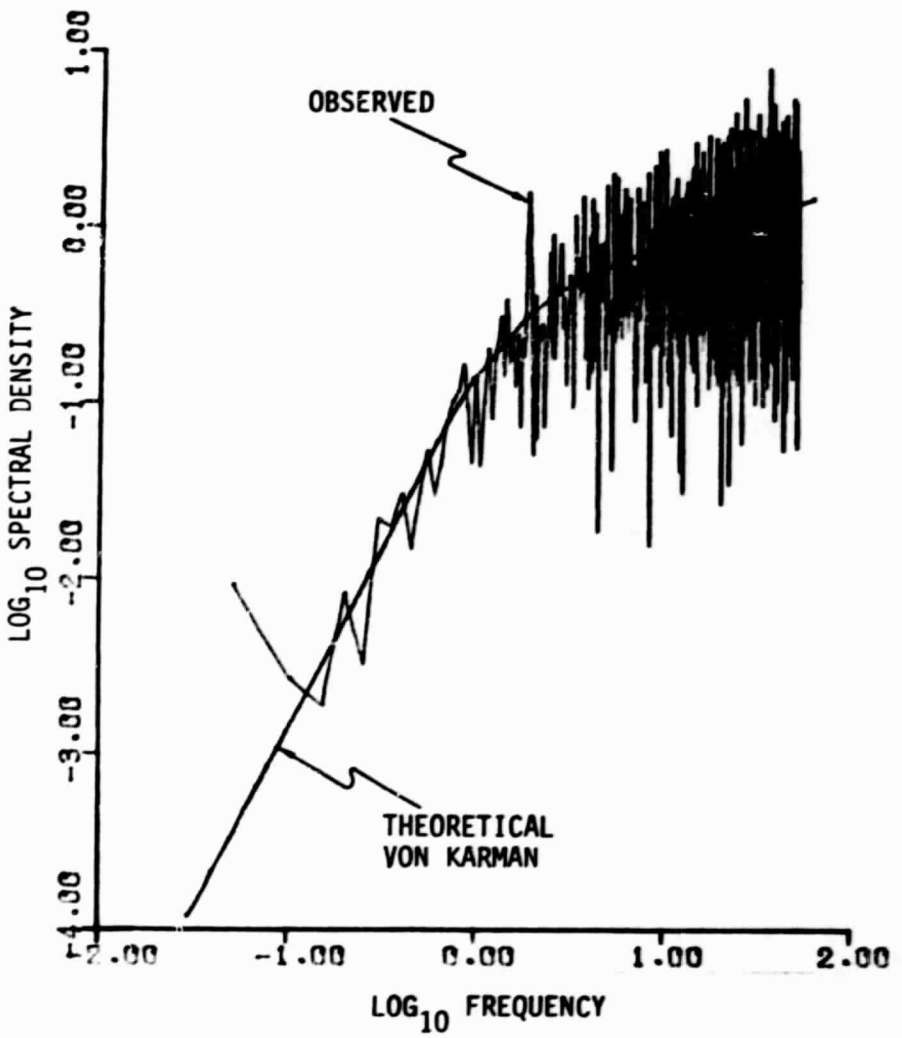


Figure C-30. $\partial u_3/\partial x_1$ - Gust Gradient Spectrum, Altitude Band #6

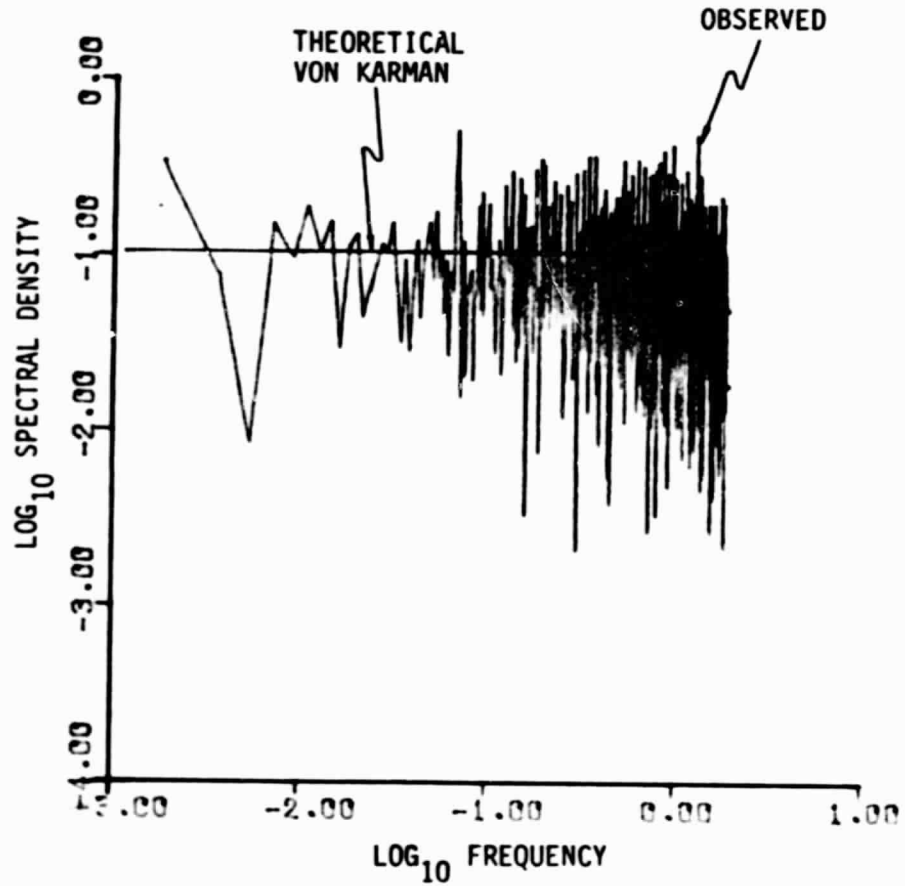


Figure C-31. $\partial u_3/\partial x_2$ - Gust Gradient Spectrum, Altitude Band #1

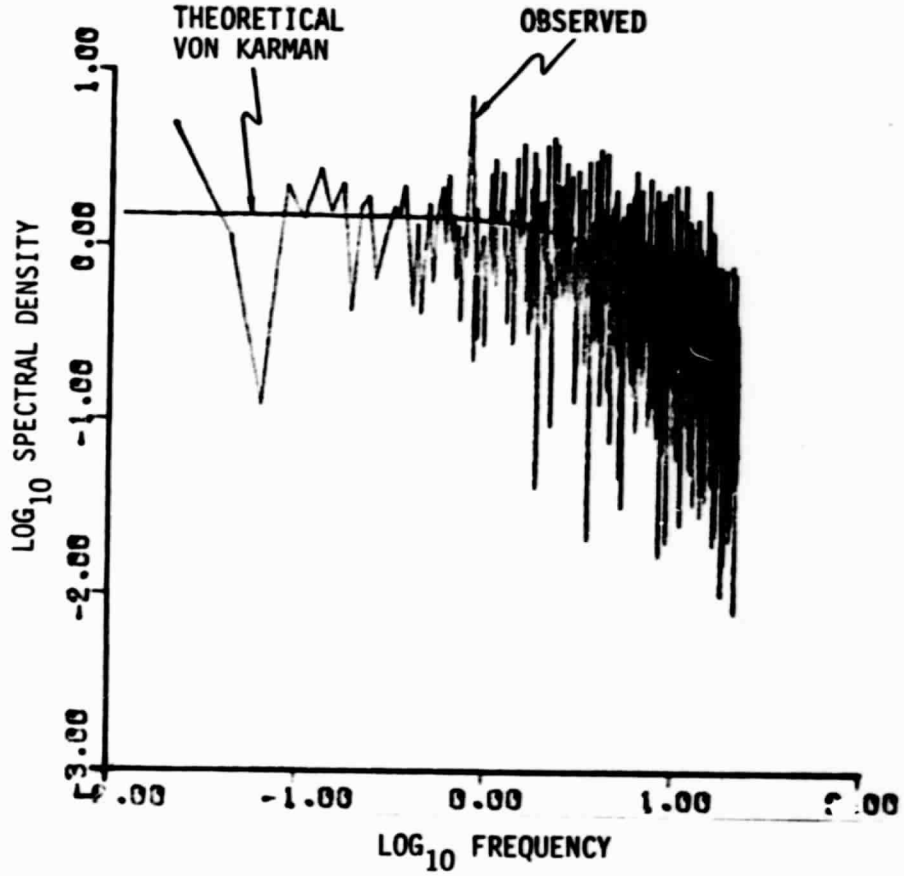


Figure C-32. $\partial u_3/\partial x_2$ - Gust Gradient Spectrum, Altitude Band #2

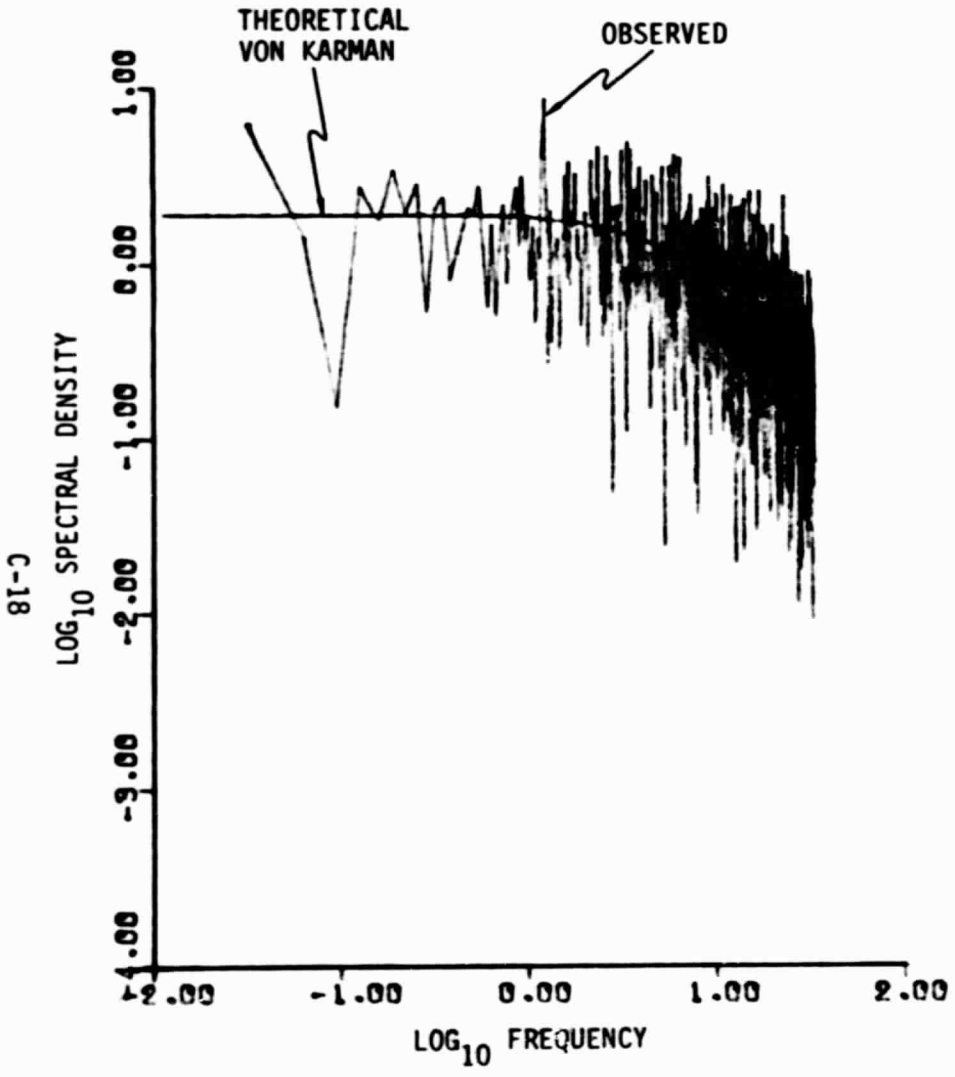


Figure C-33. $\partial u_3/\partial x_2$ - Gust Gradient Spectrum, Altitude Band #3

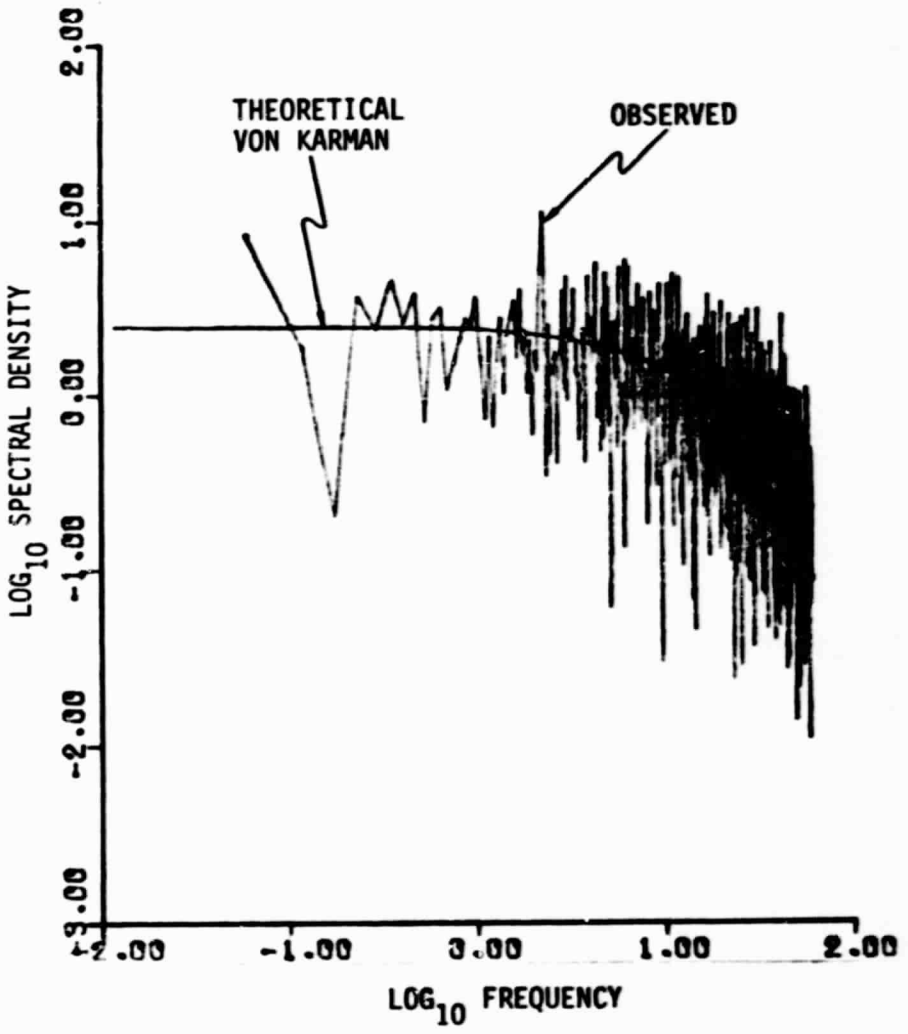


Figure C-34. $\partial u_3/\partial x_2$ - Gust Gradient Spectrum, Altitude Band #4

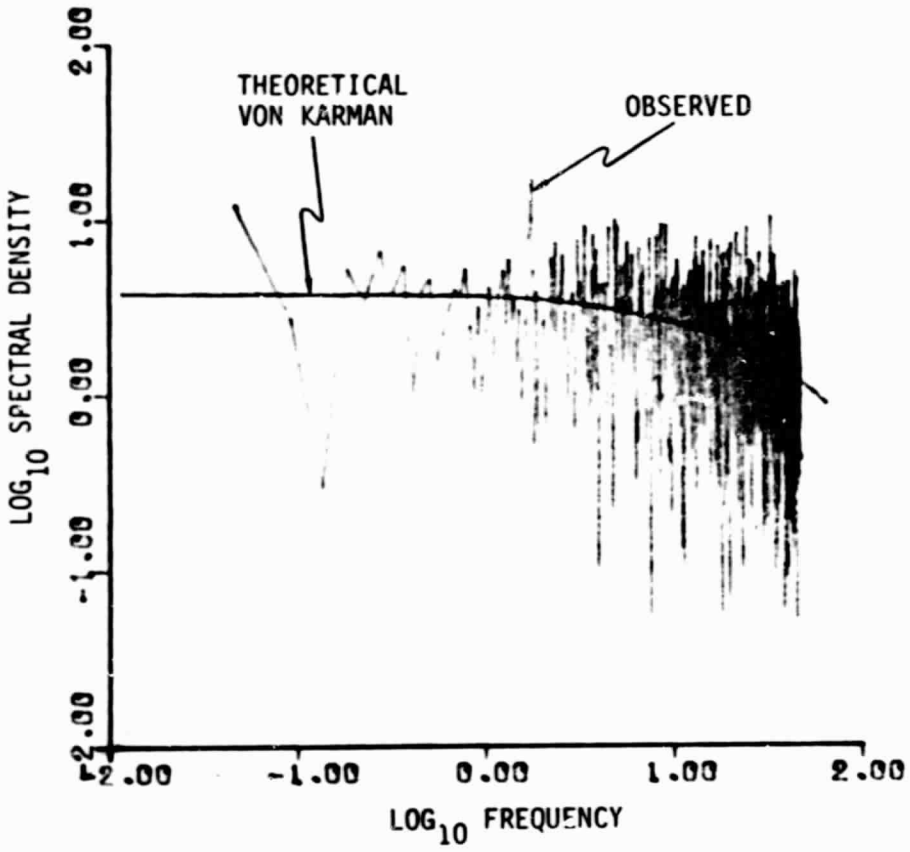


Figure C-35. $\partial u_3/\partial x_2$ - Gust Gradient Spectrum, Altitude Band #5

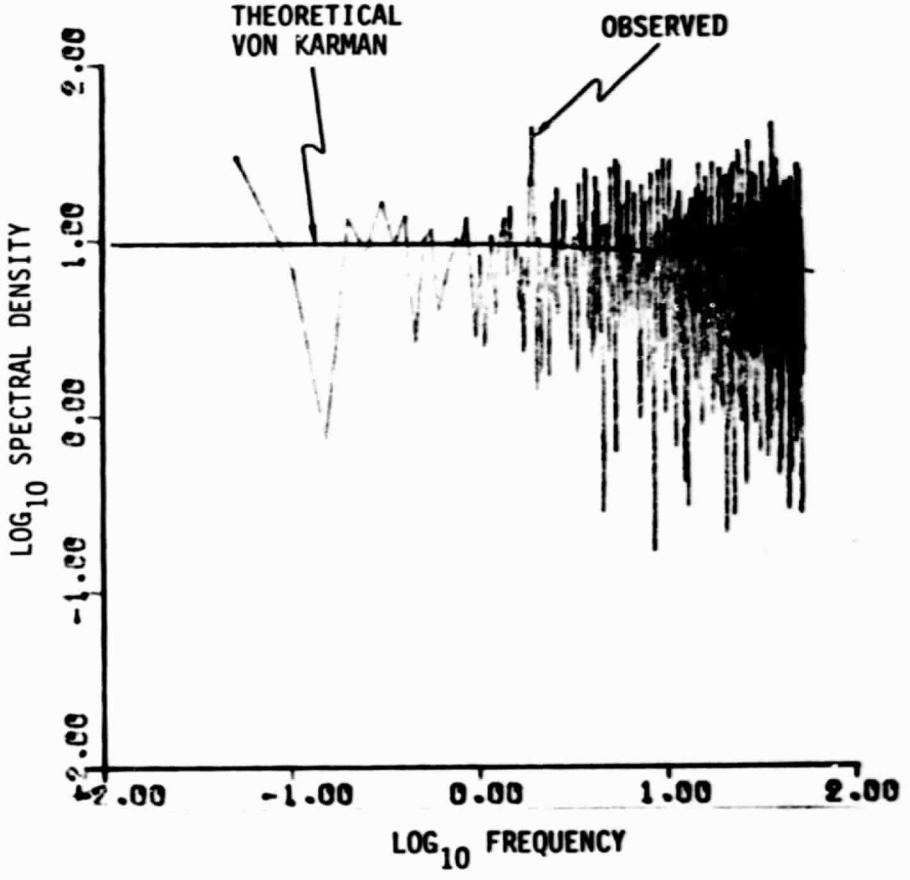


Figure C-36. $\partial u_3/\partial x_2$ - Gust Gradient Spectrum, Altitude Band #6

# APPENDIX D

## STATISTICAL ANALYSIS OF SIMULATED TURBULENCE

By means of standard statistical analysis procedures each of the SSTT has been analyzed to determine its mean value, standard deviation, and probability density distribution*. The resulting mean values are presented in Table D-1 while Table D-2 contains the resulting standard deviations. As expected all mean values were near zero. The standard deviations represent the square root of the energy content. The ratio of the theoretical energy content (from Table 2-5) to the square of the corresponding standard deviation (from Table D-2) is presented in Table D-3. The agreement appears quite satisfactory.

The gust and gust gradient probability density distributions are presented in Figures D-1 through D-36 in accordance with Table D-4. In each figure the corresponding theoretical normal distribution is also presented. The results indicate that both the gust and gust gradient time series are very close to normal distributions.

TABLE D-1. MEAN VALUE OF GUST AND GUST GRADIENTS

| SERIES TYPE | ALTITUDE BAND | | | | | |
|---|---|---|---|---|---|---|
| | 1 | 2 | 3 | 4 | 5 | 6 |
| $u_1$ | -.019295 | -.042050 | -.051852 | -.088142 | -.0455 | -.0464 |
| $u_2$ | -.010671 | -.029576 | -.0371 | -.049431 | -.0428 | -.0441 |
| $u_3$ | -.006806 | -.029652 | -.037043 | -.049370 | -.043788 | -.046637 |
| $\partial u_2/\partial x_1$ | -.000002 | -.001572 | -.002794 | -.005628 | -.172152 | -.206385 |
| $\partial u_3/\partial x_2$ | -.000001 | -.001591 | -.002798 | -.005649 | -.004293 | -.004893 |
| $\partial u_3/\partial x_1$ | -.005760 | -.073072 | -.103823 | -.160303 | -.171448 | -.288178 |

*The statistical analysis involved the first 4096 terms of each time series except for bands 5 and 6 for the $u_1$ and $u_2$ gusts. For these cases 8192 terms were used.

TABLE D-2. STANDARD DEVIATION OF GUST AND GUST GRADIENTS

| SERIES TYPE | ALTITUDE BAND | | | | | |
|---|---|---|---|---|---|---|
| | 1 | 2 | 3 | 4 | 5 | 6 |
| $u_1$ | .788959 | .927098 | .946351 | .964271 | .99888 | .99996 |
| $u_2$ | .707845 | .925201 | .94619 | .964152 | .99764 | .99863 |
| $u_3$ | .524571 | .915606 | .938552 | .958985 | .961845 | .967651 |
| $\partial u_2/\partial x_1$ | .766627 | 3.625937 | 4.976618 | 7.356808 | 41.717292 | 48.052734 |
| $\partial u_3/\partial x_2$ | .390512 | 3.488677 | 4.758426 | 7.037516 | 6.458092 | 7.216648 |
| $\partial u_3/\partial x_1$ | .394539 | 3.508280 | 4.784378 | 7.075349 | 9.778736 | 19.790119 |

TABLE D-3. RATIO OF THE THEORETICAL ENERGY CONTENT* TO THE SQUARE OF THE OBSERVED STANDARD DEVIATION†

| SERIES TYPE | ALTITUDE BAND | | | | | |
|---|---|---|---|---|---|---|
| | 1 | 2 | 3 | 4 | 5 | 6 |
| $u_1$ | 1.0001 | 1.0000 | 1.0000 | 1.0000 | .9999 | 1.0001 |
| $u_2$ | .9999 | 1.0000 | .9999 | 1.0000 | 1.0000 | 1.0000 |
| $u_3$ | 1.0001 | 1.0000 | 1.0000 | 1.0001 | 1.0000 | .9999 |
| $\partial u_2/\partial x_1$ | 1.0000 | 1.0000 | 1.0000 | 1.0000 | .9998 | 1.0000 |
| $\partial u_3/\partial x_2$ | 1.0000 | 1.0000 | 1.0000 | 1.0000 | 1.0001 | 1.0000 |
| $\partial u_3/\partial x_1$ | 1.0002 | 1.0000 | 1.0000 | 1.0000 | 1.0000 | .9999 |

*Theoretical energy content taken from Table 2-3.

†Observed standard deviation taken from Table D-2.

TABLE D-4. MATRIX OF STATISTICAL ANALYSIS FIGURES

| SERIES TYPE | ALTITUDE BAND | | | | | |
|---|---|---|---|---|---|---|
| | 1 | 2 | 3 | 4 | 5 | 6 |
| $u_1$ | D-1 | D-2 | D-3 | D-4 | D-5 | D-6 |
| $u_2$ | D-7 | D-8 | D-9 | D-10 | D-11 | D-12 |
| $u_3$ | D-13 | D-14 | D-15 | D-16 | D-17 | D-18 |
| $\partial u_2/\partial x_1$ | D-19 | D-20 | D-21 | D-22 | D-23 | D-24 |
| $\partial u_3/\partial x_1$ | D-25 | D-26 | D-27 | D-28 | D-29 | D-30 |
| $\partial u_3/\partial x_2$ | D-31 | D-32 | D-33 | D-34 | D-35 | D-36 |

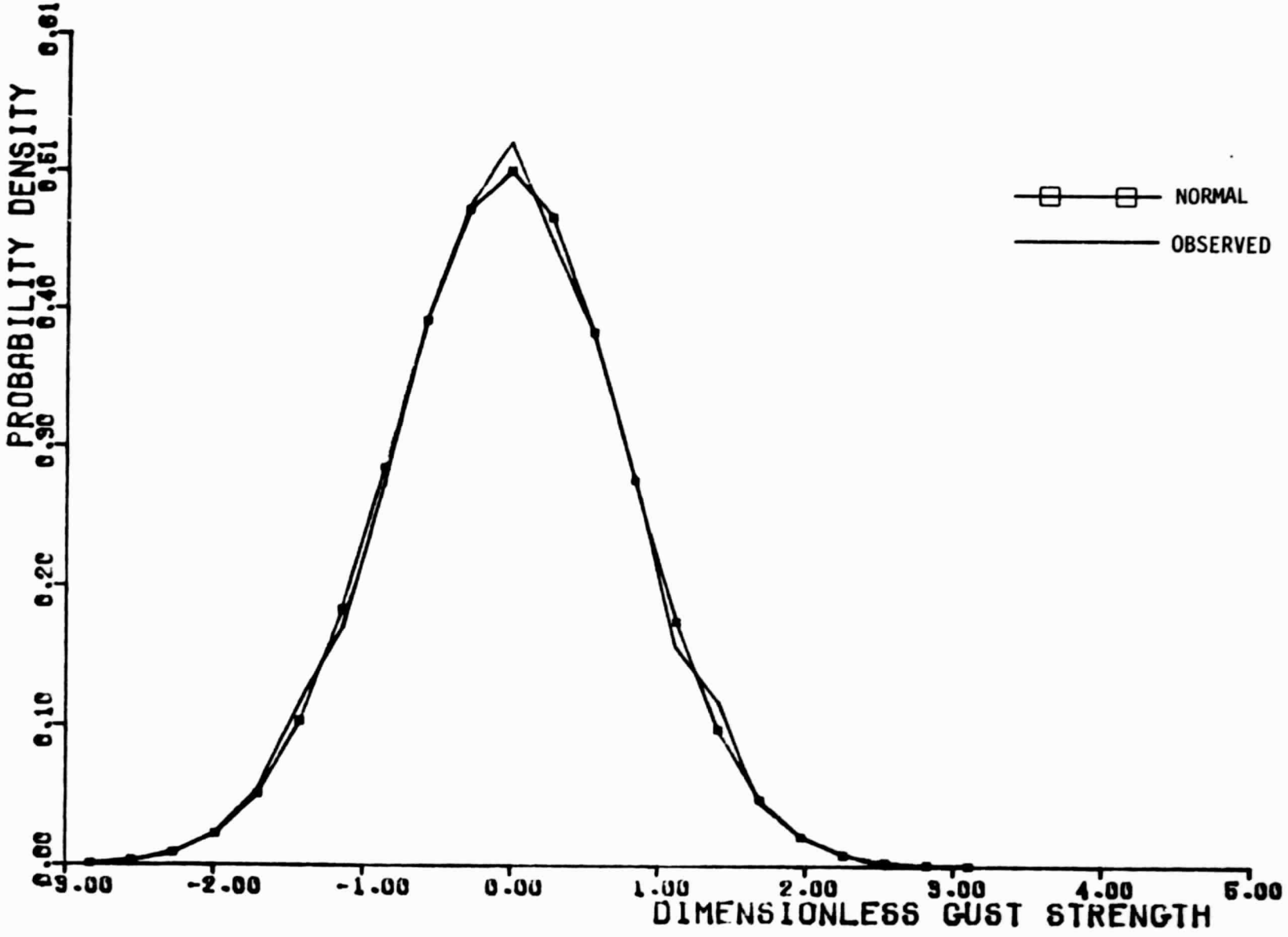


Figure D-1. $u_1$ - Gust Probability Density Distribution, Altitude Band #1

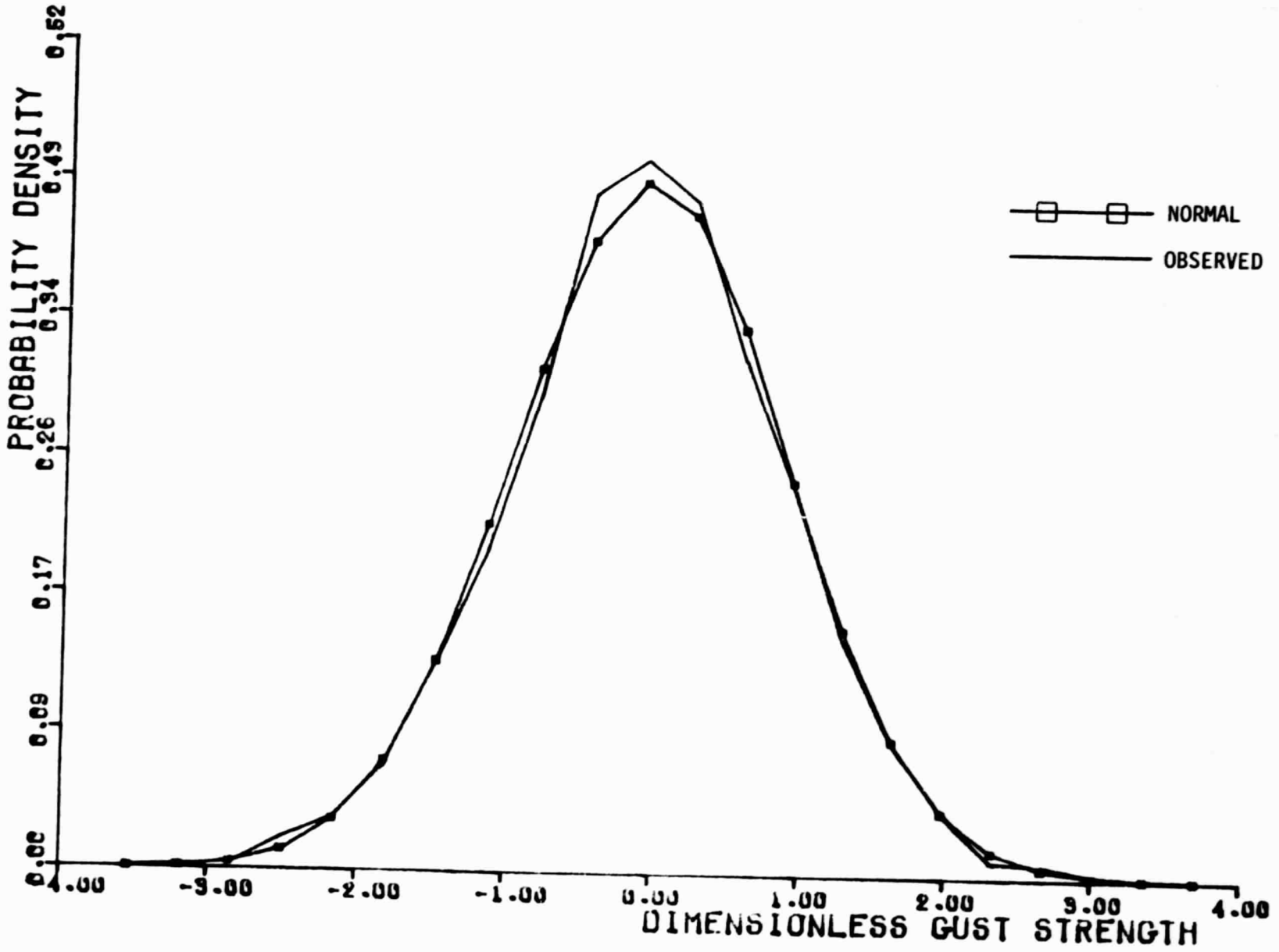


Figure D-2. $u_1$ - Gust Probability Density Distribution, Altitude Band #2

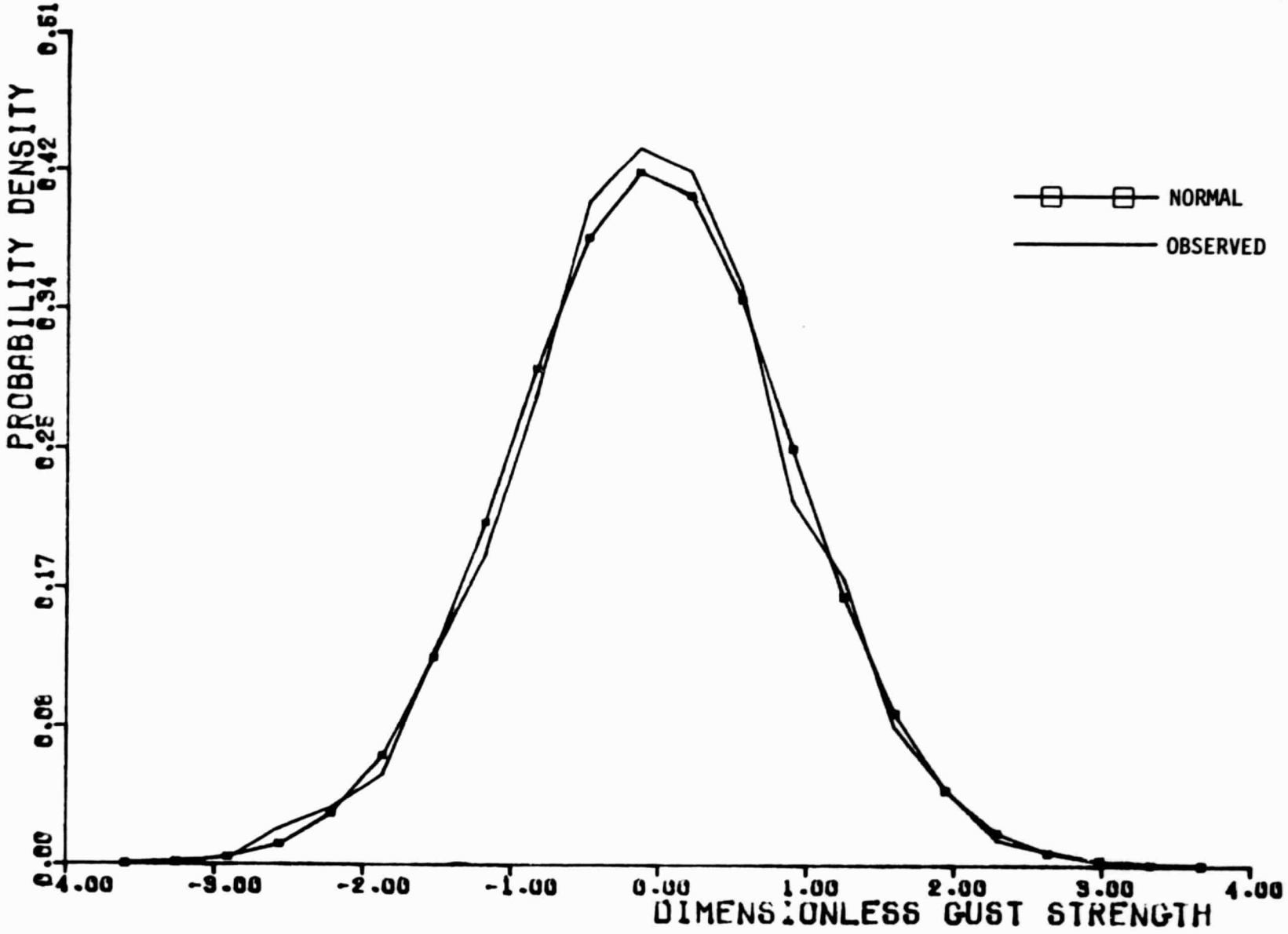


Figure D-3. $u_1$ - Gust Probability Density Distribution, Altitude Band #3

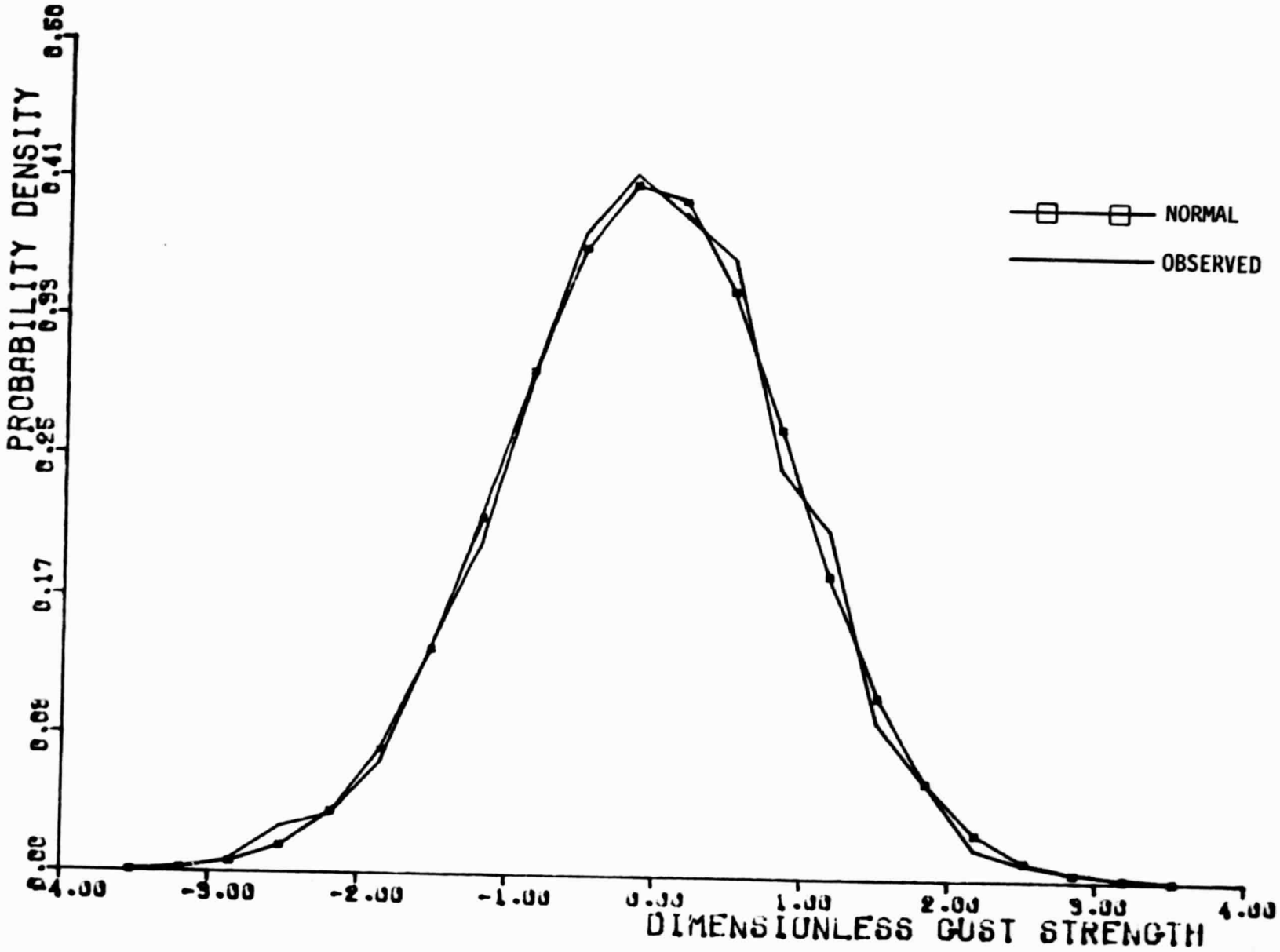


Figure D-4. $u_1$ - Gust Probability Density Distribution, Altitude Band #4

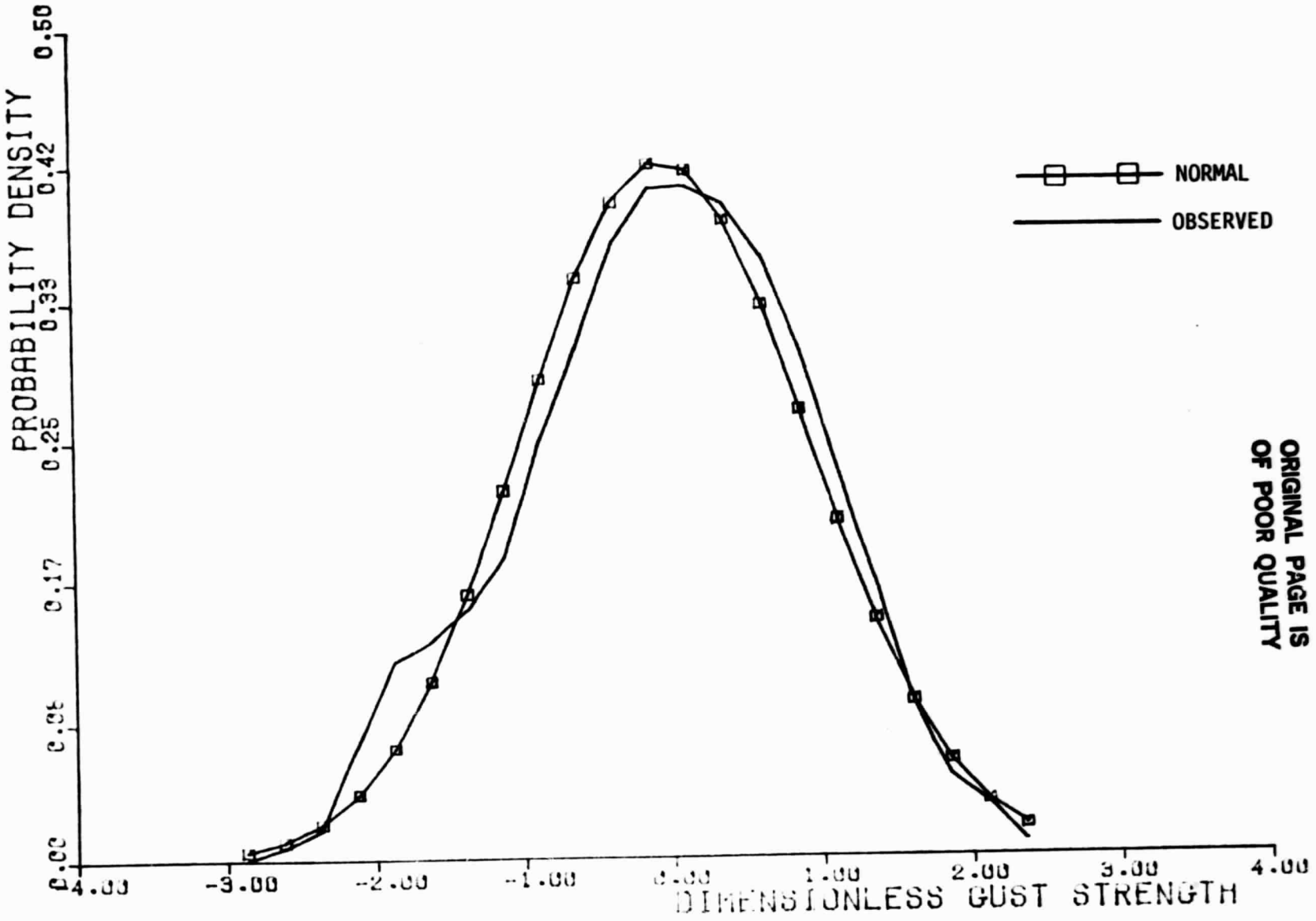




Figure D-5. $u_1$ - Gust Probability Density Distribution, Altitude Band #5

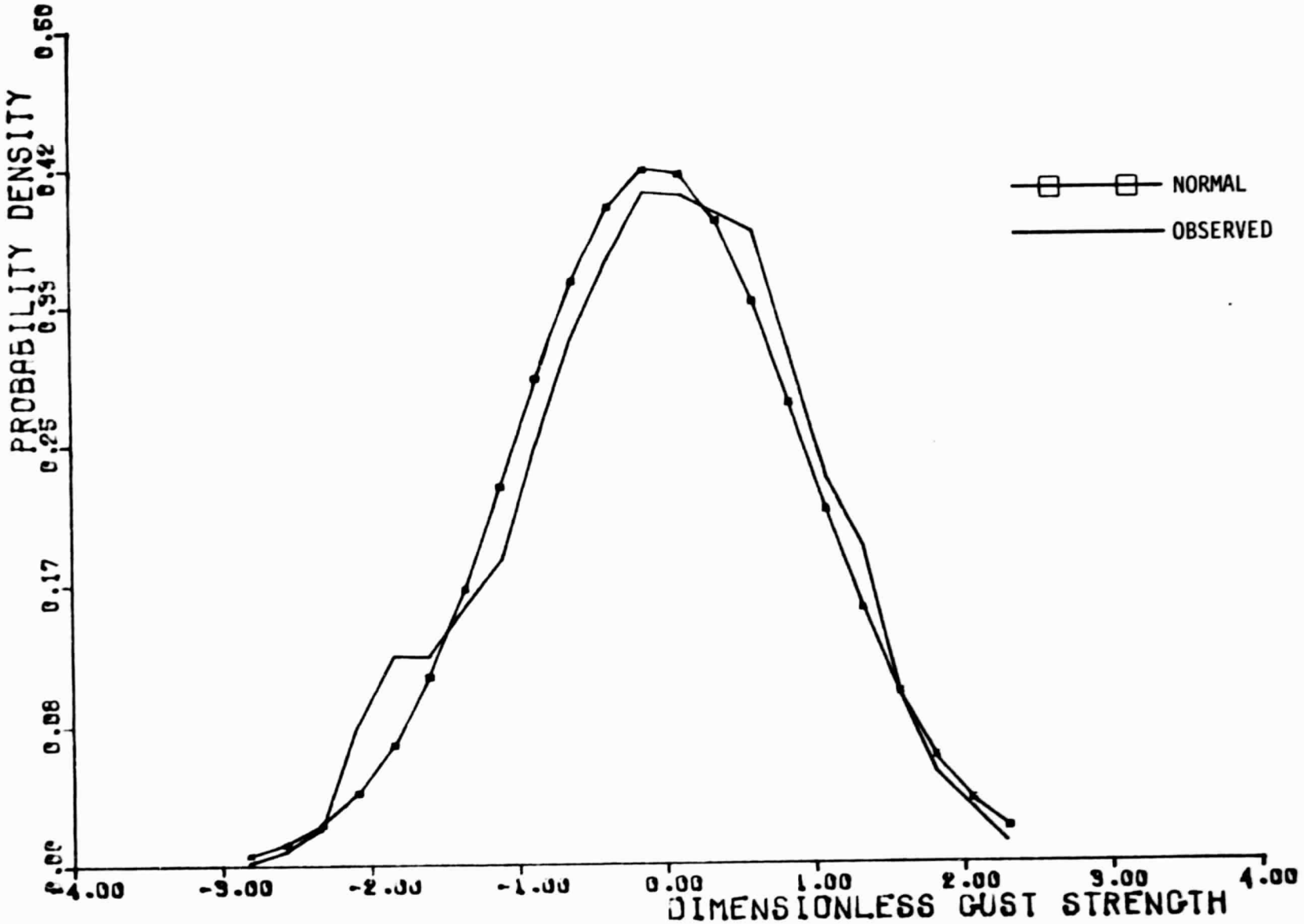


Figure D-6. $u_1$ - Gust Probability Density Distribution, Altitude Band #6

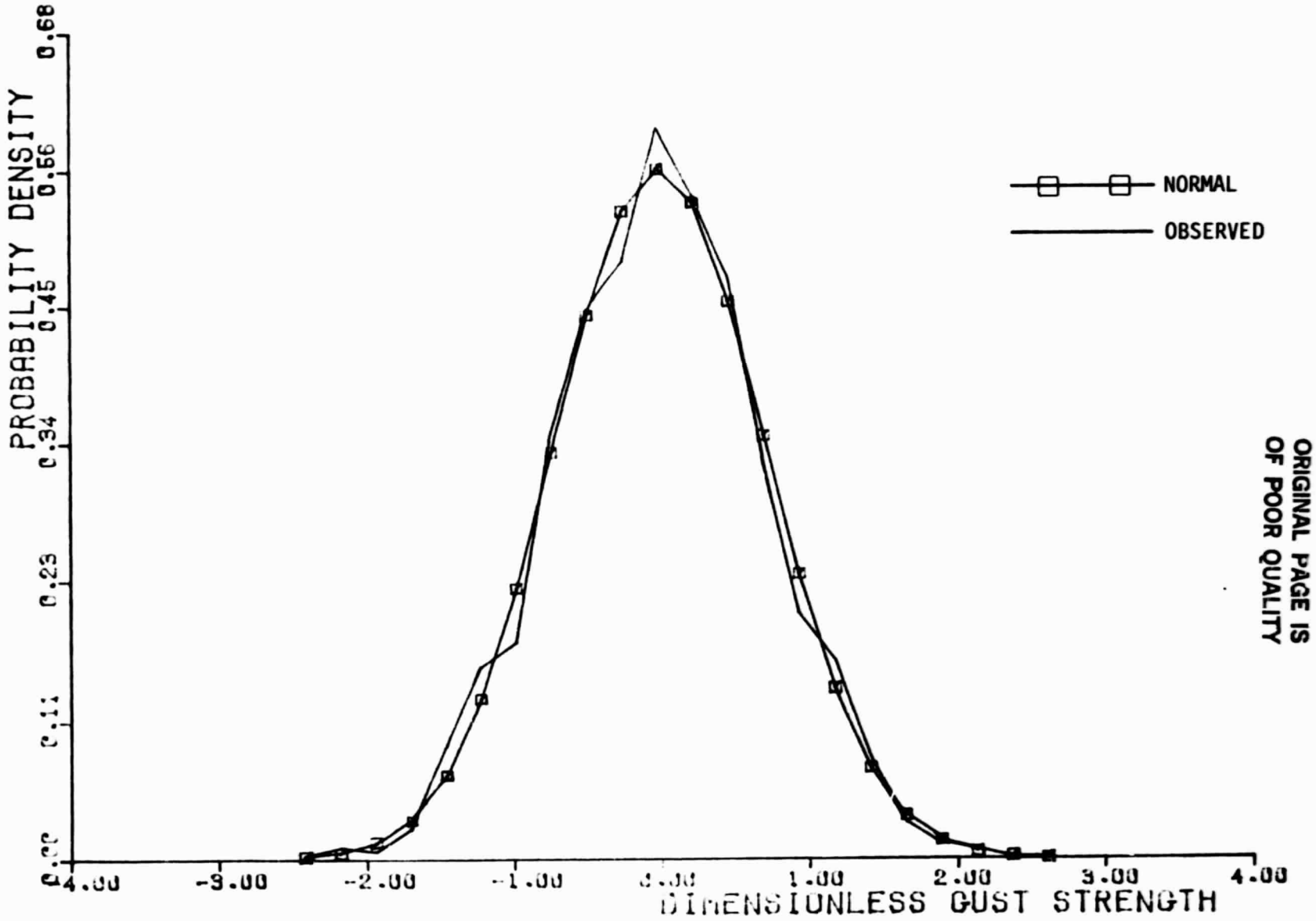






Figure D-7. $u_2$ - Gust Probability Density Distribution, Altitude Band #1

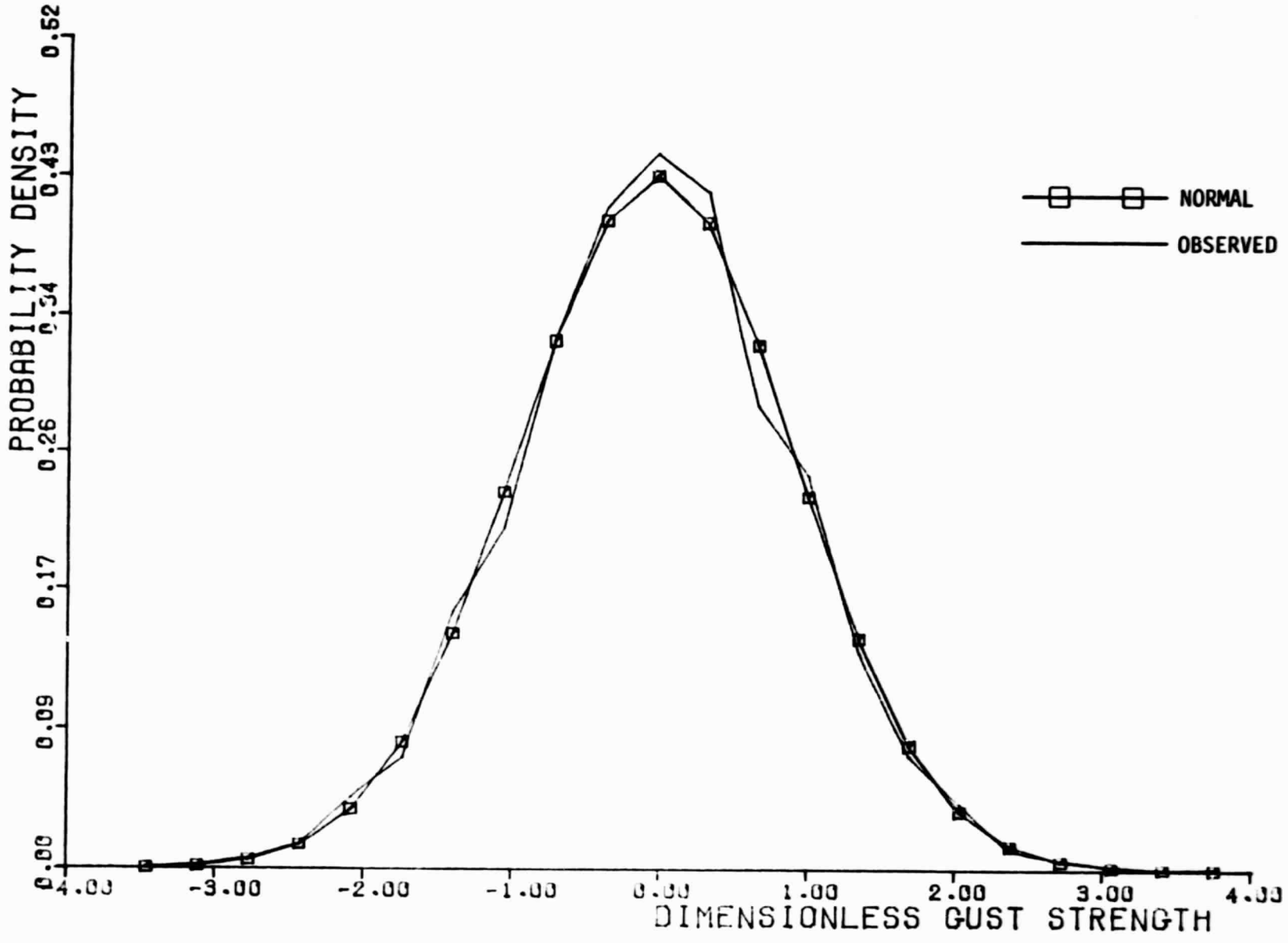


Figure D-8. $u_2$ - Gust Probability Density Distribution, Altitude Band #2

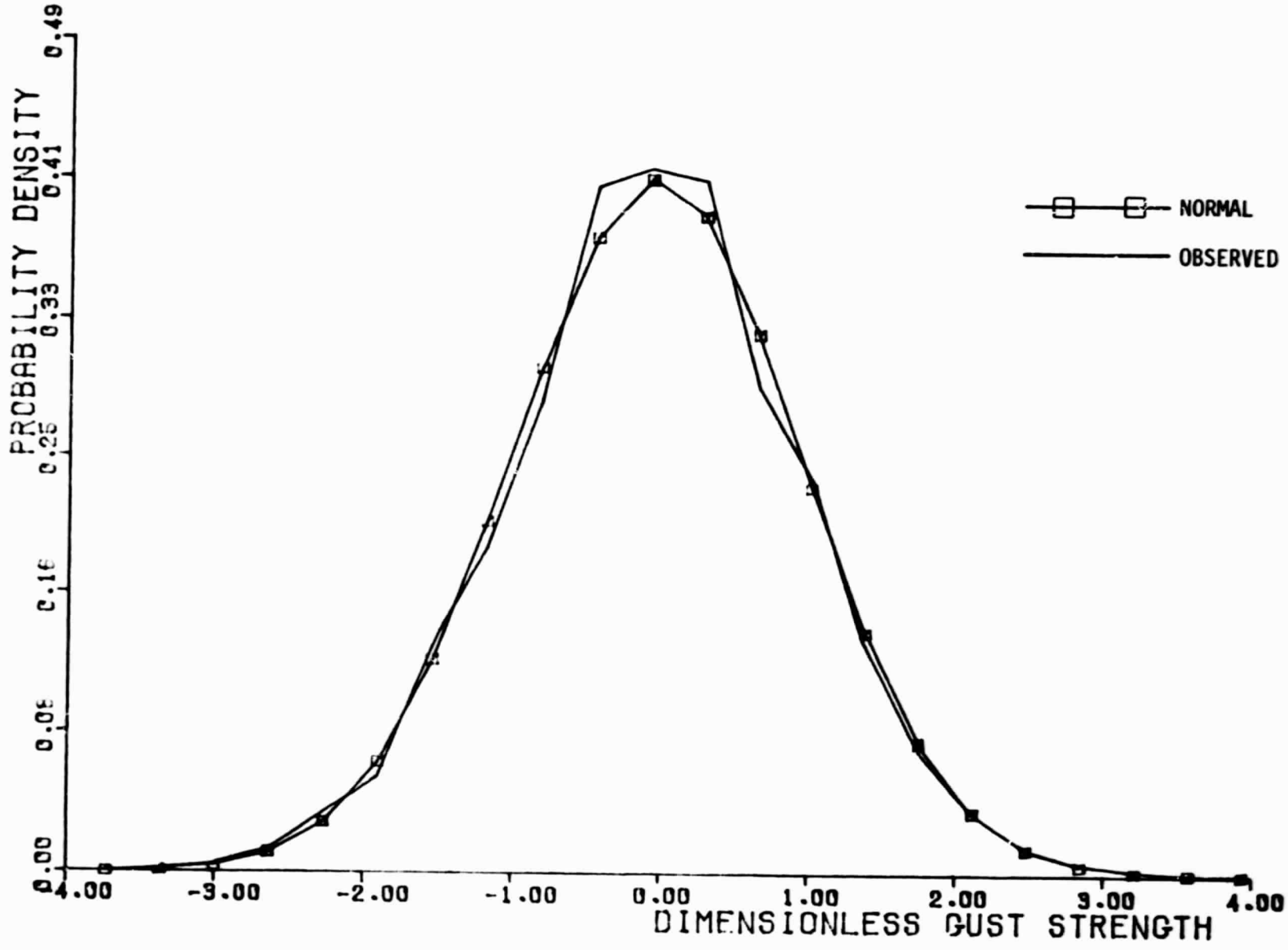


Figure D-9. $u_2$ - Gust Probability Density Distribution, Altitude Band #3

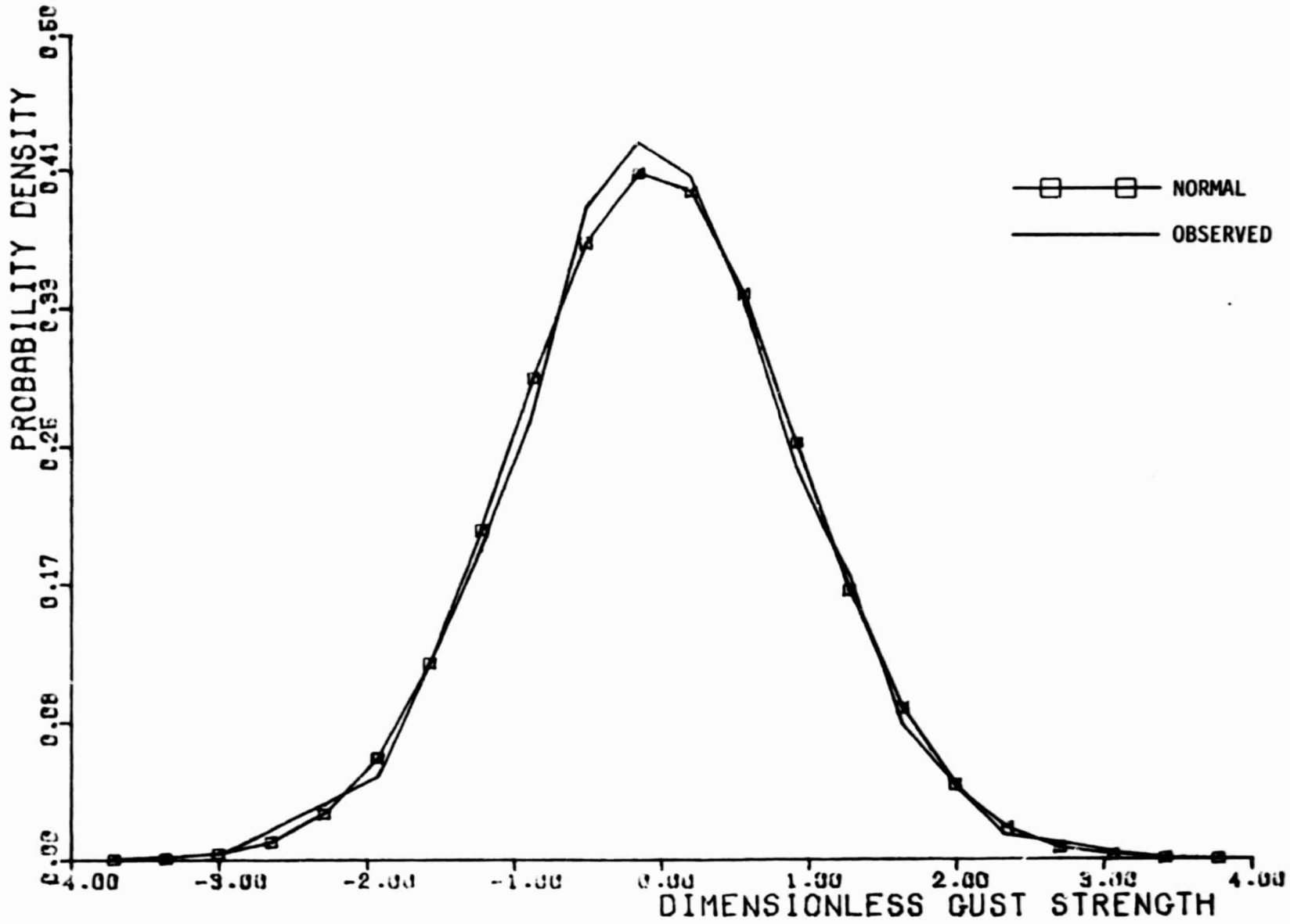


Figure D-10. $u_2$ - Gust Probability Density Distribution, Altitude Band #4

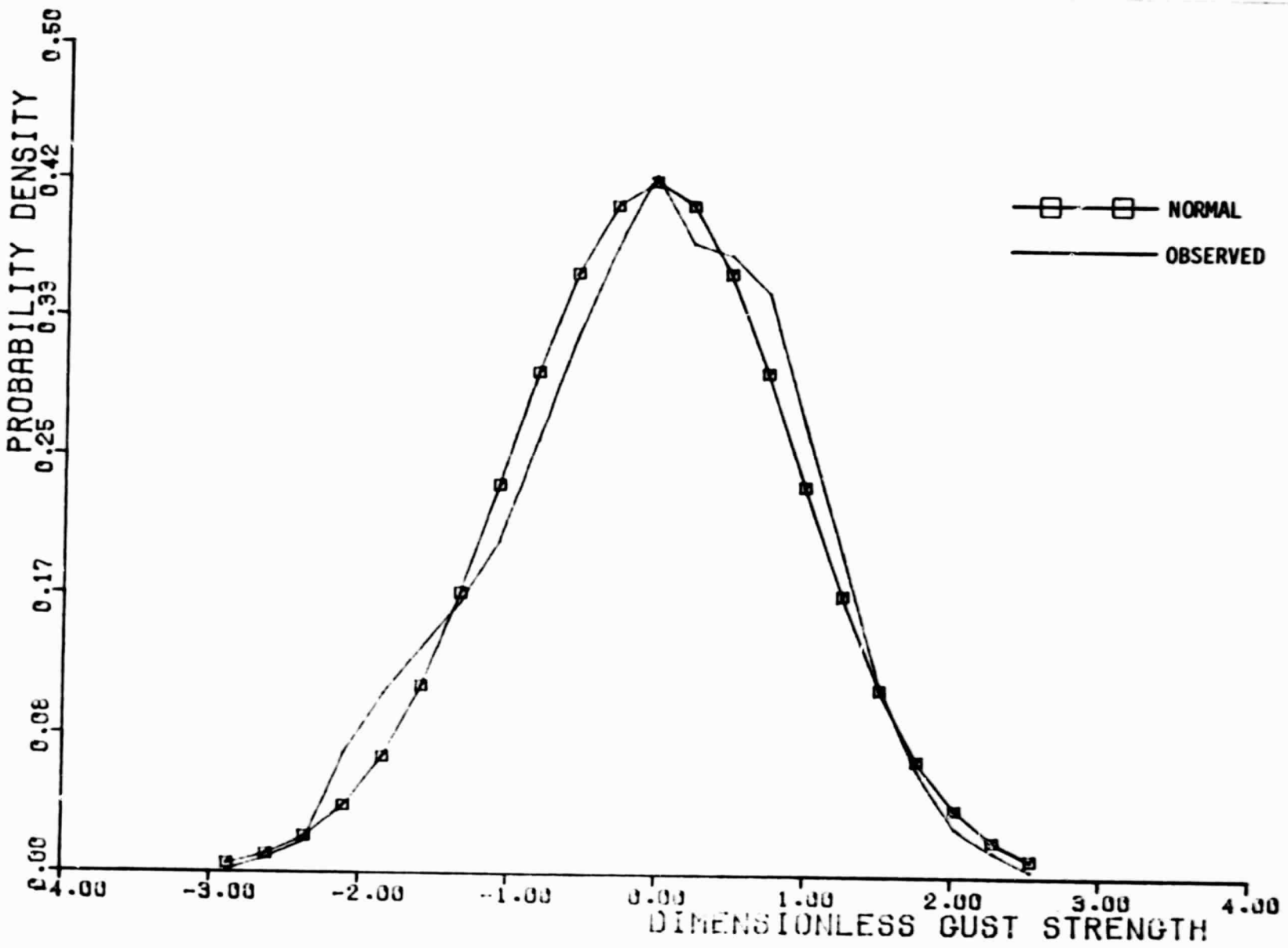


Figure D-11. $u_2$ - Gust Probability Density Distribution, Altitude Band #5

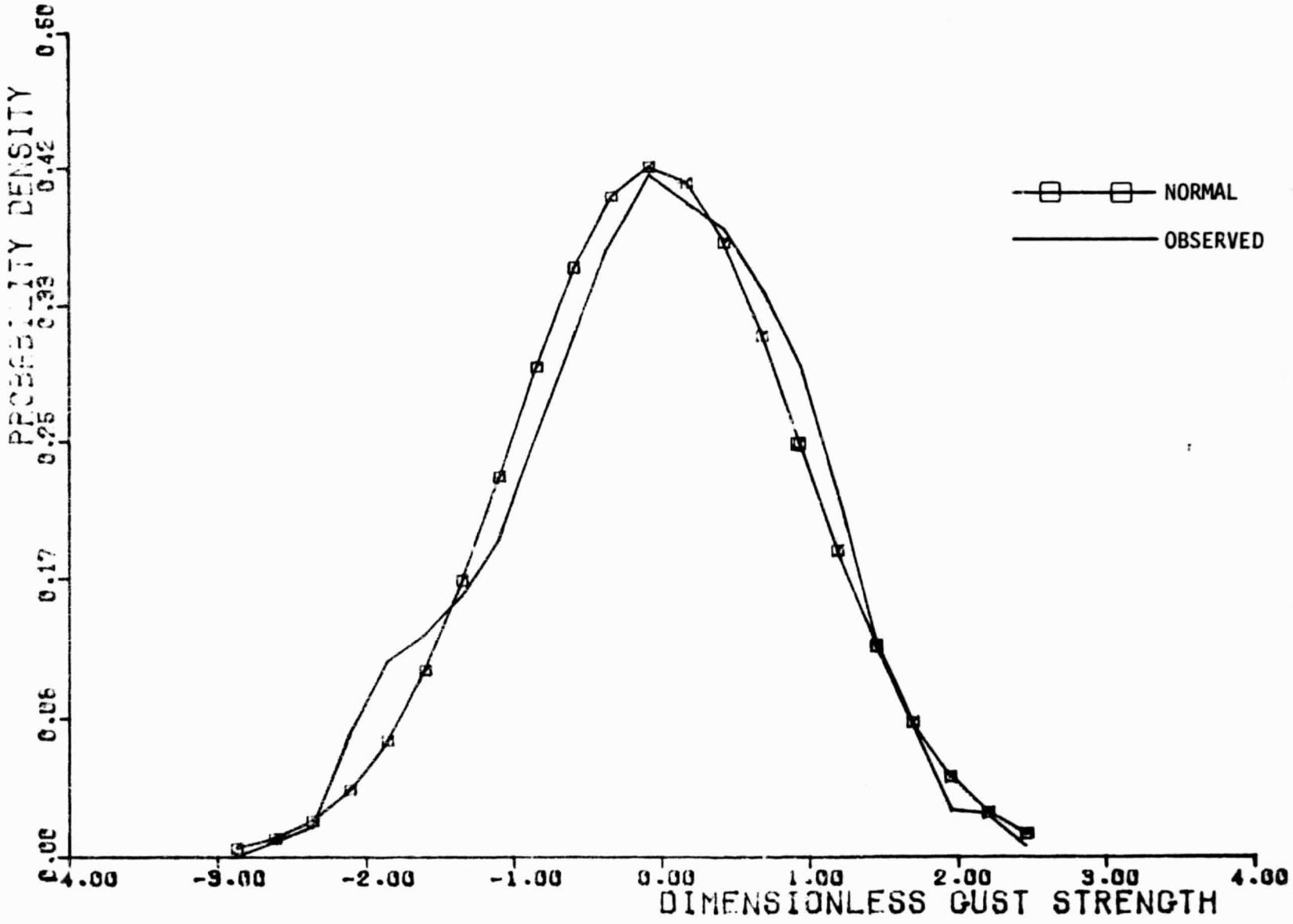


Figure D-12. $u_2$ - Gust Probability Density Distribution, Altitude Band #6

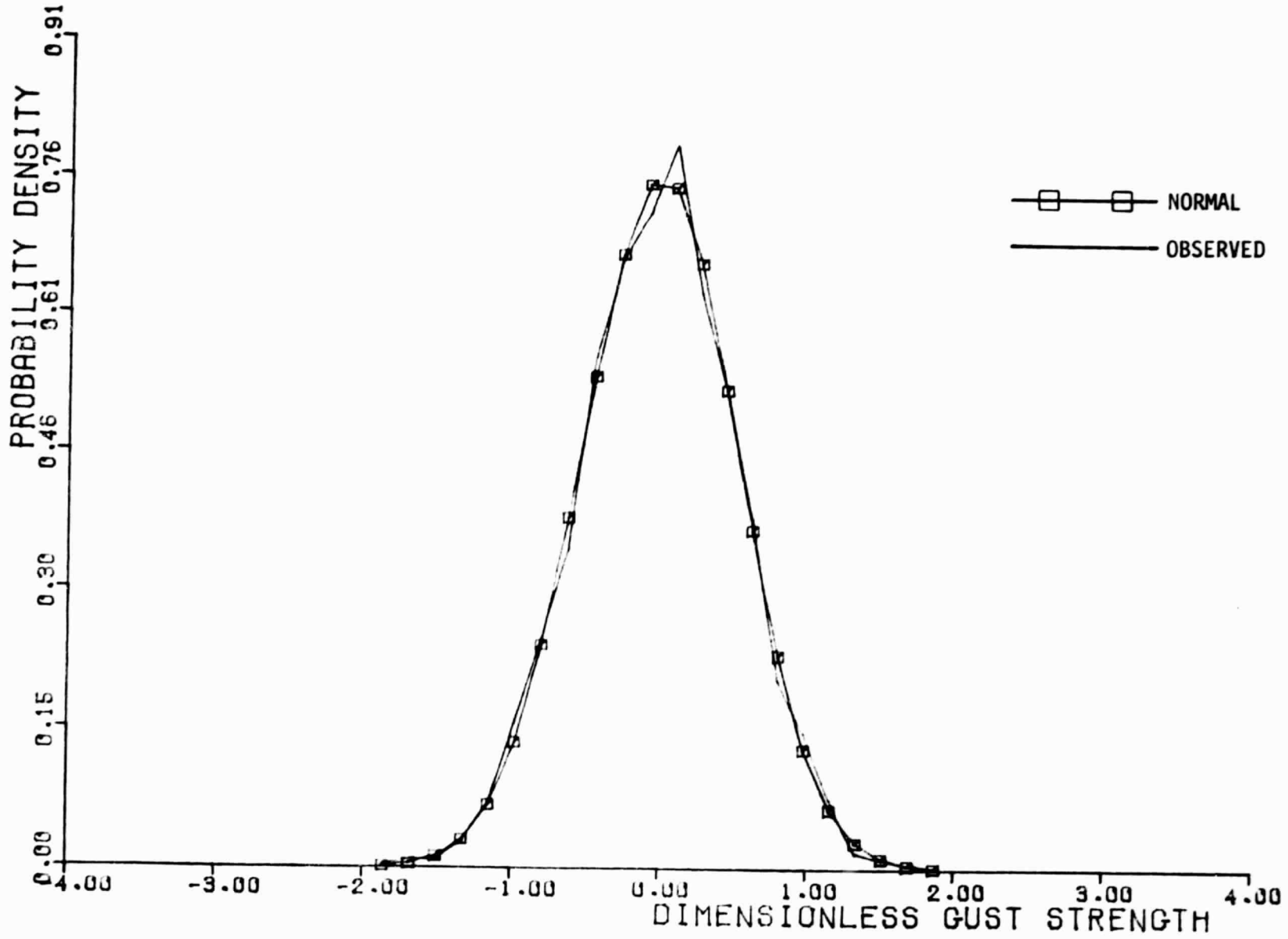


Figure D-13. $u_3$ - Gust Probability Density Distribution, Altitude Band #1

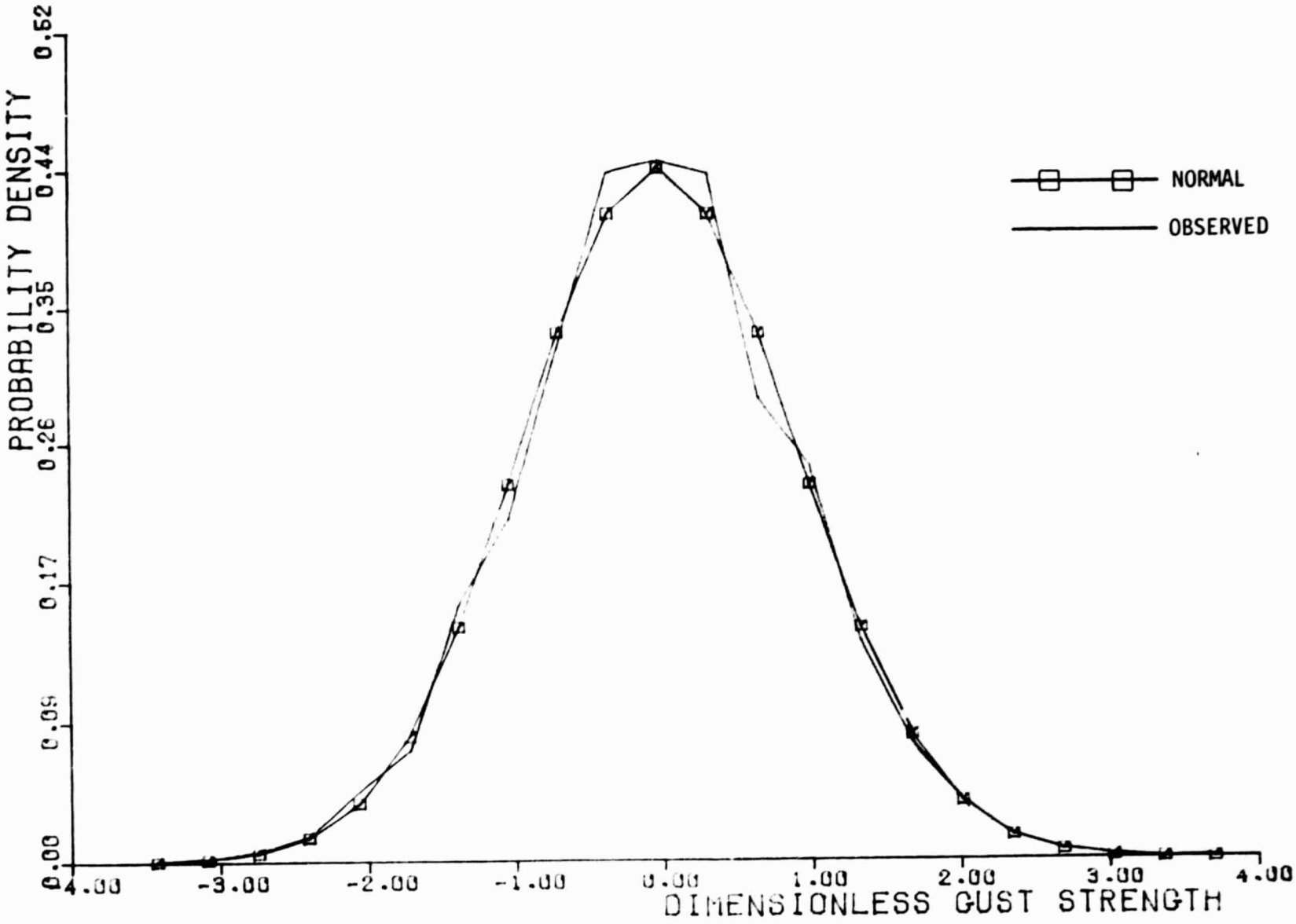


Figure D-14. $u_3$ - Gust Probability Density Distribution, Altitude Band #2

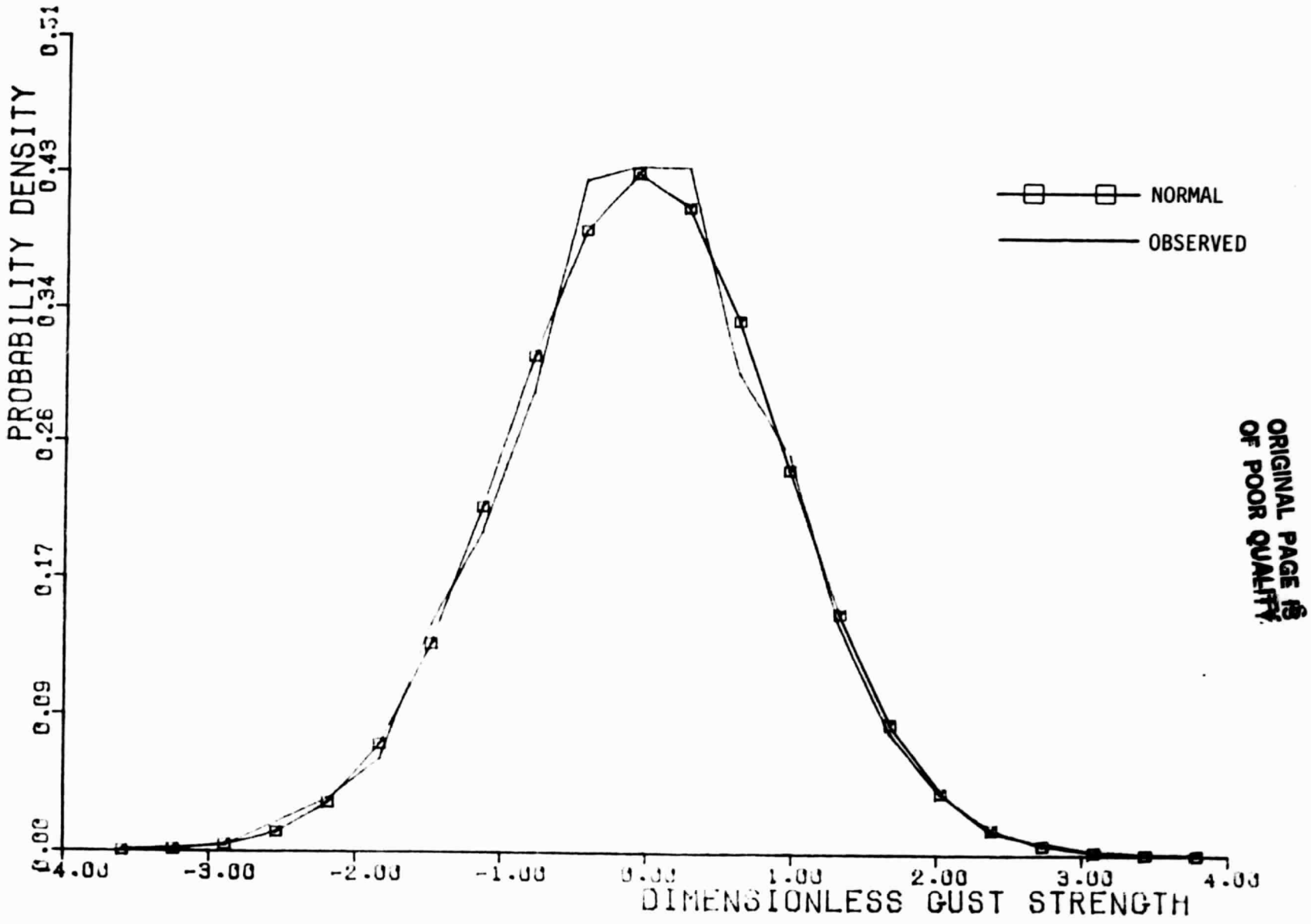




Figure D-15. $u_3$ - Gust Probability Density Distribution, Altitude Band #3

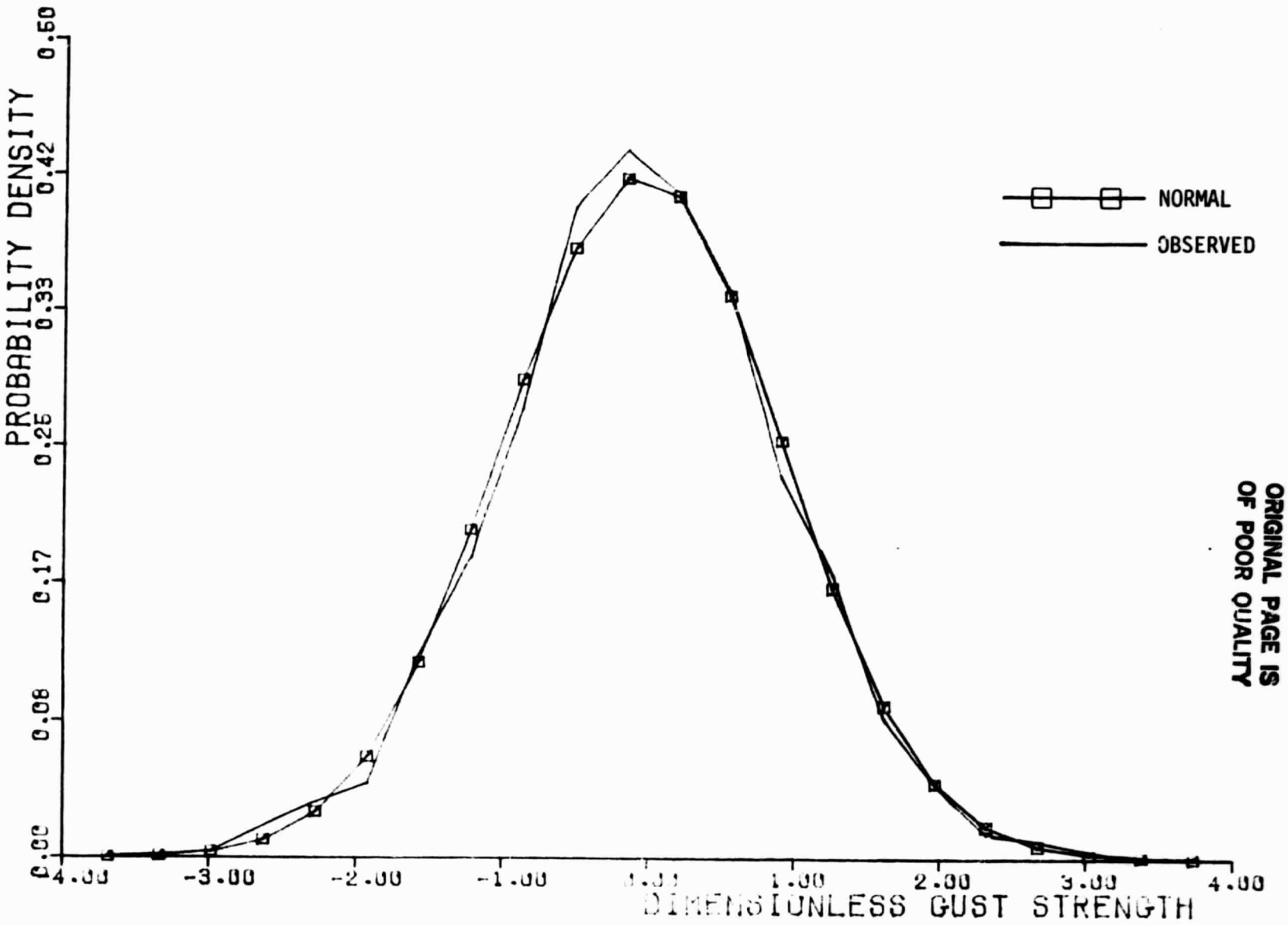




Figure D-16. $u_3$ - Gust Probability Density Distribution, Altitude Band #4

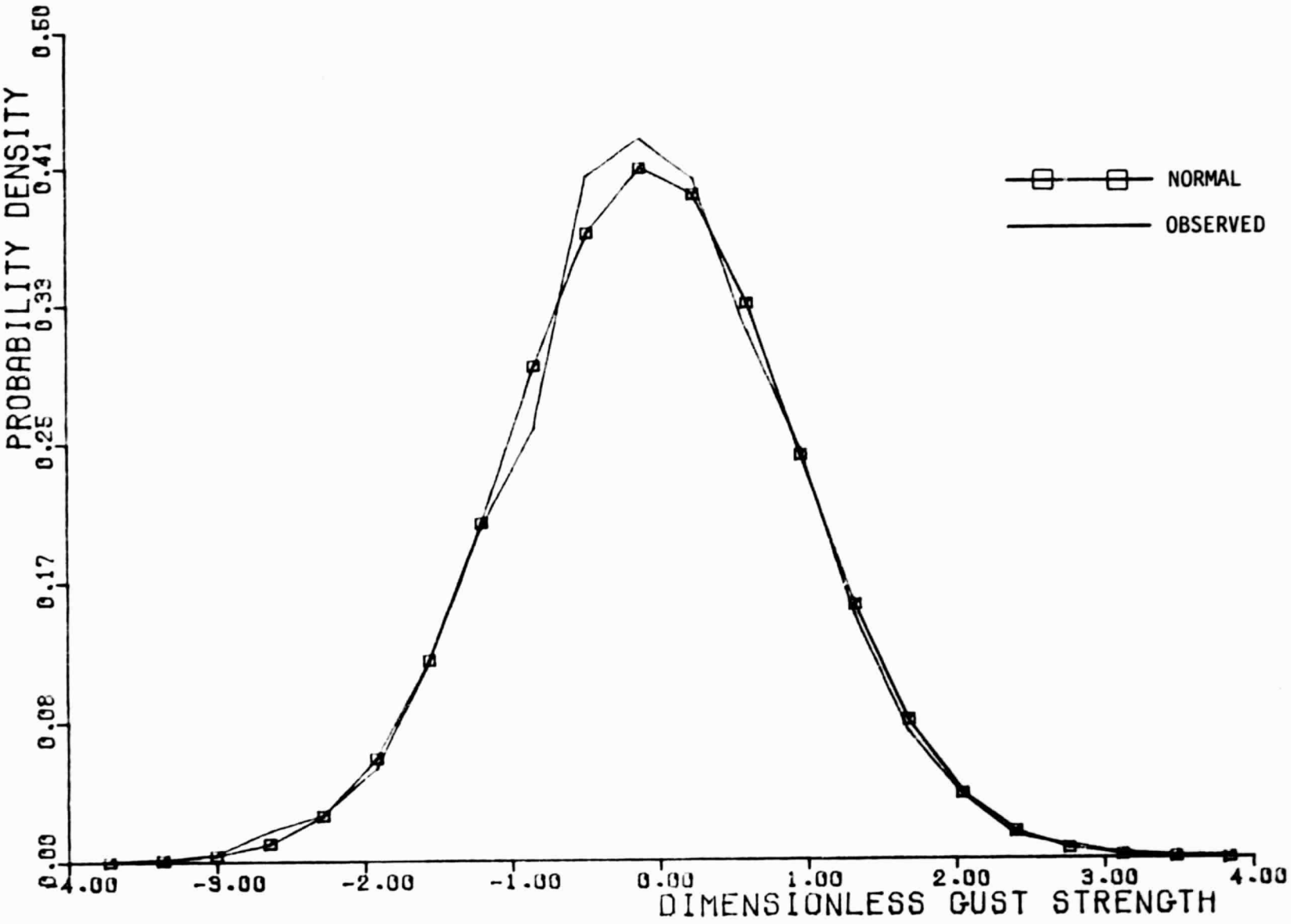


Figure D-17. $u_3$ - Gust Probability Density Distribution, Altitude Band #5

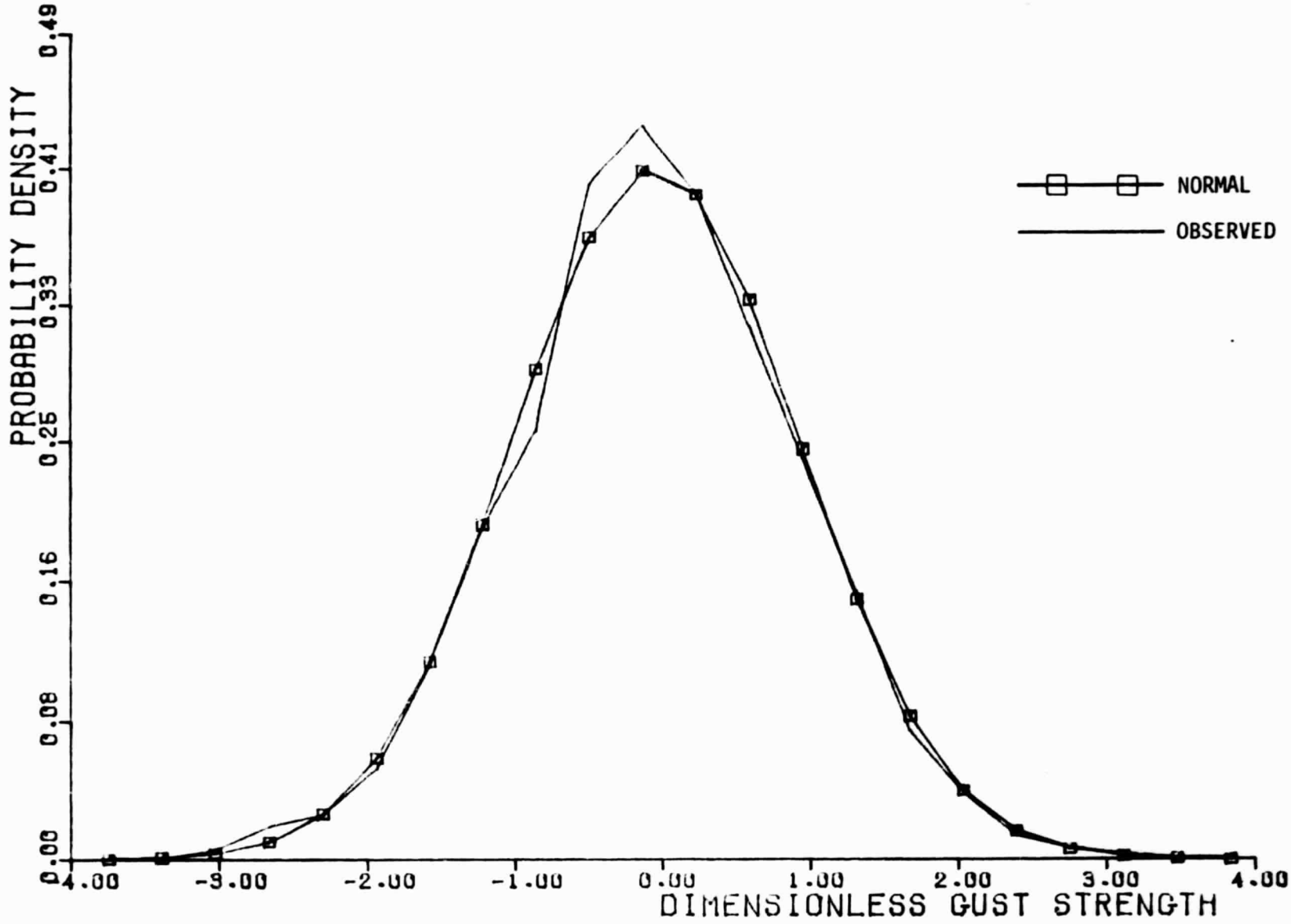


Figure D-18. $u_3$ - Gust Probability Density Distribution, Altitude Band #6

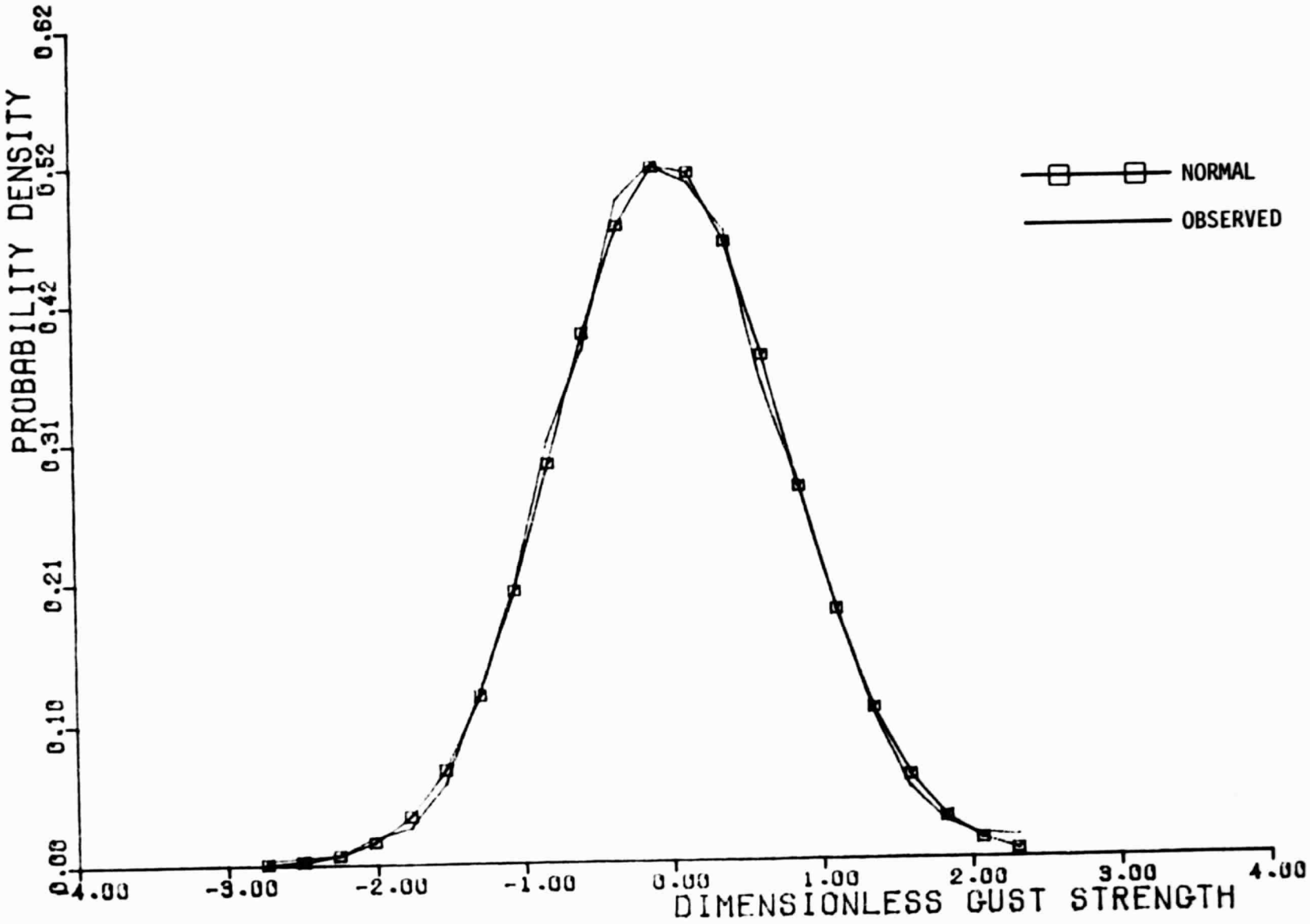


Figure D-19. $\partial u_2/\partial x_1$ - Gust Gradient Probability Density Distribution, Altitude Band #1

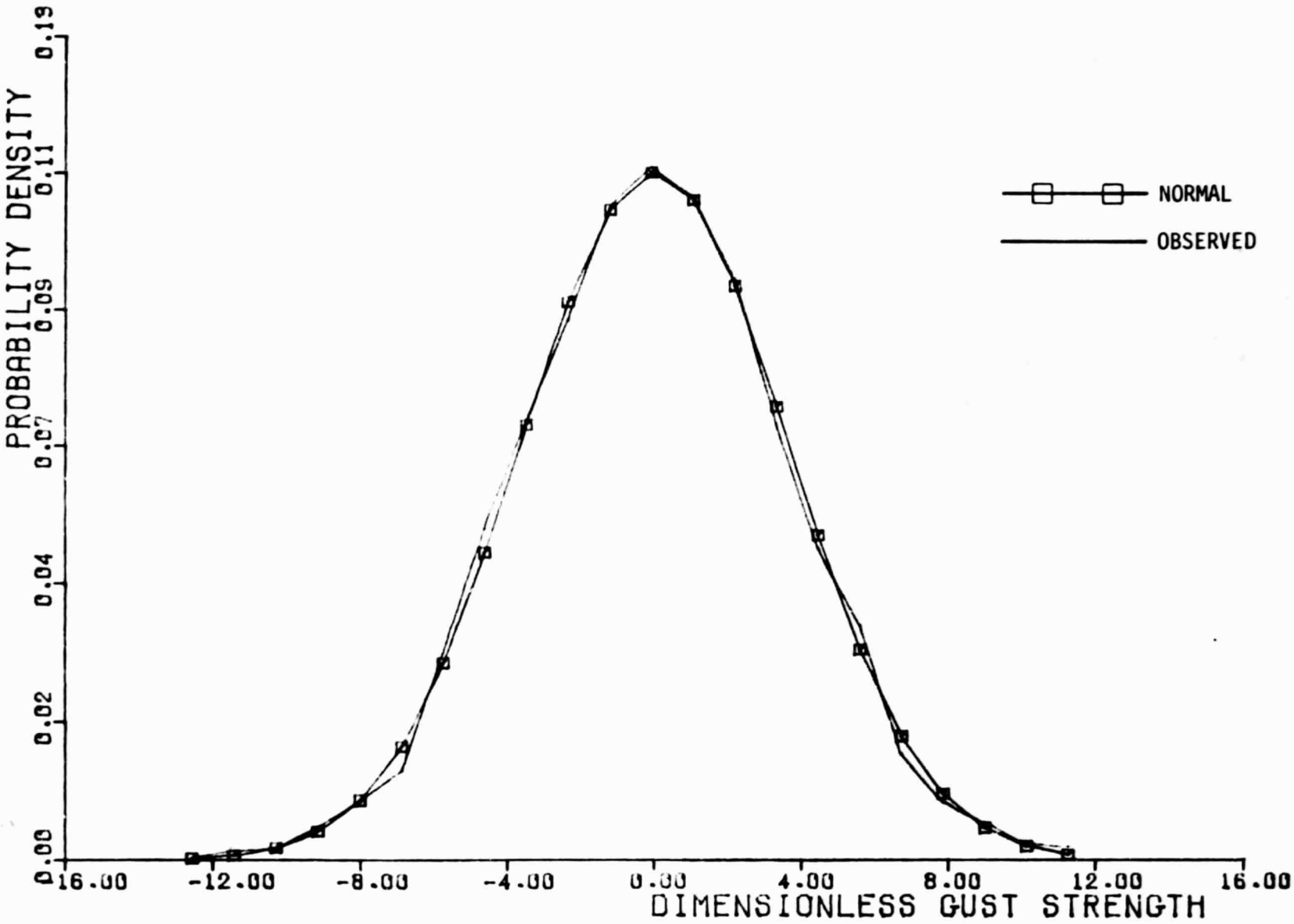


Figure D-20. $\partial u_2/\partial x_1$ - Gust Gradient Probability Density Distribution, Altitude Band #2

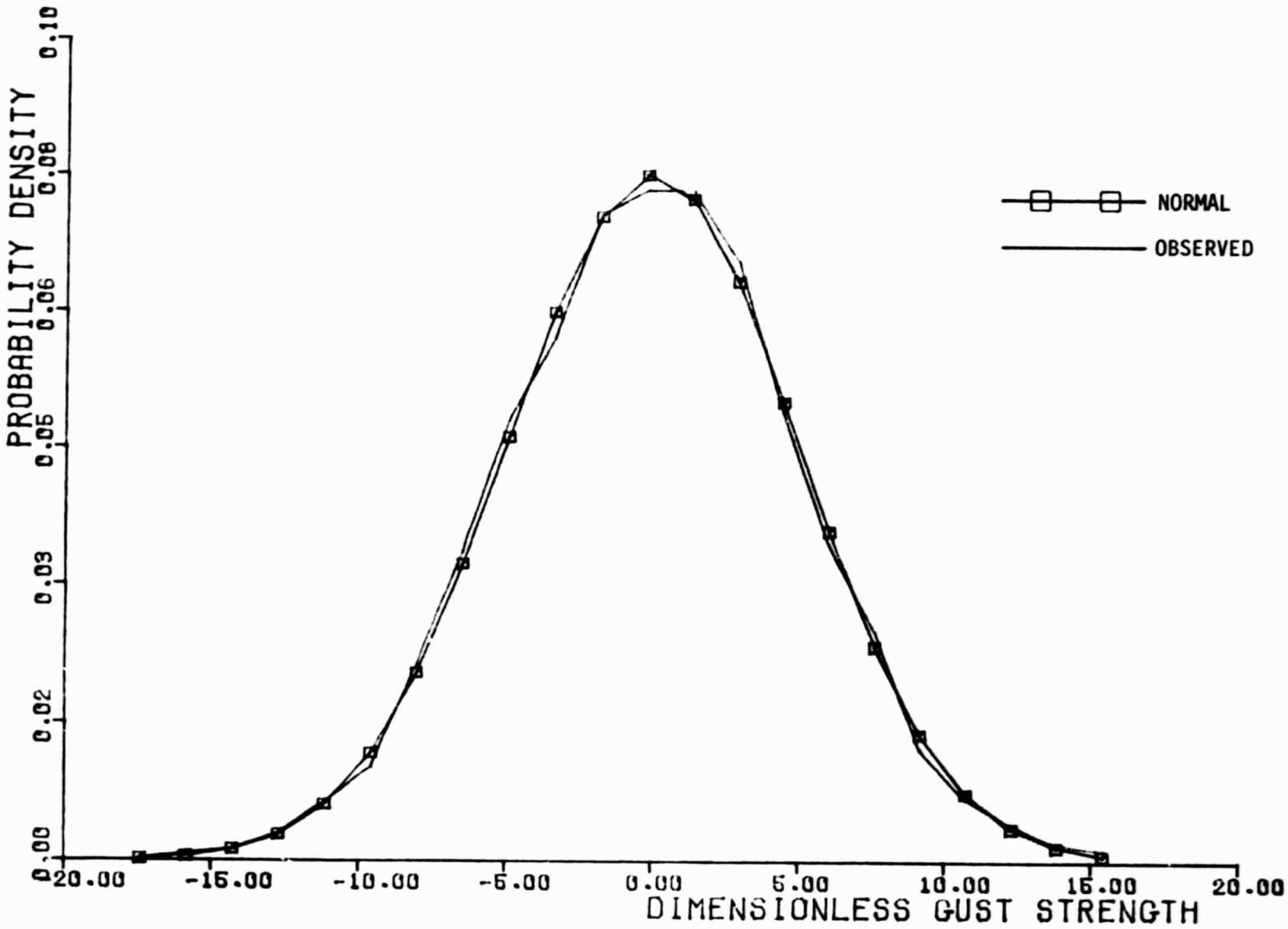


Figure D-21. $\partial u_2/\partial x_1$ - Gust Gradient Probability Density Distribution, Altitude Band #3

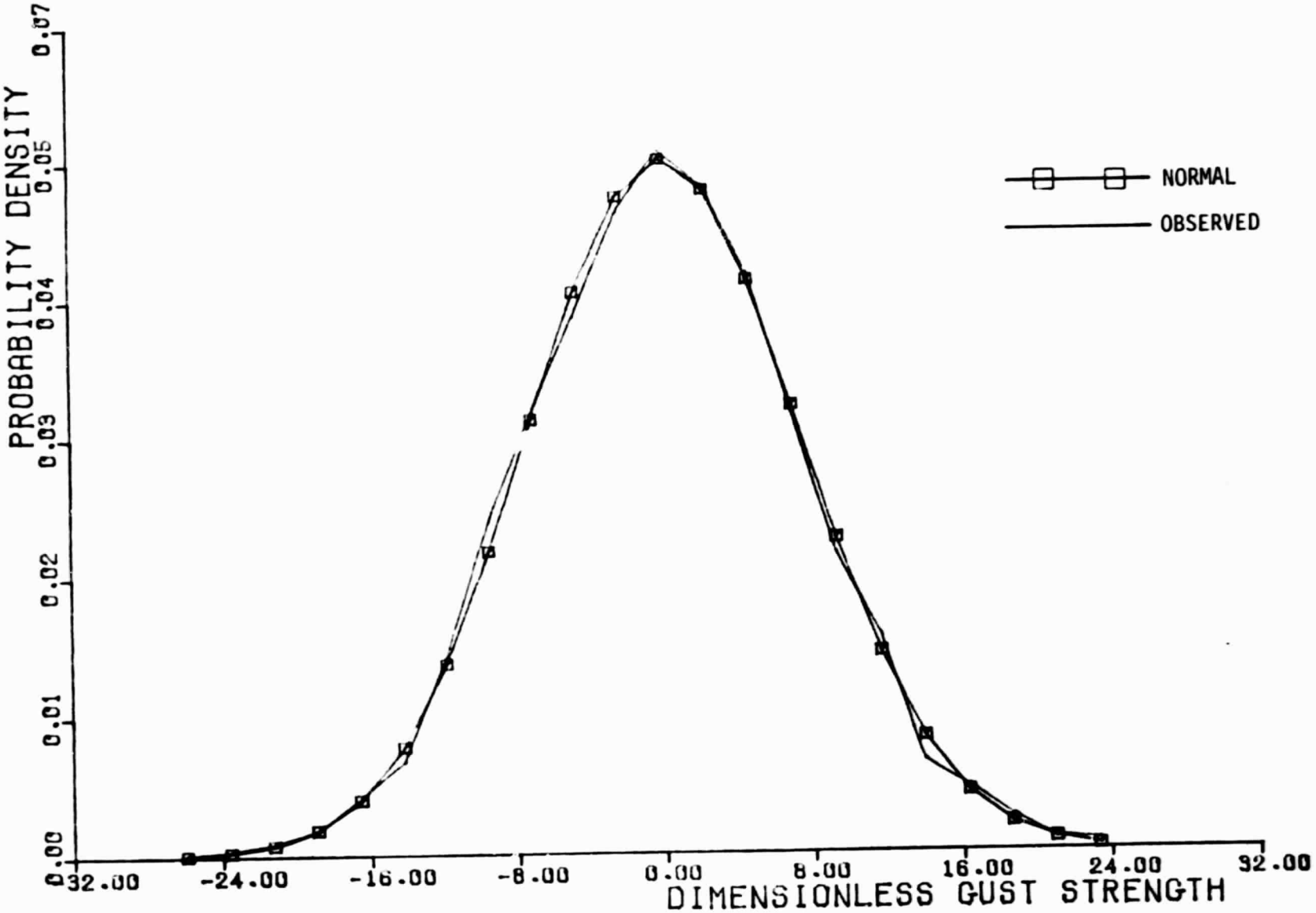


Figure D-22. $\partial u_2/\partial x_1$ - Gust Gradient Probability Density Distribution, Altitude Band #4

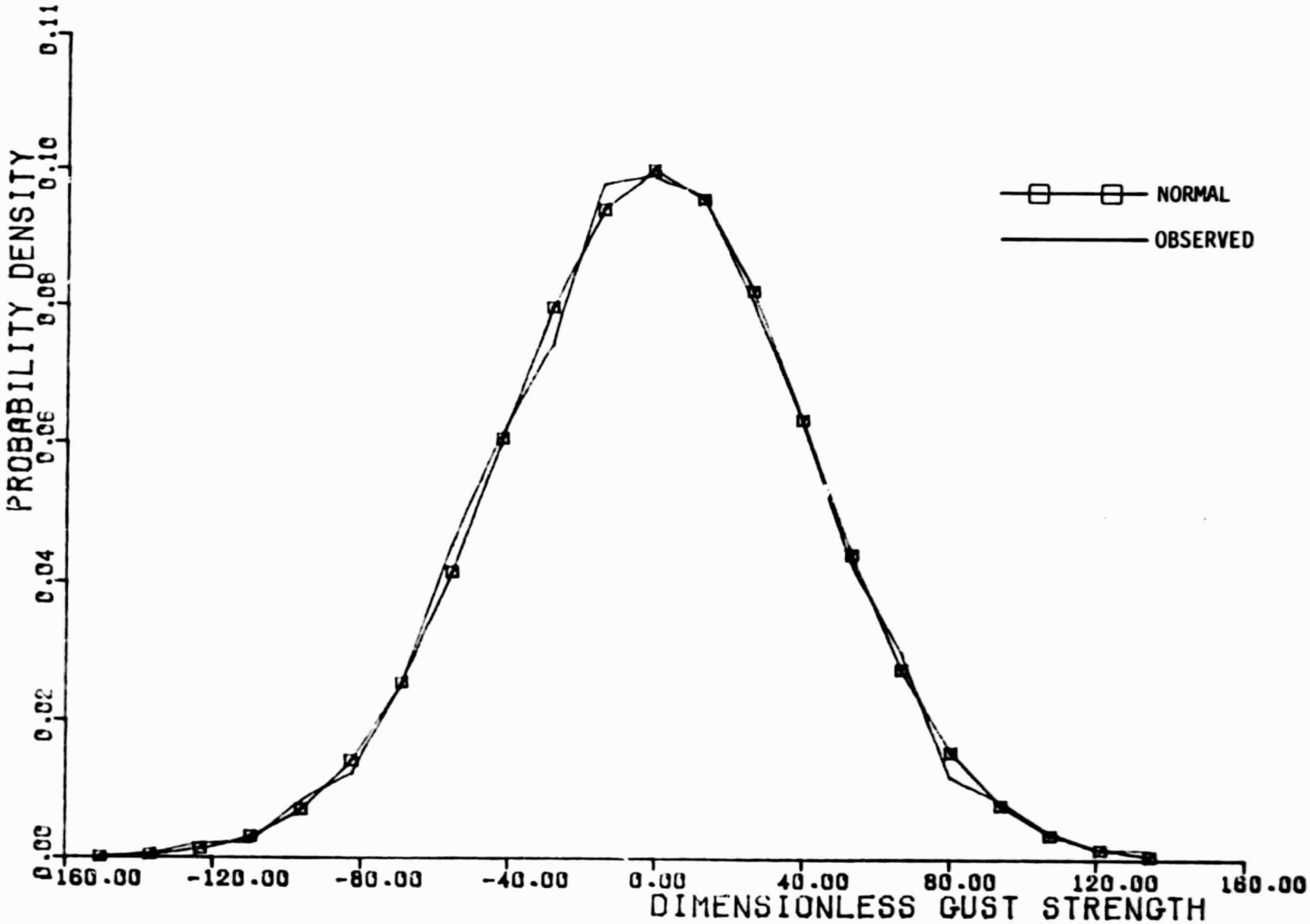


Figure D-23. $\partial u_2/\partial x_1$ - Gust Gradient Probability Density Distribution, Altitude Band #5

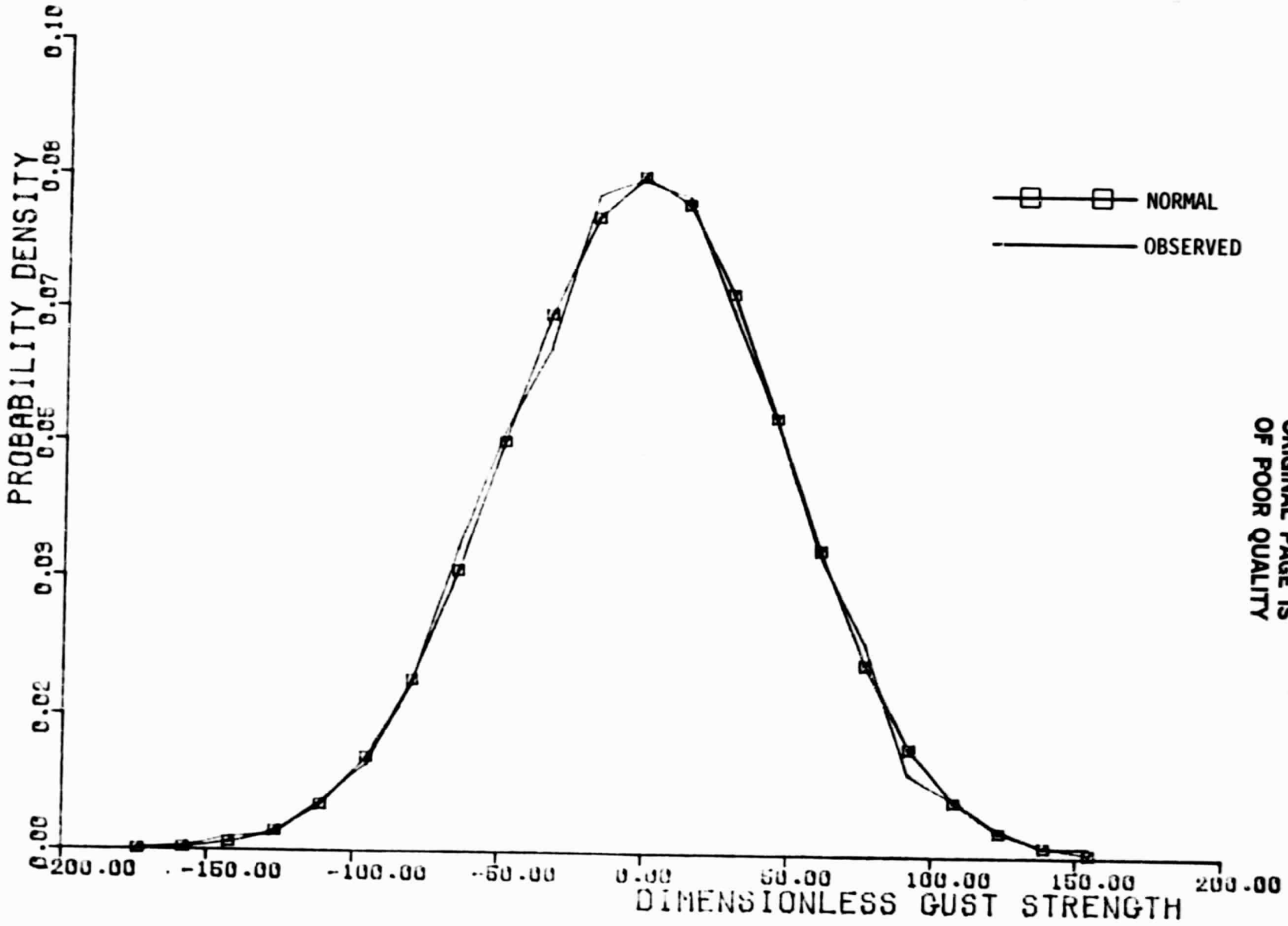




Figure D-24. $\partial u_2/\partial x_1$ - Gust Gradient Probability Density Distribution, Altitude Band #6

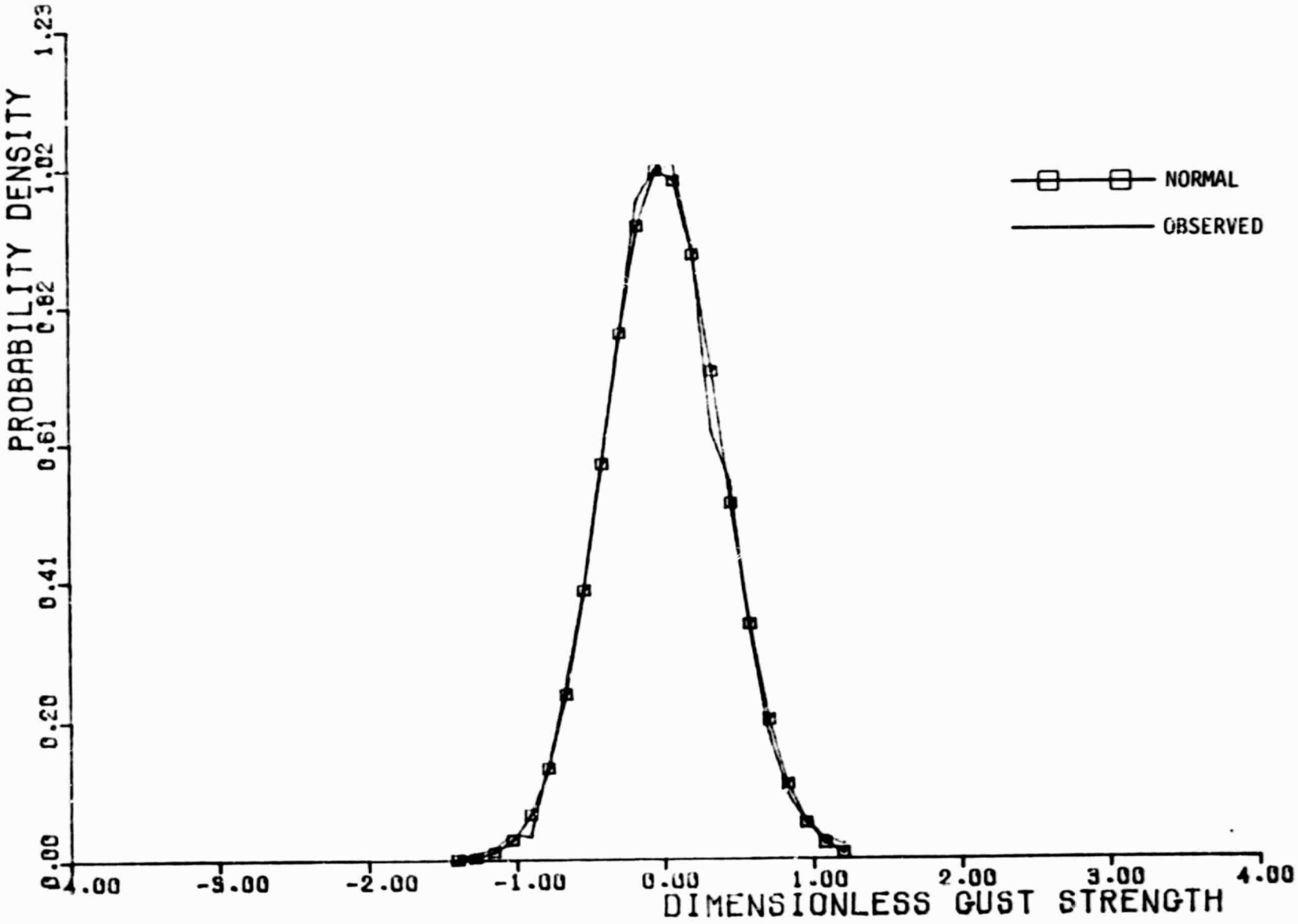


Figure D-25. $\partial u_3/\partial x_1$ - Gust Gradient Probability Density Distribution, Altitude Band #1

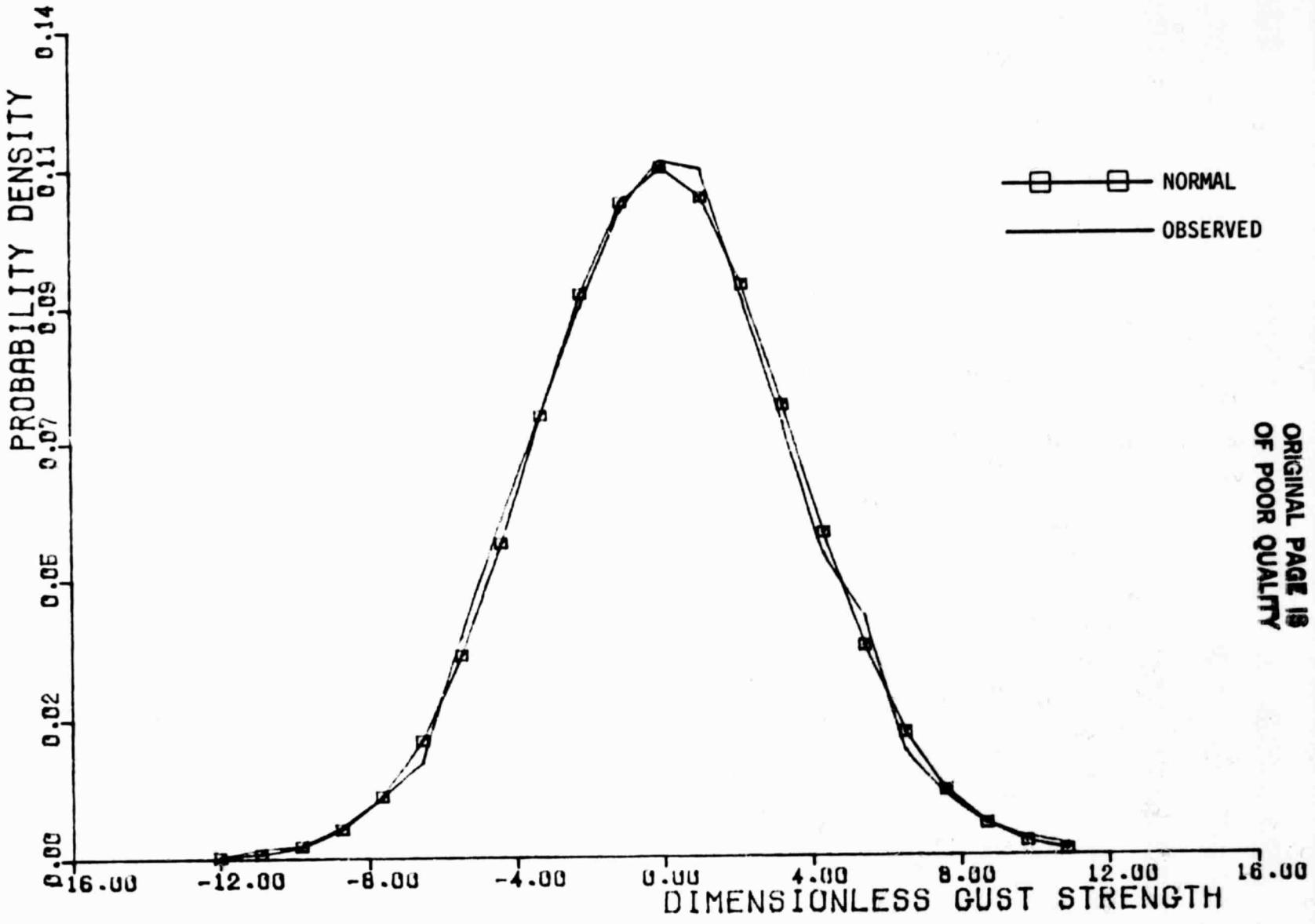




Figure D-26. $\partial u_3/\partial x_1$ - Gust Gradient Probability Density Distribution, Altitude Band #2

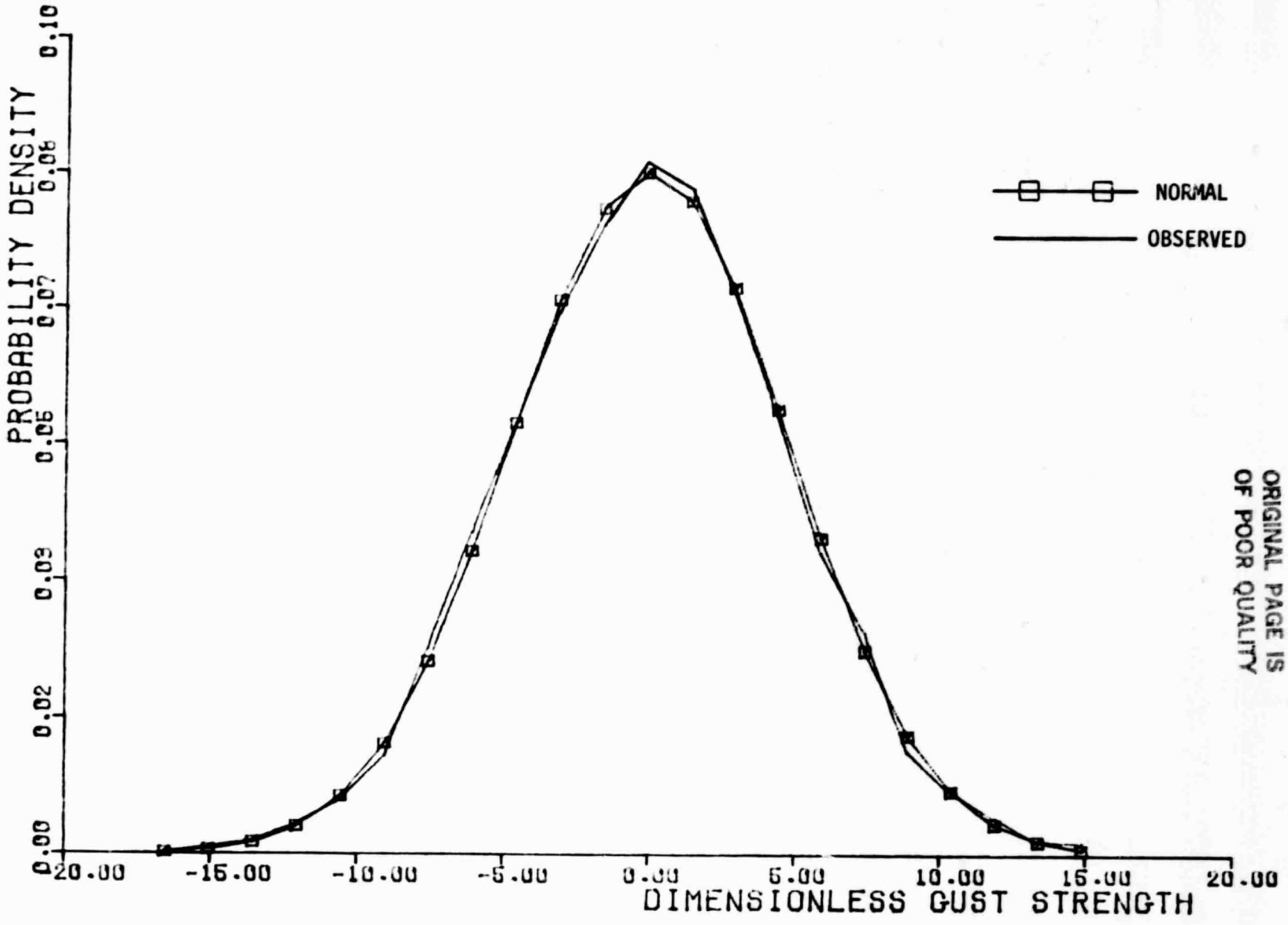


Figure D-27. $\partial u_3/\partial x_1$ - Gust Gradient Probability Density Distribution, Altitude Band #3

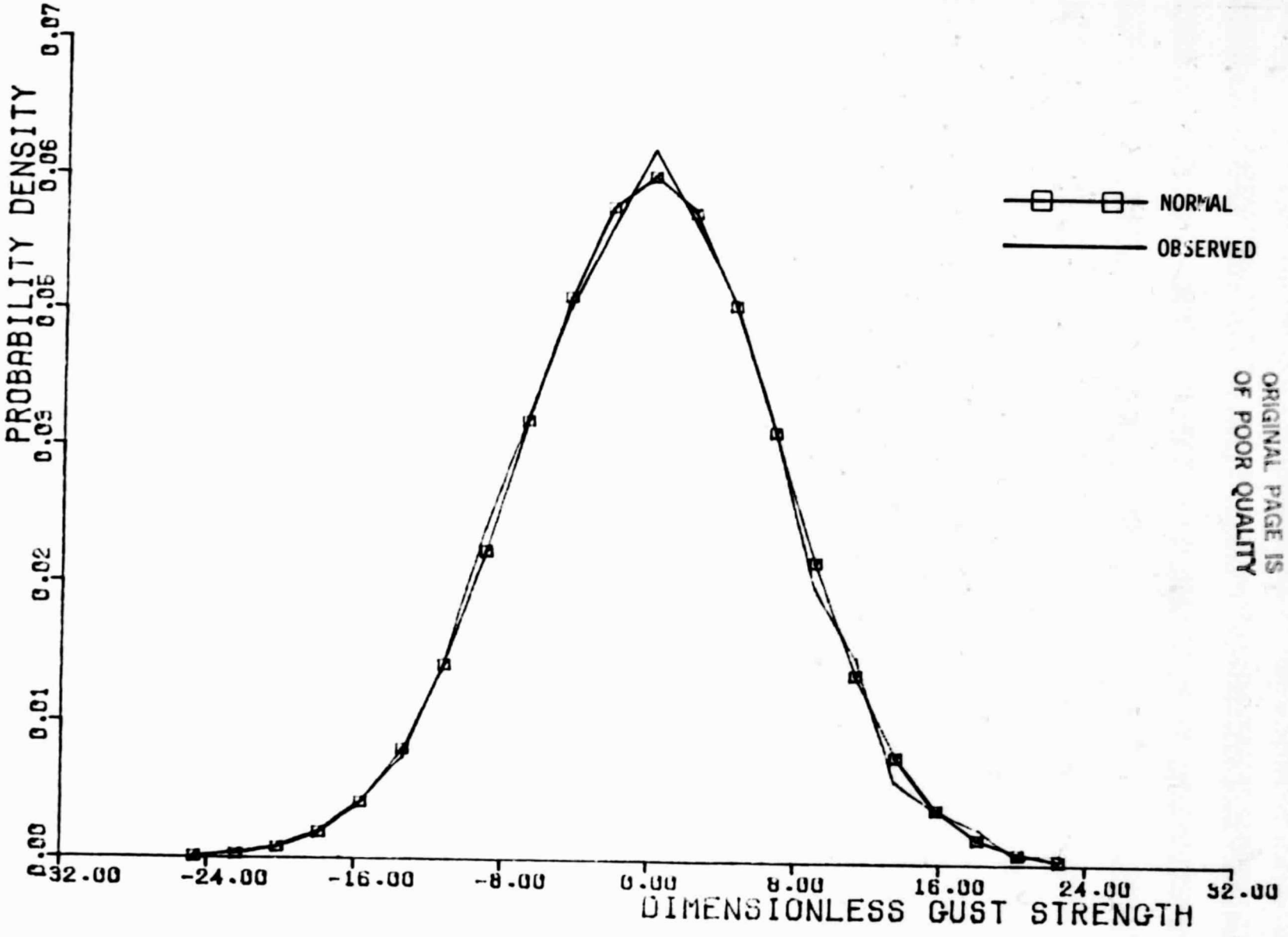




Figure D-28. $\partial u_3/\partial x_1$ - Gust Gradient Probability Density Distribution, Altitude Band #4

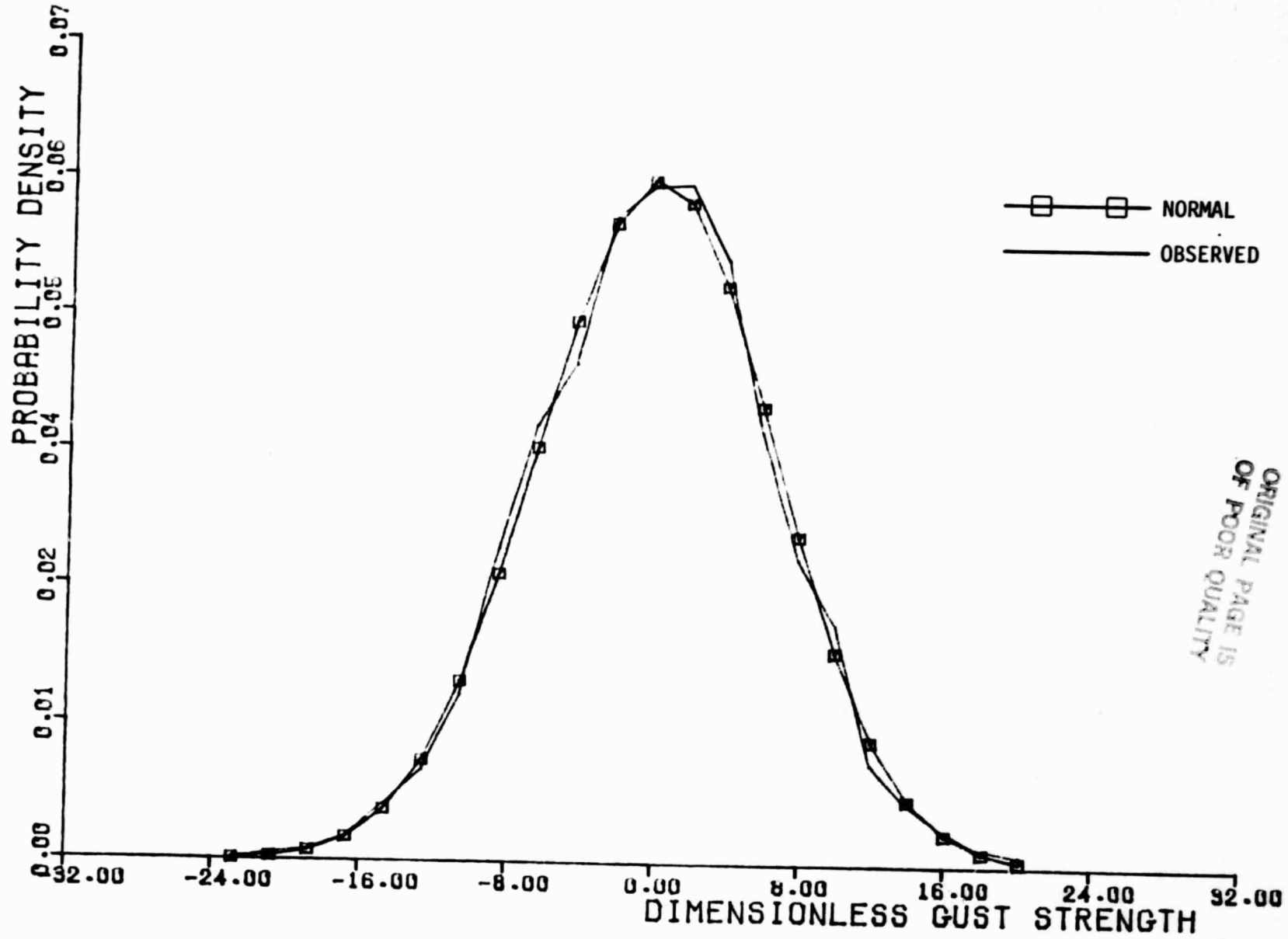




Figure D-29. $\partial u_3/\partial x_1$ - Gust Gradient Probability Density Distribution, Altitude Band #5

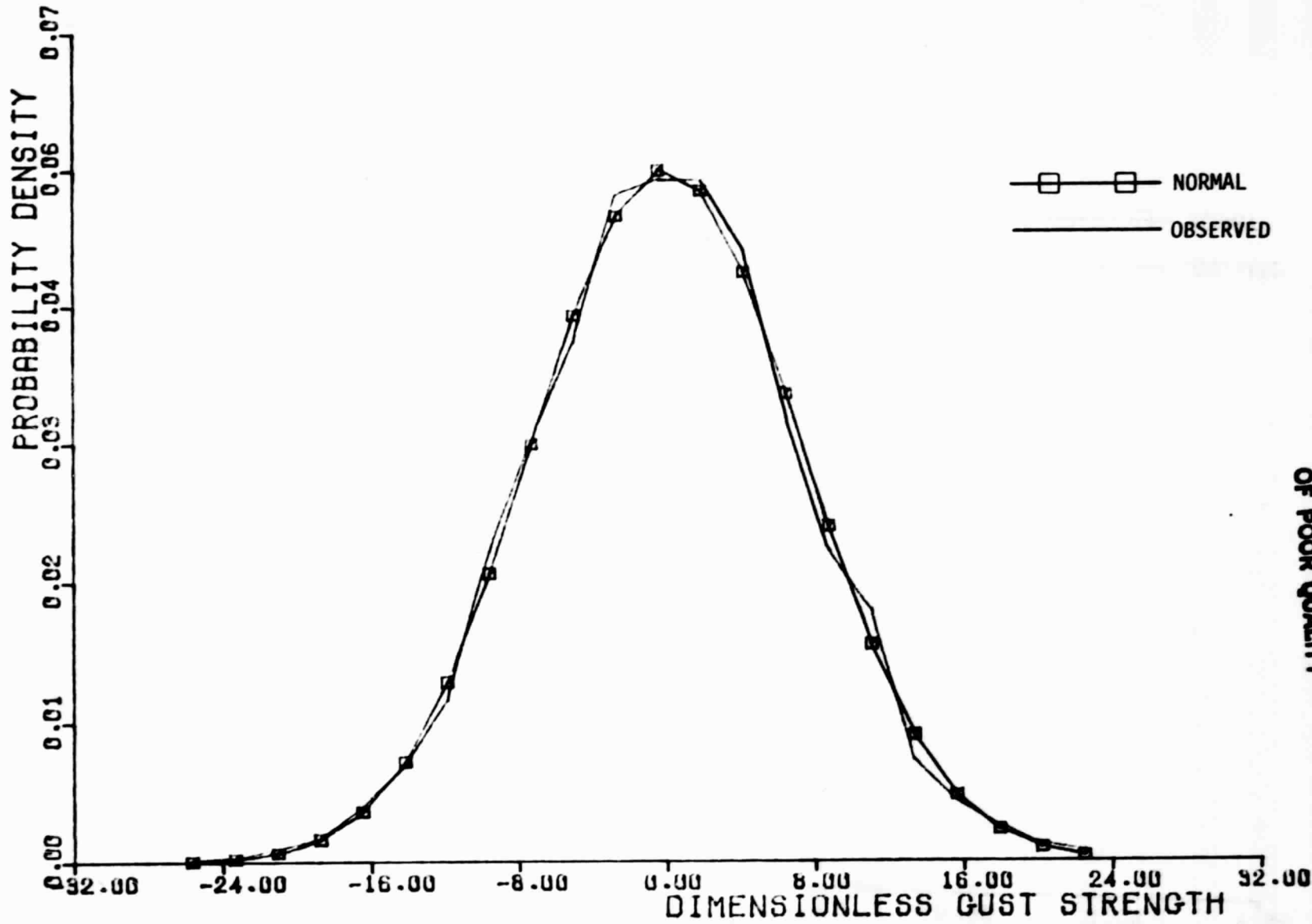




Figure D-30. $\partial u_3/\partial x_1$ - Gust Gradient Probability Density Distribution, Altitude Band #6

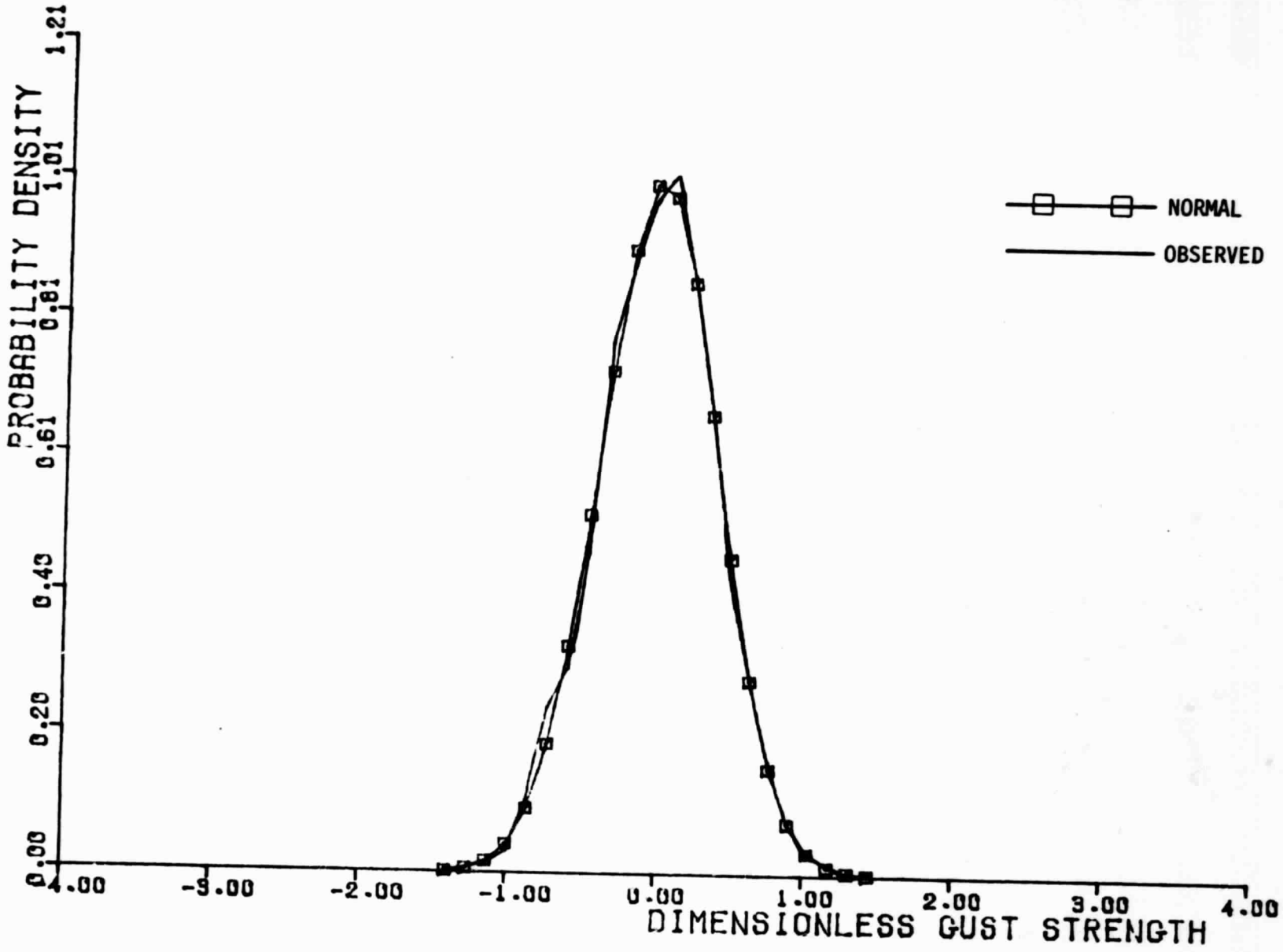


Figure D-31. $\partial u_3/\partial x_2$ - Gust Gradient Probability Density Distribution, Altitude Band #1

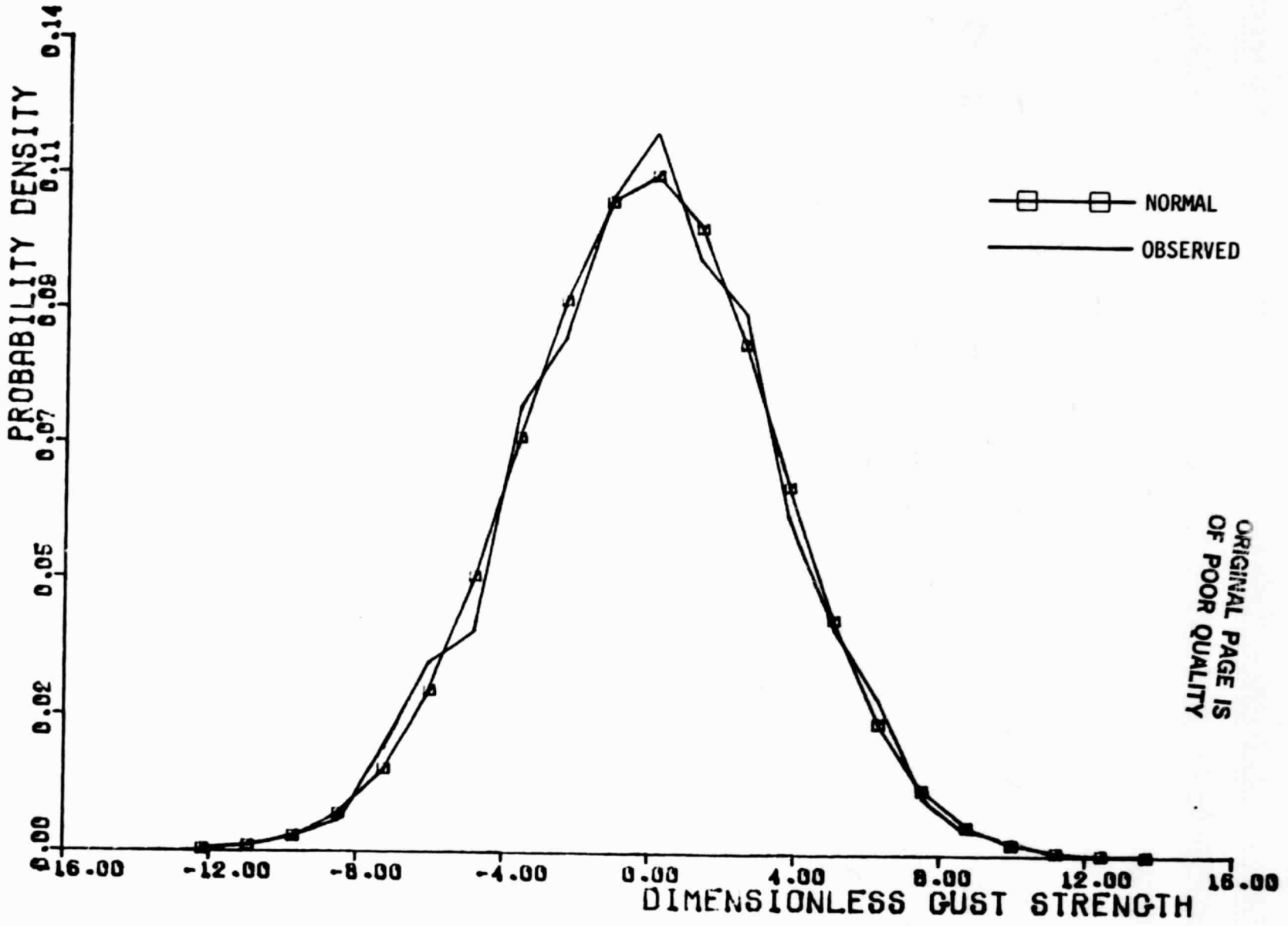


Figure D-32. $\partial u_3/\partial x_2$ - Gust Gradient Probability Density Distribution, Altitude Band #2

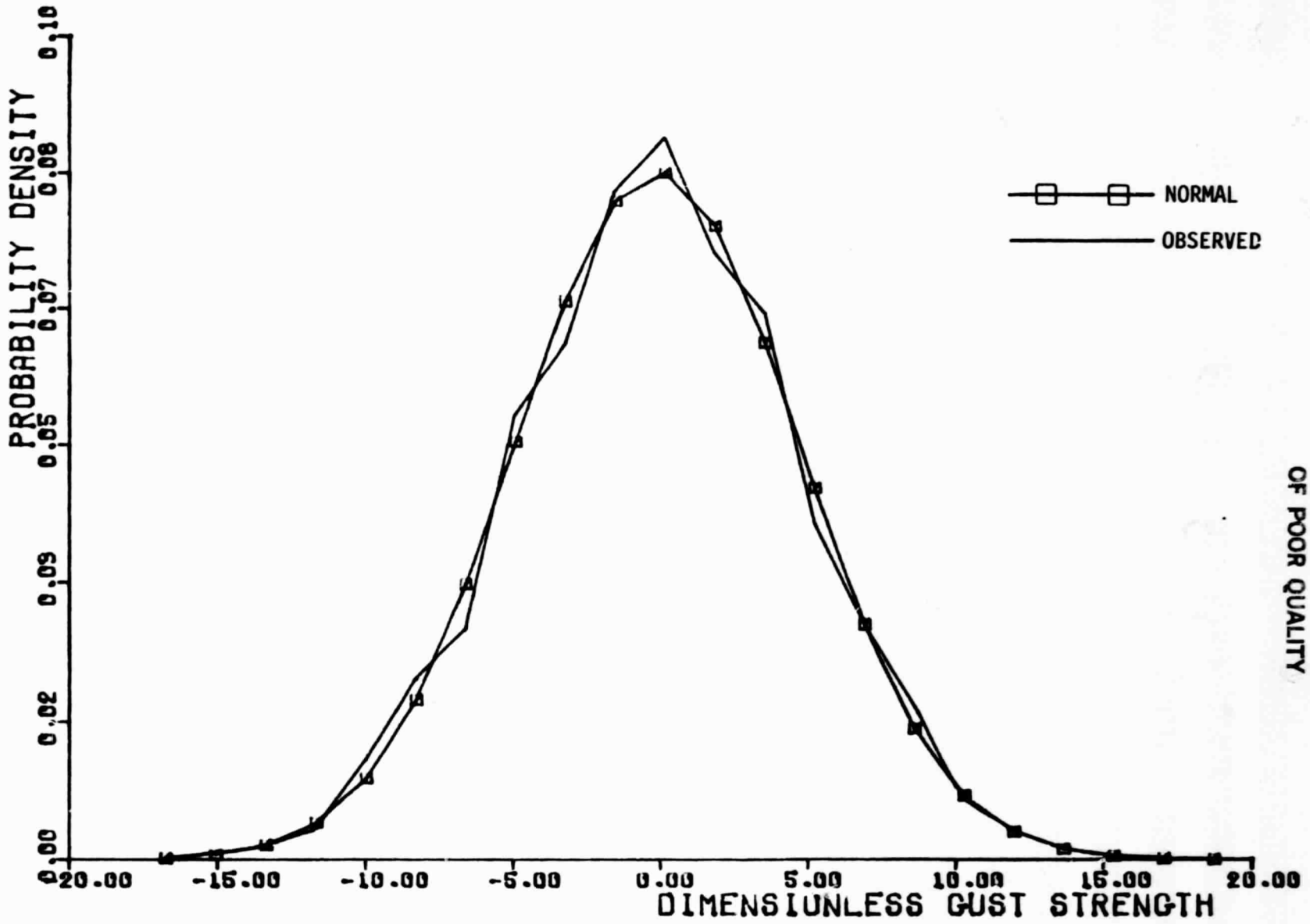


Figure D-33. $\partial u_3/\partial x_2$ - Gust Gradient Probability Density Distribution, Altitude Band #3

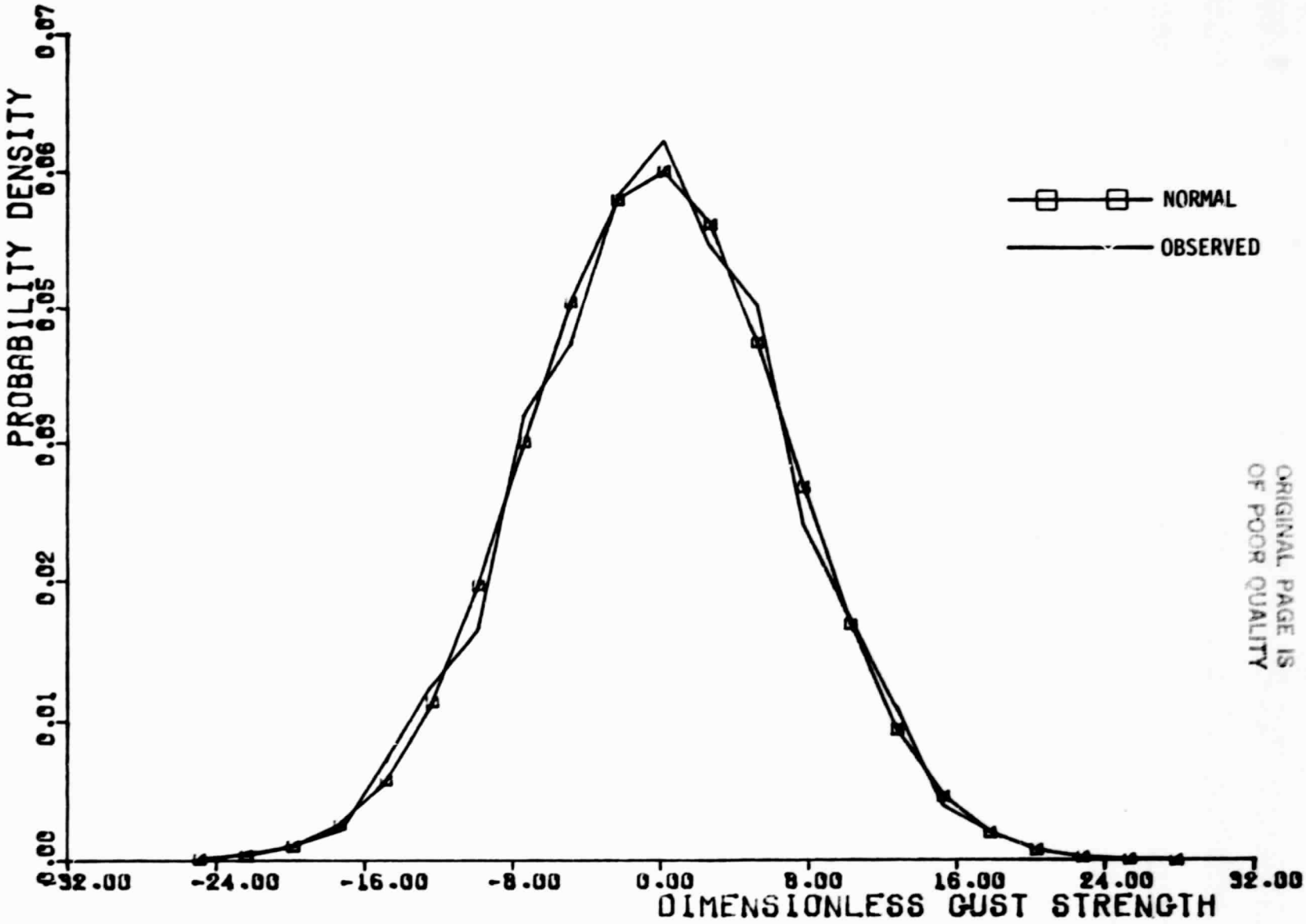




Figure D-34. $\partial u_3/\partial x_2$ - Gust Gradient Probability Density Distribution, Altitude Band #4

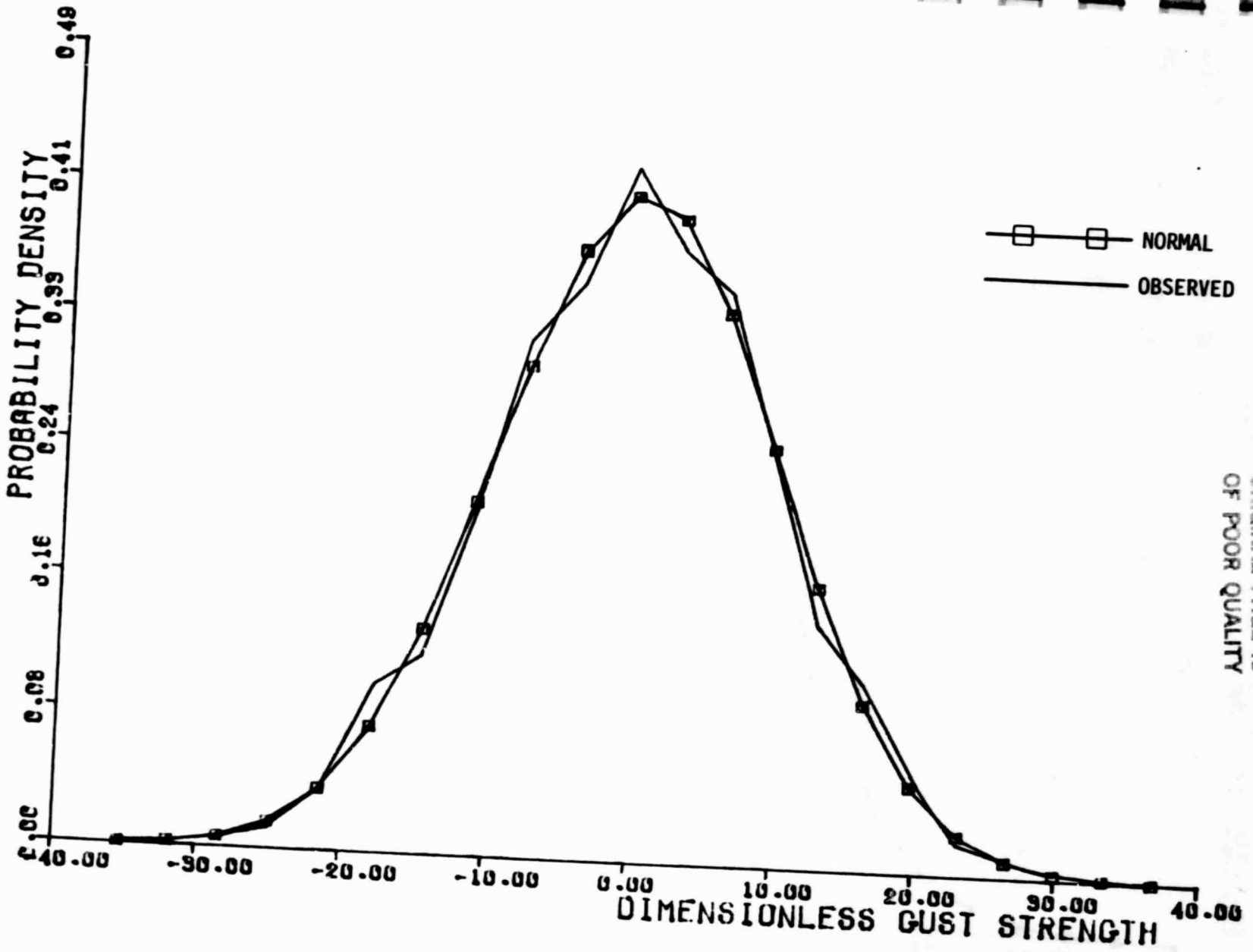


Figure D-35. $\partial u_3/\partial x_2$ - Gust Gradient Probability Density Distribution, Altitude Band #5

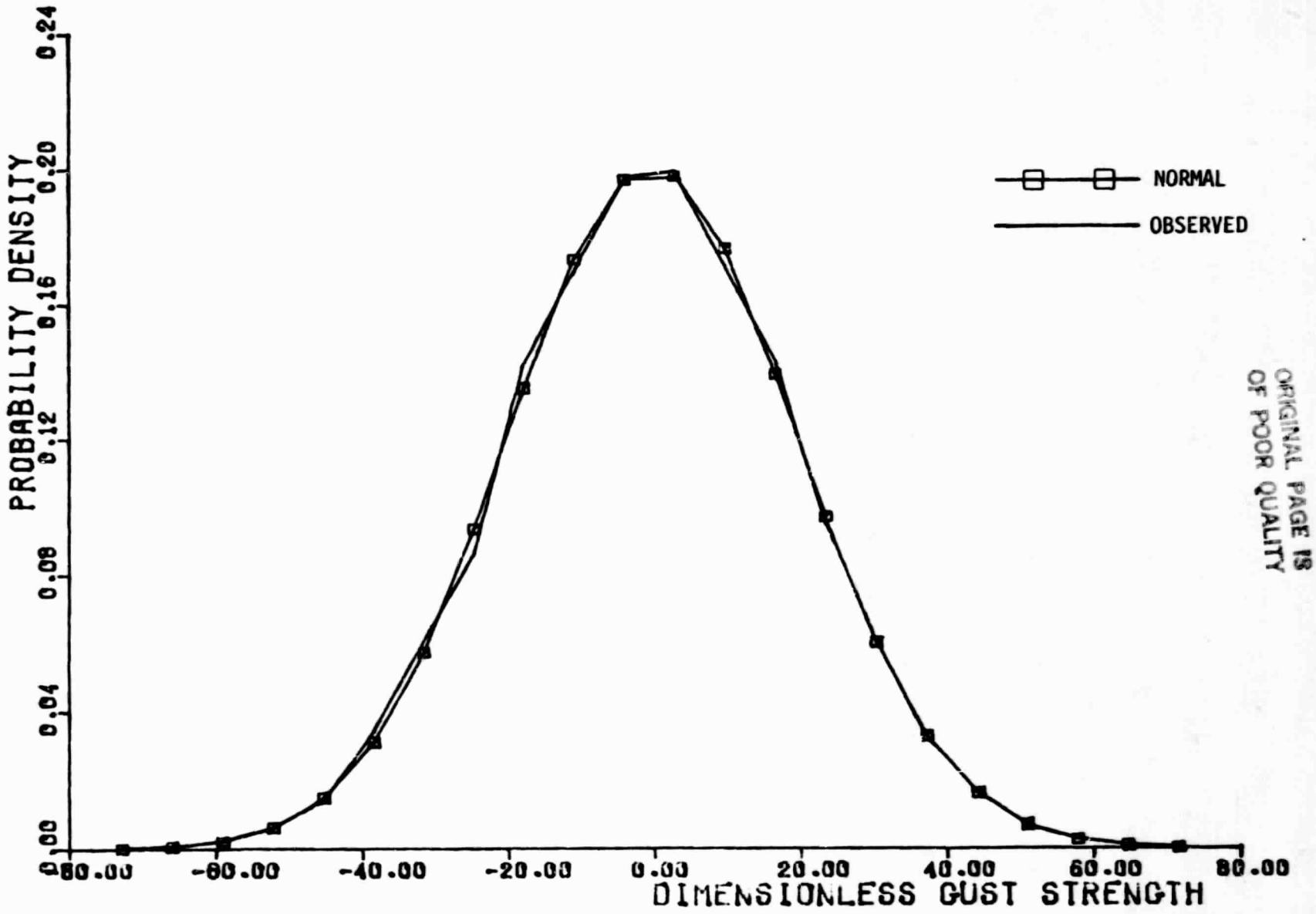




Figure D-36. $\partial u_3/\partial x_2$ - Gust Gradient Probability Density Distribution, Altitude Band #6